

An-Najah National University

Faculty of Graduate Studies

**Combined Electrochemical and Chemical Bath
Deposition Techniques to Prepare CuSe Thin
Film Electrodes for Solar Energy Purposes**

By

Khaled Ali Qasem Murtada

Supervisor

Prof. Hikmat S. Hilal

**This Thesis is Submitted in Partial Fulfillment of the Requirements for
the Degree of Master of Chemistry, Faculty of Graduate Studies, An-
Najah National University, Nablus, Palestine.**

2014

**Combined Electrochemical and Chemical Bath
Deposition Techniques to Prepare CuSe Thin
Film Electrodes for Solar Energy Purposes**

By

Khaled Ali Qasem Murtada

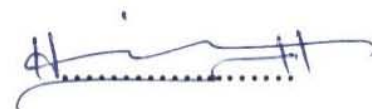
This thesis was defended successfully on 18/09/2014 and approved by:

Defense Committee Members

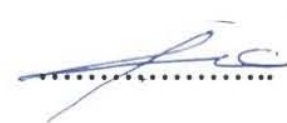
Signature

– Prof. Hikmat S. Hilal

(Supervisor)



– Dr. Abdel-Rahman Abu-Labdeh (External Examiner)



– Dr. Ahed Zyoud

(Internal Examiner)



Dedication

- *My parents: Thank you for your unconditional support with my studies. I'm honored to have you as my parents. Thank you for giving me a chance to prove and improve myself through all my walks of life. Please do not ever change. I love you.*
- *My family: Thank you for believing in me; for allowing me to further my studies. Please do not ever doubt my dedication and love for you.*
- *My brothers: Hoping that with this research I have proven to you that there is no mountain higher as long as God is on our side, hoping that you will walk again and be able to fulfill your dreams.*

Khaled A. Q. Murtada

Acknowledgments

- I thank Almighty God for giving me the courage and the determination, as well as guidance in conducting this research study, despite all difficulties.
- I wish to extend my utmost gratitude to all the research participants for their wonderful participation and cooperation.
- I also extend my heartfelt gratitude to my supervisor, Professor Hikmat S. Hilal. You were so wonderful to me. You made me believe that I had so much strength and courage to persevere even when I felt lost. You showed me light in a tunnel where everything was dark. You were very tolerant and determined to see me through. You were such wonderful motivators even when the coping seemed tough for me.
- I would also like to thank Dr. Ahed Zyoud for his patience, motivation throughout research work.
- I'll be eternally grateful to all my friends and for my Uncles Hisham & Marwan Ghanem.
- Great thanks are extended to the teaching staff and to the technical staff in the laboratories in the Department of Chemistry at An-Najah National University.
- I would like to sincerely thank my thesis committee members Dr. Abdel-Rahman Abu-Labdeh and Dr. Ahed Zyoud for the nice discussion, your questions and comments were very beneficial.

- Thanks are extended to Al-Quds University for AFM measurements. And I would also like to thank Dr. DaeHoon Park, Dansuk Industrial Co., South Korea for XRD measurements.
- Finally, I thank all those who assisted, encouraged and supported me during this research, be assured that the God will bless you all for the contributions

Khaled A. Q. Murtada

الإقرار

انا الموقع ادناه مقدم الرسالة التي تحمل عنوان:

Combined Electrochemical and Chemical Bath Deposition Techniques to Prepare CuSe Thin Film Electrodes for Solar Energy Purposes

اقر بان ما اشتملت عليه هذه الرسالة انما هو نتاج جهدي الخاص، باستثناء ما تمت الاشارة اليه
حيثما ورد وان هذه الرسالة ككل من او جزء منها لم يقدم من قبل لنيل أي درجة او بحث علمي او
بحثي لدى أي مؤسسة تعليمية او بحثية اخرى.

Declaration

The work provided in this thesis, unless otherwise referenced, is the
researcher's own work, and has not been submitted elsewhere for any other
degree or qualification.

Student's name:

فالدعق قائم مرتضى

اسم الطالب:

Signature:



التوقيع:

Date:

18.9.2014

التاريخ:

List of Contents

NO.	Contents	Page
	Dedication	III
	Acknowledgements	IV
	Declaration	VI
	List of Contents	VII
	List of Tables	XI
	List of Figures	XII
	Abstract	XV
	Chapter One: Introduction	1
1.1	Solar energy	2
1.2	Semiconductor (SCs)	3
1.3	Popular Semiconductor Materials Used in Solar Cells	3
1.4	Types of Semiconductor (SCs)	3
1.4.1	Intrinsic SCs	4
1.4.2	Extrinsic SCs	5
1.4.2.1	n-type	5
1.4.2.2	p-type	5
1.5	Fermi Level (E_F)	6
1.6	Solar Energy Conversion Technologies	7
1.6.1	Photovoltaic Devices (PV)	7
1.6.2	Photoelectrochemical Solar Cell (PEC)	7
1.7	Dark Current in n-type PEC Systems	8
1.8	Photo Current in n-type PEC Systems	10
1.9	Thin Film Technology	10
1.10	Copper Selenide (CuSe)	11
1.10.1	Some Basics Properties of Copper Selenide (CuSe)	12
1.11	Objectives	12
1.12	Hypothesis	13
	Chapter Two: Experimental	15
2.1	Materials	16
2.1.1	Chemicals	16
2.1.2	FTO/Glass Substrate Cleaning Process	16
2.1.3	Preparations of Selenium Ions	16
2.2	Preparation of CuSe Films	17
2.2.1	Electrochemical Deposition (ECD) Technique	17
2.2.2	Chemical Bath Deposition (CBD) Technique	18
2.2.3	Preparation of Electro-active (MP-Sil) Matrix	19
2.3	Modification of CuSe Thin Films	21
2.3.1	Annealing Process	21
2.3.2	Cooling Process	22

2.3.2.1	Fast Cooling (Quenching)	22
2.3.2.2	Slow Cooling	22
2.3.3	Coating with MP-Sil	22
2.4	Film Characterization	23
2.4.1	Electronic Absorption Spectra	23
2.4.2	Fluorescence Spectroscopy	23
2.4.3	Atomic Force Microscopy (AFM)	23
2.4.4	X-Ray Diffraction (XRD)	23
2.5	Photo-Electrochemical Cell (PEC)	24
2.6	Current Density-Potential Plots	25
2.7	Electrode Stability Testing	27
	Chapter Three: Results	28
3.1	Electronic absorption spectra	29
3.1.1	Effect of deposition time on the CuSe thin film electrodes	29
3.1.1.1	Effect of deposition time on the ECD-CuSe thin film electrodes	30
3.1.1.2	Effect of deposition time on the CBD-CuSe thin film electrodes	30
3.1.1.3	Effect of deposition time on the CBD/ECD-CuSe thin film electrodes	31
3.1.1.4	Comparison of CuSe thin film electrodes prepared by different techniques	32
3.1.2	Effect of cooling rate on the CuSe thin film electrodes	33
3.1.2.1	Effect of cooling rate on the CBD-CuSe thin film electrodes	33
3.1.2.2	Effect of cooling rate on the CBD/ECD-CuSe thin film electrodes	34
3.2	Photoluminescence spectra (PL)	35
3.2.1	Effect of deposition time on the CuSe thin film electrodes	35
3.2.1.1	Effect of deposition time on the ECD-CuSe thin film electrodes	36
3.2.1.2	Effect of deposition time on the CBD-CuSe thin film electrodes	36
3.2.1.3	Effect of deposition time on the CBD/ECD-CuSe thin film electrodes	37
3.2.1.4	Comparison of CuSe thin film electrodes prepared by different techniques	38
3.2.2	Effect of cooling rate on the CuSe thin film electrodes	39
3.2.2.1	Effect of cooling rate on the CBD-CuSe thin film electrodes	39

3.2.2.2	Effect of cooling rate on the CBD/ECD-CuSe thin film electrodes	40
3.3	Atomic force microscopy (AFM)	41
3.4	X-Ray diffraction (XRD)	44
3.4.1	Effect of deposition time on the CBD-CuSe thin film electrodes	45
3.4.2	Effect of deposition time on the CBD/ECD-CuSe thin film electrodes	47
3.4.3	Effect of cooling rate on the CBD/ECD-CuSe thin film electrodes	49
3.5	PEC studies	51
3.5.1	Effect of deposition time on the CuSe thin film electrodes	51
3.5.1.1	Photo <i>J-V</i> plots measured for ECD-CuSe thin film electrodes	51
3.5.1.2	Photo <i>J-V</i> plots measured for CBD-CuSe thin film electrodes	52
3.5.1.3	Dark <i>J-V</i> plots measured for CBD-CuSe thin film electrodes	53
3.5.1.4	Photo <i>J-V</i> plots measured for CBD/ECD-CuSe thin film electrodes	53
3.5.1.5	Dark <i>J-V</i> plots measured for CBD/ECD-CuSe thin film electrodes	55
3.5.1.6	Photo <i>J-V</i> plots measured for CuSe thin film electrodes prepared by different techniques	55
3.5.2	Effect of cooling rate on the CuSe thin film electrodes	57
3.5.2.1	Photo <i>J-V</i> plots measured for CBD-CuSe thin film electrodes	57
3.5.2.2	Photo <i>J-V</i> plots measured for CBD/ECD-CuSe thin film electrodes	58
3.6	Stability of the CuSe thin film electrodes	59
3.7	Electronic Absorption Spectra	61
3.7.1	Effect of coating with MP-Sil matrix on the CBD-CuSe thin film electrodes	61
3.7.2	Effect of coating with MP-Sil matrix on the CBD/ECD-CuSe thin film electrodes	62
3.8	Photoluminescence Spectra (PL)	62
3.8.1	Effect of coating with MP-Sil matrix on the CBD-CuSe thin film electrodes	62
3.8.2	Effect of coating with MP-Sil matrix on the CBD/ECD-CuSe thin film electrodes	63
3.9	PEC Studies	64

3.9.1	Photo J - V plots measured for coated CBD-CuSe thin film electrodes	64
3.9.2	Photo J - V plots measured for coated CBD/ECD-CuSe thin film electrodes	65
	Chapter Four: Discussion	67
4.1	Naked CuSe thin film electrodes	69
4.1.1	ECD-CuSe thin film electrodes	69
4.1.2	CBD-CuSe thin film electrodes	69
4.1.3	CBD/ECD-CuSe thin film electrodes	72
4.1.4	Comparison between different preparation techniques: ECD (15 min), CBD (2 hr) and CBD/ECD (2 hr)	76
4.2	Coating with MP-Sil	77
4.2.1	CBD-CuSe thin film electrodes	78
4.2.2	CBD/ECD-CuSe thin film electrodes	79
	Conclusions	80
	Suggestions for Further Work	81
	References	82
	المخلص	ب

List of Tables

No.	Table	Page
Table 1.1	Popular semiconductor materials used in solar cells	3
Table 1.2	Some basic properties of copper selenide (CuSe)	12
Table 3.1	XRD measurements for CBD-CuSe thin films	46
Table 3.2	XRD measurements for CBD/ECD-CuSe thin film electrodes	48
Table 3.3	XRD results for annealed CBD/ECD-CuSe thin film electrodes	50
Table 3.4	The PEC characteristics of ECD-CuSe thin film electrode deposited in 15 min	51
Table 3.5	Effect of deposition time on PEC characteristics of CBD-CuSe thin film electrodes	52
Table 3.6	Effect of deposition time on PEC characteristics of CBD/ECD-CuSe thin film electrodes	54
Table 3.7	Comparison of CuSe thin film electrodes prepared by different techniques	56
Table 3.8	Effect of annealing on PEC characteristics of CBD-CuSe thin film electrodes	58
Table 3.9	Effect of annealing on PEC characteristics of CBD/ECD-CuSe thin film electrodes	59
Table 3.10	Effect of coating with MP-Sil matrix on PEC characteristics of CBD-CuSe thin film electrodes	65
Table 3.11	Effect of coating with MP-Sil matrix on PEC characteristics of CBD/ECD-CuSe thin film electrodes	66

List of Figures

No.	Figures	Page
Figure 1.1	Band gap in conductor, semiconductor, and insulator	4
Figure 1.2	Schematic showing thermally excited electron in intrinsic semiconductor	4
Figure 1.3	Dopant energy levels in n-type SC and p-type SC	5
Figure 1.4	Fermi level diagram, a) n-type semiconductor, b) intrinsic semiconductor, c) p-type semiconductor	6
Figure 1.5	Energy level diagrams of an n-type SC before and after equilibrium with an electrolyte containing the redox couple A/A ⁻	8
Figure 1.6	Dark and photocurrent voltammograms for an n-type SC	9
Figure 1.7	Dark current in n-type SC	9
Figure 1.8	Photocurrent generation at n-type SC	10
Figure 1.9	Crystal structure of CuSe, a) cubic structure, b) hexagonal structure	11
Figure 2.1	Preparing the (Na ₂ SeSO ₃) by refluxing the reactant (2.0 g Se powder, 20.0 g of Na ₂ SO ₃ , 100 mL distilled water) at 80°C for 10 hour	17
Figure 2.2	The experimental arrangement for the ECD-CuSe film. 1) magnetic stirrer plate, 2) magnetic stirrer, 3) CuSe thin film, 4) platinum electrode, 5) counter electrode (Ag/AgCl), 6) nitrogen, 7) ECD cell, 8) glass cover, 9,10,11) electrodes holders, 12) Potentiostat	18
Figure 2.3	Experimental setup for solution growth of CBD-CuSe thin film	19
Figure 2.4	Tetra(-4-pyridyl)porphyrinatomanganese (III)sulfate (MP) complex	20
Figure 2.5	Photoluminescence spectra of: a) MP embedded in Sil polymer coated on FTO/Glass substrate, b) FTO/Glass substrate	21
Figure 2.6	The annealing system, 1) nitrogen input, 2) nitrogen output, 3) CuSe thin film	22
Figure 2.7	Two-electrode photo-electrochemical cell (PEC). 1) Beaker, 2) rubber seal, 3) CuSe working electrode, 4) platinum counter electrode and internal reference electrode 5) electrolytic solution, 6) nitrogen, 7) light source	25
Figure 2.8	Reduction of copper ion in HCl electrolyte solution, on glassy carbon electrode	26
Figure 3.1	Electronic absorption spectra for ECD of the CuSe thin films deposited in 15 min	30
Figure 3.2	Electronic absorption spectra for CBD of CuSe thin films, deposited in different times, a) 2 hr, b) 4 hr and c) 6 hr	31

Figure 3.3	Electronic absorption spectra for the CBD/ECD of CuSe thin films, deposited in different times, a) 2 hr, b) 4 hr and c) 6 hr	32
Figure 3.4	Electronic absorption spectra for CBD of the CuSe thin films, deposited in different techniques, a) CBD/ECD for 2 hr, b) CBD for 2 hr and c) ECD for 15 min	33
Figure 3.5	Electronic absorption spectra for CBD of the CuSe thin films deposited in 2 hr, a) non-annealed, b) annealed at 250°C for 1 hr, quickly cooled and c) annealed at 250°C for 1 hr, slowly cooled	34
Figure 3.6	Electronic absorption spectra for CBD/ECD of the CuSe thin films deposited in 2 hr, a) non-annealed, b) annealed at 250°C for 1 hr, quickly cooled, and c) annealed at 250°C for 1 hr, slowly cooled	35
Figure 3.7	Photoluminescence spectra for ECD of CuSe thin films, deposited in 15 min	36
Figure 3.8	Photoluminescence spectra for CBD of CuSe thin films, deposited in different times, a) 2 hr, b) 4 hr and c) 6 hr	37
Figure 3.9	Photoluminescence spectra for CBD/ECD of CuSe thin films, deposited in different times, a) 2 hr, b) 4 hr and c) 6 hr	38
Figure 3.10	Photoluminescence spectra for CBD of CuSe thin films, deposited in different techniques, a) CBD/ECD for 2 hr, b) CBD for 2 hr and c) ECD for 15 min	39
Figure 3.11	Photoluminescence spectra for CBD of CuSe thin films deposited in 2 hr: a) non-annealed, b) annealed at 250°C, for 1 hr, quickly cooled and c) annealed at 250°C, for 1 hr, slowly cooled	40
Figure 3.12	Photo-luminescence spectra for CBD/ECD of CuSe thin films deposited in 2 hr: a) non-annealed, b) annealed at 250°C, for 1 hr, quickly cooled and c) annealed at 250°C, for 1 hr, slowly cooled	41
Figure 3.13	2D AFM image for CuSe thin films deposited in 2 hr, and prepared by different techniques: (a) by CBD/ECD, and (b) by CBD	42
Figure 3.14	Average surface roughness analysis for CuSe films deposited in 2 hr, prepared by different techniques: (a) by CBD, and (b) by CBD/ECD	43
Figure 3.15	Effect of annealing on 2D AFM image for CBD/ECD-CuSe thin films deposited in 2 hr, (a) non-annealed, and (b) annealed (at 250°C for 1 hr and slowly cooled)	43
Figure 3.16	Effect of annealing on average surface roughness analysis for CBD/ECD-CuSe thin films deposited in 2 hr, (a) non-annealed, and (b) annealed (at 250°C for 1 hr and slowly cooled)	44

Figure 3.17	XRD spectra for CBD-CuSe thin films electrodes, deposited in different times, a) 2 hr, b) 4 hr and c) 6 hr	46
Figure 3.18	XRD spectra for CBD/ECD-CuSe thin films electrodes, deposited in different times, a) 2 hr, b) 4 hr and c) 6 hr	48
Figure 3.19	XRD spectra for CBD/ECD of CuSe thin films deposited in 2 hr: a) annealed at 250°C, for 1 hr, quickly cooled and b) annealed at 250°C, for 1 hr, slowly cooled	50
Figure 3.20	Photo <i>J-V</i> plots for ECD of CuSe thin films, deposited in 15 min	51
Figure 3.21	Photo <i>J-V</i> plots for CBD of CuSe thin films, deposited in different times, a) 2 hr, b) 4 hr and c) 6 hr	52
Figure 3.2	Dark <i>J-V</i> plots for CBD of CuSe thin films, deposited in different times, a) 2 hr, b) 4 hr and c) 6 hr	53
Figure 3.23	Photo <i>J-V</i> plots for CBD/ECD of CuSe thin films, deposited in different times, a) 2hr, b) 4hr and c) 6hr	54
Figure 3.24	Dark <i>J-V</i> plots for CBD/ECD of CuSe thin films, deposited in different times, a) 2 hr, b) 4 hr and c) 6 hr	55
Figure 3.25	Photo <i>J-V</i> plots for CuSe thin films, deposited in different techniques, a) CBD/ECD for 2 hr, b) CBD for 2 hr and c) ECD for 15 min	56
Figure 3.26	Photo <i>J-V</i> plots for CBD of CuSe thin films, deposited in 2 hr, a) non-annealed b) annealed at 250°C, 1 hr with fast cooling and c) annealed at 250°C, 1 hr with slow cooling	57
Figure 3.27	Photo <i>J-V</i> plots for CBD/ECD of CuSe thin films, deposited in 2 hr, a) non-annealed b) annealed at 250°C, 1 hr with fast cooling and c) annealed at 250°C, 1 hr with slow cooling	58
Figure 3.28	Short circuit current density vs. time measured for CBD/ECD of CuSe thin film electrodes, deposited in 2 hrs. The measurement was conducted in aqueous $K_3Fe(CN)_6/K_4Fe(CN)_6/LiClO_4$ redox system at room temperature	60
Figure 3.29	Electronic absorption spectra for CBD of CuSe thin films, deposited on FTO in 2 hr, a) naked, b) coated	61
Figure 3.30	Electronic absorption spectra for CBD/ECD CuSe thin films, deposited in 2 hr, a) naked, b) coated	62
Figure 3.31	Photoluminescence spectra for CBD of CuSe thin films, deposited in 2 hr, a) naked, b) coated	63
Figure 3.32	Photoluminescence spectra for CBD/ECD of CuSe thin films, deposited in 2 hr: a) naked, b) coated	64
Figure 3.33	Photo <i>J-V</i> plots for CBD of CuSe thin films, deposited in 2 hr, a) naked, b) coated	65
Figure 3.34	Photo <i>J-V</i> plots for CBD/ECD of CuSe thin films, deposited in 2 hr, a) naked, b) coated	66

**Combined Electrochemical and Chemical Bath Deposition Techniques
to Prepare CuSe Thin Film Electrodes for Solar Energy Purposes****By****Khaled Ali Qasem Murtada****Supervisor****Prof. Hikmat S. Hilal****Abstract**

The copper selenide (CuSe) thin films were prepared using electrochemical deposition (ECD), chemical bath deposition (CBD) and combined CBD/ECD preparation techniques on fluorine-doped tin oxide (FTO) coated glass substrates. Enhancement of deposited CuSe thin film characteristics in photo-electrochemical (PEC) systems was investigated. Deposited CuSe thin films were exposed to different treatment methods and different experimental conditions (deposition time 2, 4 and 6 hr). The films were annealed at 250°C under N₂ atmosphere for 1 hour. Cooling of annealed films to room temperature was done using two different methods (slow and fast cooling). K₃Fe(CN)₆/K₄Fe(CN)₆/LiClO₄ as redox couple was also used in the PEC measurements. The effect of such treatment on electrode PEC characteristics, such as: open-circuit voltage (V_{oc}), short-circuit current density (J_{sc}), dark current density-potential (J - V) plots, photo J - V plots, conversion efficiency (η), fill factor (FF), Surface Morphology and stability, was studied.

The characteristics of CuSe thin films in PEC systems were enhanced by using different experimental conditions, annealing and cooling rates.

Improving the stability of the prepared CuSe electrode by cleaning and using suitable redox couple was also achieved.

The dark and photo-current density versus potential plots were non-improved by annealing. Cell efficiency (η), fill factor (FF), and short-circuit current densities (J_{sc}) were enhanced by CuSe films annealing. The best CuSe films are naked and non-annealed CBD/ECD film which the photo J - V plots and cell efficiency was improved significantly.

The effect of coating the CuSe electrodes with MP/polysiloxane (1:4 ratios) was also studied. The (J_{sc}) values of coated CuSe films were significantly enhanced. The MP/polysiloxane coating introduces a charge-transfer mediator species that enhances current and electrode stability.

The PEC studies and characteristics showed that the 2 hr deposition time (prepared by CBD/ECD) gave films with more uniform, smoother, more homogeneous surfaces, higher conversion efficiency (14.6%) than other counterparts.

Chapter One

Introduction

Chapter One

Introduction

1.1 Solar Energy

In recent years the world has begun to change slowly from using non-renewable energy to renewable energy. Renewable energy sources are very important in helping us save of non-renewable resources like oil. The sun is the most important source of renewable energy available today.

Solar energy technology converts sunlight into heat, hot water, and electricity, for homes and industry. One of the alternative energy sources for decreasing the effects of global warming and climate change is solar energy. This environmentally friendly energy source is promising in combating the hazardous emissions of fossil fuels. Daily, the sun radiates a large amount of energy. It radiates additional energy in one second than the planet has used since time began. This energy comes from inside the sun itself [1-4].

The sun is a huge gas ball involving mostly hydrogen and helium atoms. It makes energy in its internal core in a process called nuclear fusion [1-4].

Solar energy is an important part of life. Humans use the daylight to provide vitamin D in their bodies. Animals and plants use solar light to produce important nutrients in their cells. The sun doesn't emit toxic gases into our environment. Importance of solar energy lies in the benefits, it does not cause pollution, can be used in remote areas where it is too expensive to extend the electricity, and solar energy is infinite. On the other hand, the oil is limited [5-6].

1.2 Semiconductors (SCs)

A semiconductor is material that has electrical conductivity in between a conductor (such as copper) and an insulator (such as glass). Semiconductors are used in modern electronics, as computers, radio, telephones, and solar cells. Semiconductor solar PV panels or PEC cells directly convert sunlight into electricity [7].

1.3 Popular Semiconductor Materials Used in Solar Cells

Many semiconductor materials can be used in solar cells, but the most common semiconductors can be categorized by groups; such as, Table (1.1) [8].

Table (1.1): Popular semiconductor materials used in solar cells.

Class	Example
Elements	Si and Ge
III-V Compounds	GaAs, GaP and InP
II-VI Compounds	CdS, CdSe and CdTe
Transition Metal Di-chalcogenides	MoSe ₂ and ZrS ₂
Ternary Compounds	CuInS ₂ and CdIn ₂ Se ₄
Oxide Semiconductors	TiO ₂ , WO ₃ and ZnO
Zinc Phosphides	ZnP ₂

1.4 Types of Semiconductors (SCs)

The properties of a solid material depend on the difference in energy between the valence band and the conduction band is called the energy band gap E_g [13-14]. Materials are classified according to their E_g into three types: Conductors (with overlapping between the valence and conduction bands and its E_g equal zero), insulators (that have E_g above ~ 4 eV), and semiconductors (with E_g in between), Figure (1.1) [15-16].

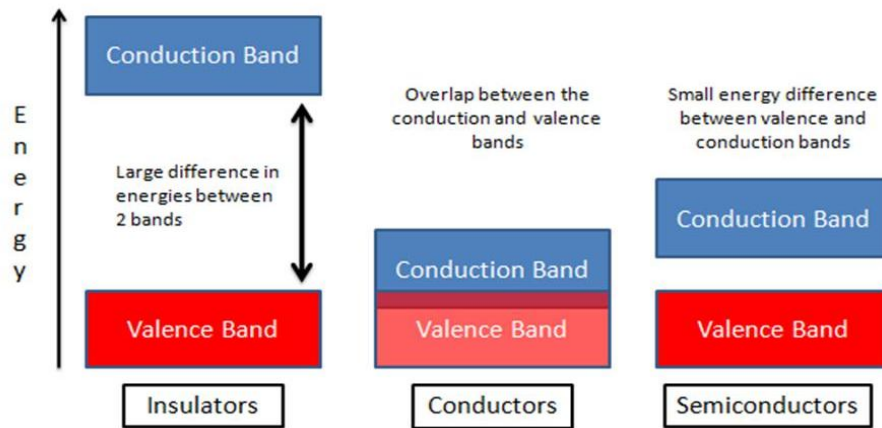


Figure (1.1): Band gap in conductor, semiconductor, and insulator [13].

Semiconductors are categorized into two groups: intrinsic and extrinsic

1.4.1 Intrinsic SCs

An intrinsic SC is a pure semiconductor without impurity (dopant) species present. When an electron gets enough energy, it moves to the conduction band and leaves a hole behind in the valence band, Figure (1.2). This method is termed (electron-hole pair creation). In intrinsic SC, since electrons and holes can be created in pairs at room temperature, relatively few electrons have enough thermal energy to jump. Therefore, intrinsic SC has only limited conductivity [9-12].

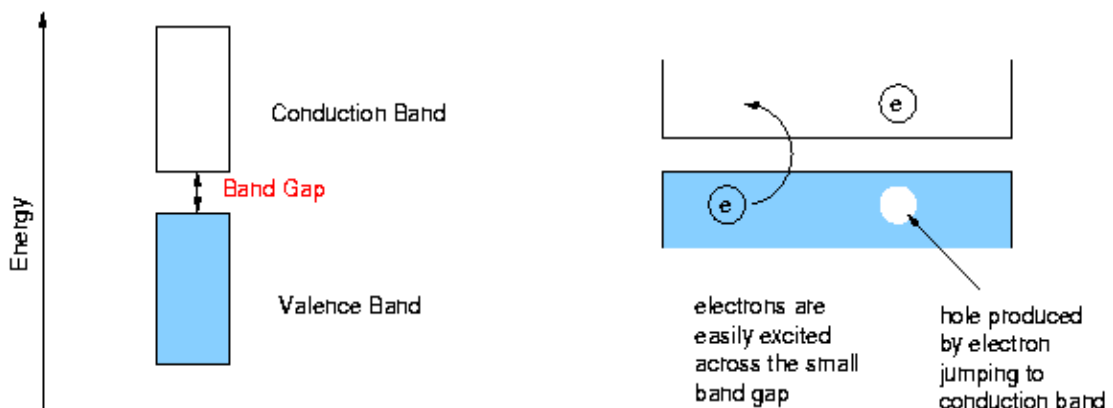


Figure (1.2): Schematic showing thermally excited electron in intrinsic semiconductor [9].

1.4.2 Extrinsic SCs

An extrinsic SC is a semiconductor that is doped. Doping involves adding impurity (dopant) to an intrinsic semiconductor, and improves conductivity of the wider band gap SC. Extrinsic semiconductors are divided into two types:

1.4.2.1 n-type

In this type the dopant atoms (impurity) are donor atoms. For silicon, phosphorus (P) or arsenic (As) can be used as donors, with five electrons in their outer shell. When these atoms are present, one of the electrons in this shell will simply jump to the conduction band. This type is called negative type semiconductor (n-type) [17-20].

1.4.2.2 p-type

In this type the dopant atoms (impurity) are acceptor atoms. For silicon, boron (B) or Aluminum (Al) can be used as acceptors, with three electrons in their outer shell. When these atoms are present in the silicon crystal, electrons in the silicon valence band will jump to the valence shell of one of the acceptor atoms. The name positive type (p-type) is suitable for these SCs [17-22].

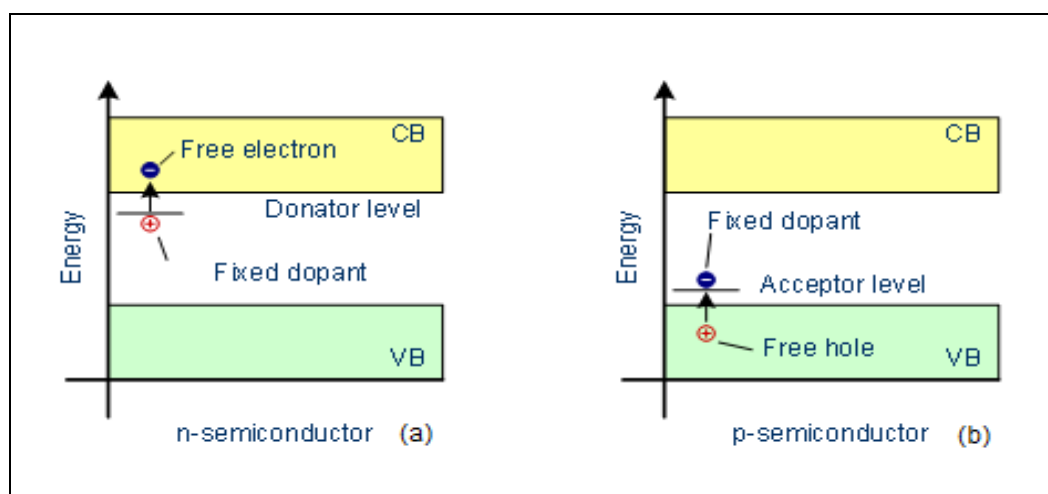


Figure (1.3): Dopant energy levels in n-type SC and p-type SC [21].

If the dopant energy level lies close to the conduction band, CB (the case of electron donor), then electrons will be thermally excited to CB. The SC is thus known as n-type. If the dopant energy level lies close to the valance band, VB (the case of electron acceptors), then electrons are captured from the VB leaving excess positive charge carrier holes. Figure (1.3) [17-22].

1.5 Fermi Level (E_F)

The Fermi level is an extremely important parameter for metal and semiconductor electrochemistry, because it is the property which is controlled by the externally applied potential. The Fermi level is the energy, at which the probability of an energy level being occupied by an electron is exactly 1/2 [23].

In metal the Fermi level in effect marks the division between occupied and empty levels. For semiconductors the Fermi level resides in the band gap forbidden region. For an intrinsic semiconductor the Fermi level is approximately midway between valance band and conduction band as shown in Figure (1.4 b). It shifts towards the conduction band for n-type SC as shown in Figure (1.4 a), while for p-type SC, it shifts towards the valance band edge, as show in Figure (1.4 c).

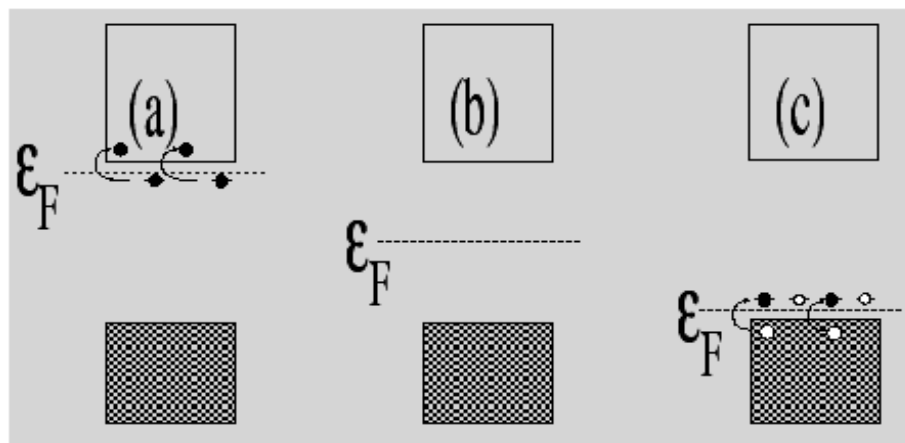


Figure (1.4): Fermi level diagram, a) n-type semiconductor, b) intrinsic semiconductor, c) p-type semiconductor [24].

1.6 Solar Energy Conversion Technologies

Solar energy may be used by using several active technologies to convert it into useful electric energy. Two main techniques are known:

1.6.1 Photovoltaic Devices (PV)

PV means conversion of solar energy into electricity (light-electricity), by photovoltaic effect. The photovoltaic effect means that the generation of a potential difference at the p-n junction of two different materials. p-n junctions could be homo-junctions (having same type of crystal) or hetero-junction (having two different types of crystals). PV has some advantages, in being environmentally friendly, having long life time up to 30 years and no used of fuels and water. On the other hand, it has some disadvantages as it cannot operate without light and large area needed [25-26].

1.6.2 Photoelectrochemical Solar Cell (PEC)

Like PV cells, a PEC cell may convert solar power into electricity. The operation relies on the contact potential between a semiconductor and a redox solution. Instead of the solid state p-n junction that is employed within the photo-voltaic (PV) solar cells, a SC electrolyte junction is used in PEC cells [9, 22].

In n-type SC, before equilibrium (contact) the E_F can stay higher than E_{redox} . Electrons can flow right down to E_{redox} . After connection between two phases the electrons transfer from the SC to electrolyte until the Fermi energy of the two phases become equal. As a result, E_F will be lowered, Figure (1.5). The space charge layer (SCL) is made as results of n-type

semiconductor electrolyte junction. For SC, the Fermi level (E_F) within the SC is set by chemical potential of electrons [27-29].

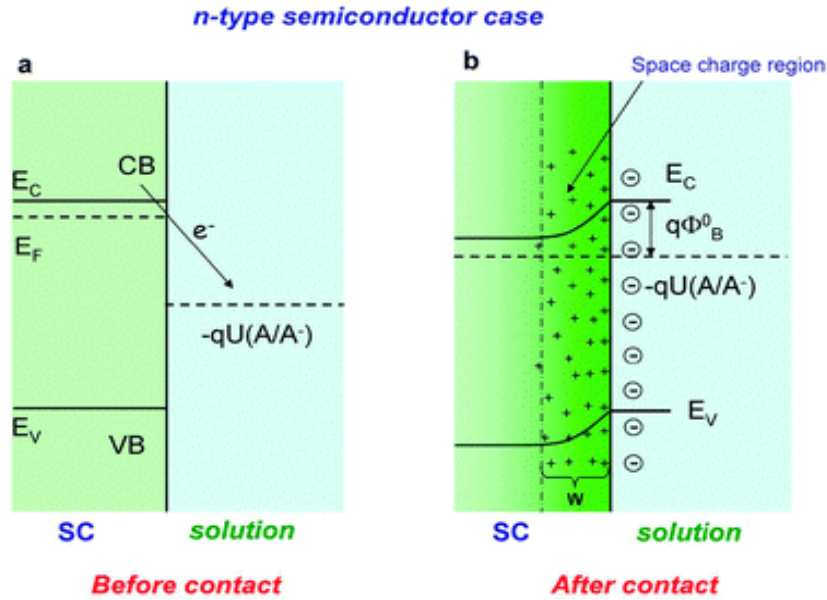


Figure (1.5): Energy level diagrams of an n-type SC before and after equilibrium with an electrolyte containing the redox couple A/A^- [30].

1.7 Dark Current in n-type PEC Systems

Dark current occurs in the dark. At equilibrium, there exists a potential barrier between the surface and the bulk of the electrode. The band bending in each valence and conduction bands represents this potential. Dark current occurs because electrons transfer from the n-type SC conduction band to the electrolyte across the interface, Figure (1.6). To realize this, a negative potential (ΔE) should be applied, to provide electrons with enough energy to overcome this barrier, consequently no SCL will exist (flat band), Figure (1.7). Therefore, dark current occurs in cases of flat band system [31-32].

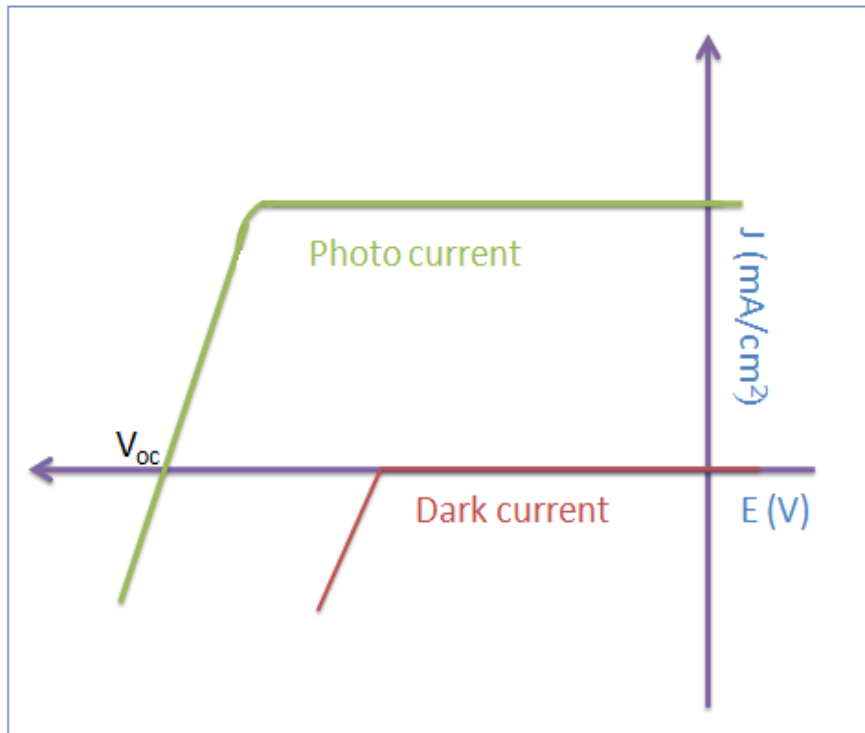


Figure (1.6): Dark and photocurrent voltammograms for an n-type SC [33].

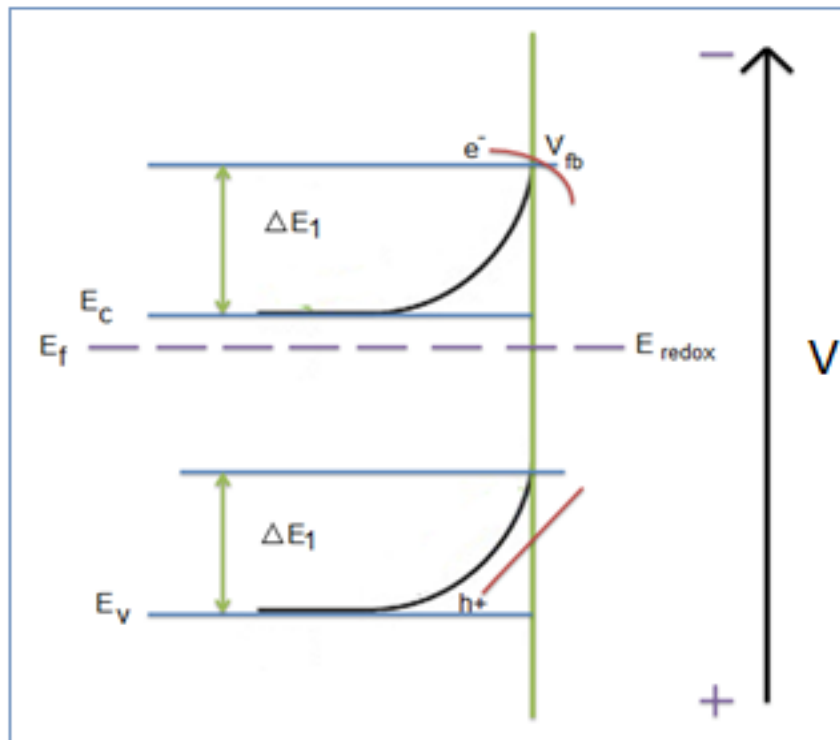


Figure (1.7): Dark current in n-type SC [33].

1.8 Photo Current in n-type PEC Systems

When light absorption generates excited electrons and holes, the majority carrier concentration changes relatively very little and therefore the minority carrier concentration is relatively greatly enhanced, Figure (1.8). Thus photo-effects are greatest when minority carriers dominate the electrode response. This occurs when the electrode is biased to create a depletion layer (with positive potential) and also the photo-generated minority carriers migrate towards the electrode/electrolyte interface [32].

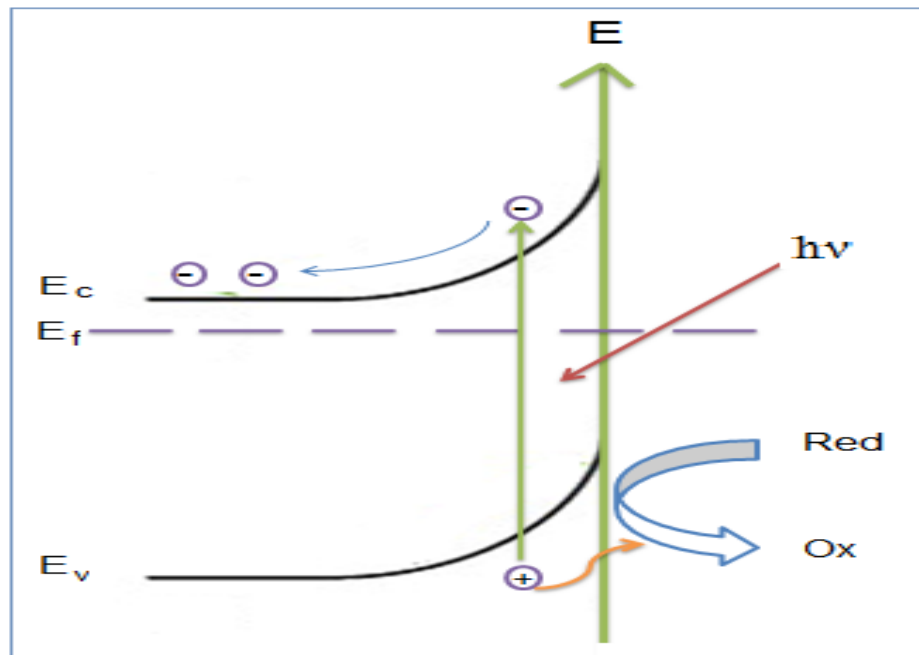


Figure (1.8): Photocurrent generation at n-type SC [33].

1.9 Thin Film Technology

Thin film technologies reduce the number of material needed in making the active material of solar cell. Thin films of metal compounds can be deposited onto glass, metal, plastics and other substrates by a variety of techniques, such as, electrochemical (ECD) and chemical bath deposition (CBD). These metal compounds are often encapsulated in building

materials which permit photovoltaic cells to use in some circumstances where glass coated solar modules wouldn't be allowable or would be impractical. The majority of thin film solar modules have significantly lower conversion efficiencies than mono-crystalline solar cells, but are cheaper to produce. Many semiconductors have been examined as thin film electrodes in solar cells, such as CuSe, CdSe, CdTe, CuS, ZnS, CdS and others [34-36].

1.10 Copper Selenide (CuSe)

CuSe is a semiconducting material, which has electrical and optical properties suitable for photovoltaic application. Copper selenide is a direct band gap p-type semiconductor with an energy gap value in the range 2.1 - 2.3 eV. This makes the material suitable to make solid/ liquid junction solar cells. CuSe exists in widely different crystal structures depending on the method of preparation. It normally exists in cubic structure and hexagonal structure [37-46], Figure (1.9).

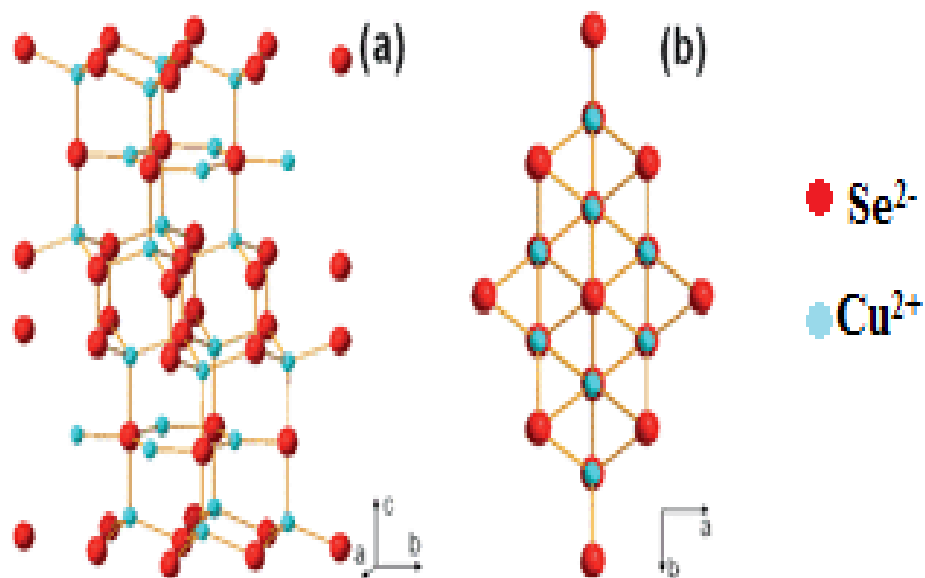


Figure (1.9): Crystal structure of CuSe, a) cubic structure, b) hexagonal structure [47].

Thin films of copper selenide are obtained by different techniques like vacuum evaporation, sputtering, molecular beam epitaxy, spray pyrolysis, electrochemical deposition and chemical bath deposition [48-50]. Electrochemical deposition is attractive because it is simple and non-costly. It is used in producing products for our everyday lives, appropriate for the preparation of large scale thin films and may control film thickness and morphology [51-52].

Chemical bath deposition is used to prepare thin films of certain materials on a substrate in a liquid bath containing suitable reagents at temperatures starting from room temperature to 100°C. It has been known as a method suitable for the preparation of large area thin films [53-54].

1.10.1 Some Basic Properties of Copper Selenide (CuSe)

Table (1.2): Some basic properties of copper selenide (CuSe).

Property	Value
Physical state	Crystalline solid
Molar mass	142.506 g mol ⁻¹
Color	Blue-black
Melting point	550°C (decomposes)
Density	6000 kg m ⁻³
Solubility	Insoluble in hot and cold water

1.11 Objectives

The main objective of this work is to prepare new type of nano-sized environmentally friendly CuSe film onto fluorine doped tin oxide (FTO)/glass for the purpose of PEC conversion of light to electricity. We look for an efficient and stable nano-film under PEC conditions.

The prepared a new type of CuSe film will be prepared by combined ECD and CBD techniques together. The ECD technique gives good contact

between the CuSe and the FTO surface. The CBD technique gives thick layers suitable enough for light-to-electricity conversion. Therefore, the CBD/ECD technique gives a CuSe/FTO/glass film that has good contact and suitable thickness. The final CuSe film, prepared by CBD/ECD, will be followed by annealing, to give higher conversion efficiency and better stability than either ECD, CBD films separately.

In this study, the work has two routes and two aims as well. Firstly, we will prepare CuSe films by ECD, CBD and CBD/ECD techniques, anneal them and compare between them. Secondly, we will coat CuSe films by a special electro-active matrix and study the effect on conversion efficiency and stability.

1.12 Hypothesis

It is often desirable to control the properties of semiconductors. Therefore, considerable efforts are being devoted to enhance PEC characteristics of the CuSe film. Our objective (described earlier) can be achieved based on the following assumptions:

- 1) The ECD method is expected to give good contact between the CuSe film and the FTO/glass surface.
- 2) The CBD method gives soundly thick layers suitable for light-to-electricity conversion.
- 3) The CBD/ECD technique is expected to give a film that has good contact and suitable thickness.
- 4) The CBD/ECD method may yield two different distinct layers within the produced CuSe film. Such a shortcoming may be avoided

by annealing the two layers together to give a homogeneous single layer film, with the preferred properties.

- 5) The final CuSe film, prepared by CBD/ECD, followed by annealing, is expected to give highest conversion efficiency and stability, as compared to earlier ECD and CBD films.
- 6) Coating CuSe thin films with polymeric matrices having electroactive species such as metalloporphyrine (MP) is assumed to enhance its PEC characteristics.

Chapter Two
Experimental

Chapter Two

Experimental

2.1 Materials

2.1.1 Chemicals

CuCl₂·2H₂O, CuSO₄·5H₂O and methanol were purchased in pure form from Riedel. HCl and Na₃C₆H₅O₇·2H₂O were purchased from Merck. NH₄Cl, and CH₂Cl₂ were purchased in pure form from Frutarom. Na₂SO₃ (purchased from Fluka) and Se powder (from Aldrich) were used as starting materials for Se²⁻ ions. FTO/glass substrates were purchased from Aldrich. All chemicals used were of analytical reagent grade and used without further purification.

2.1.2 FTO/Glass Substrate Cleaning Process

Highly conducting FTO/Glass (Aldrich) substrates were cleaned before CuSe film deposition process. FTO/Glass slides were used as substrates and they were cleaned well with detergent and distilled water, and were kept in HCl (10% v/v) for about 1 hour. The substrates were then washed first under running tap water to clean the acid off and then cleaned with acetone. They were then washed with running tap water and finally cleaned with distilled water and were dried in air prior to film deposition.

2.1.3 Preparation of Selenium Ions

At first, selenium element was used for the preparation of sodium selenosulfate (Na₂SeSO₃) by mixing the sodium sulphite (Na₂SO₃) with selenium powder and refluxed at 80°C for about 10 hours [55], Figure (2.1).

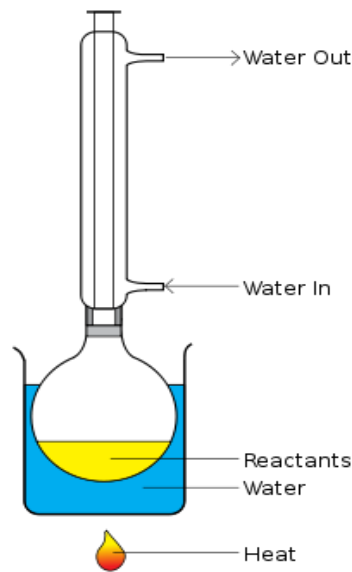


Figure (2.1): Preparing the (Na_2SeSO_3) by refluxing the reactant (2.000 g Se powder, 20.0 g of Na_2SO_3 , 100 mL distilled water) at 80°C for 10 hour [56].

To prepare 100 mL of Na_2SeSO_3 solution, Na_2SO_3 20.000 g was added to 100 mL of distilled water, then Se powder 2.000 g was added to the solution. After stirring for 10 hours at 80°C , fresh Na_2SeSO_3 solution was filtered and stored while tightly covered for electrochemical deposition processes.

2.2 Preparation of CuSe Films

Preparation techniques involved electrochemical deposition (ECD), followed by chemical bath deposition (CBD). Both techniques were combined together to yield CBD/ECD film.

2.2.1 Electrochemical Deposition (ECD) Technique

CuSe films were deposited on pre-cleaned FTO/Glass substrates using electrochemical deposition (ECD) technique, as shown in Figure (2.2)

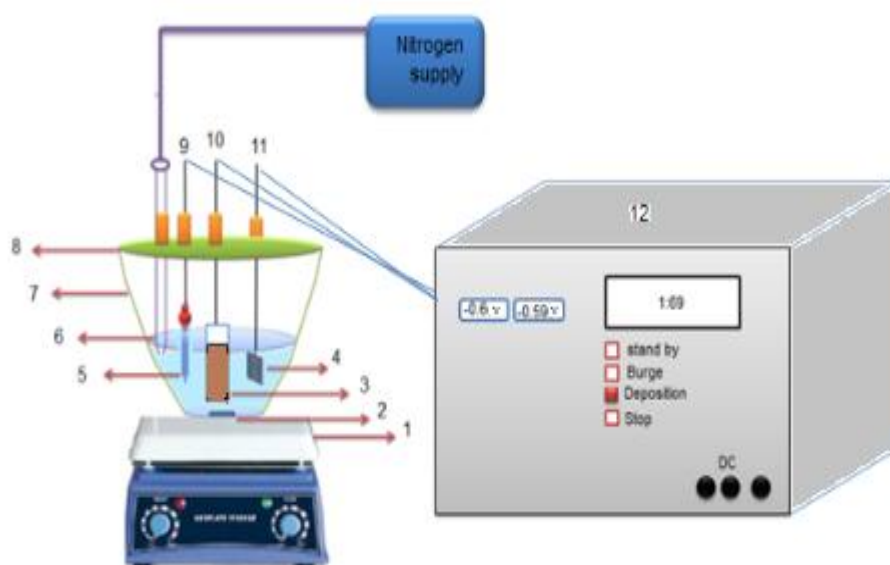


Figure (2.2): The experimental arrangement for the ECD-CuSe film. 1) magnetic stirrer plate, 2) magnetic stirrer, 3) CuSe thin film, 4) platinum electrode, 5) counter electrode (Ag/AgCl), 6) nitrogen, 7) ECD cell, 8) glass cover, 9,10,11) electrodes holders, 12) Potentiostat [46].

The experimental arrangement for CuSe film preparation is shown in Figure (2.2). It involved a solution containing Na_2SeSO_3 (20.0 mL, 0.008 M), $\text{CuCl}_2 \cdot 2\text{H}_2\text{O}$ (20.0 mL, 0.008 M) and NH_4Cl (10.0 mL, 3.0 M) which was used as supporting electrolyte. The deposition was done at room temperature; the nitrogen inlet was then above the solution and stirring was continued during deposition to avoid O_2 leakage. Deposition was performed by an applied potential of a DC stripping at fixed potential (-0.6V vs. Ag/AgCl) which is assumed to be the best working potential.

2.2.2 Chemical Bath Deposition (CBD) Technique

CuSe thin films were deposited on FTO/Glass substrates using CBD technique. The experimental setup for CuSe film preparation is shown in

Figure (2.3). It involves a chemical bath containing $\text{CuSO}_4 \cdot 5\text{H}_2\text{O}$ (4.0 mL, 0.5M), $\text{Na}_3\text{C}_6\text{H}_5\text{O}_7 \cdot 2\text{H}_2\text{O}$ (4.0 mL, 0.1M), Na_2SeSO_3 (4.0 mL, 0.25M), a few drops of dilute HCl and distilled water to make a total volume of (50.0 mL). The deposition was allowed to proceed at room temperature (20°C) for different time durations. The pH of the solution was about 6.5 and very slow stirring was continued during the deposition. After deposition, the glass slides were taken out from the bath, washed with distilled water and were dried in blowing air. To our knowledge, this procedure has not been used for CuSe films.

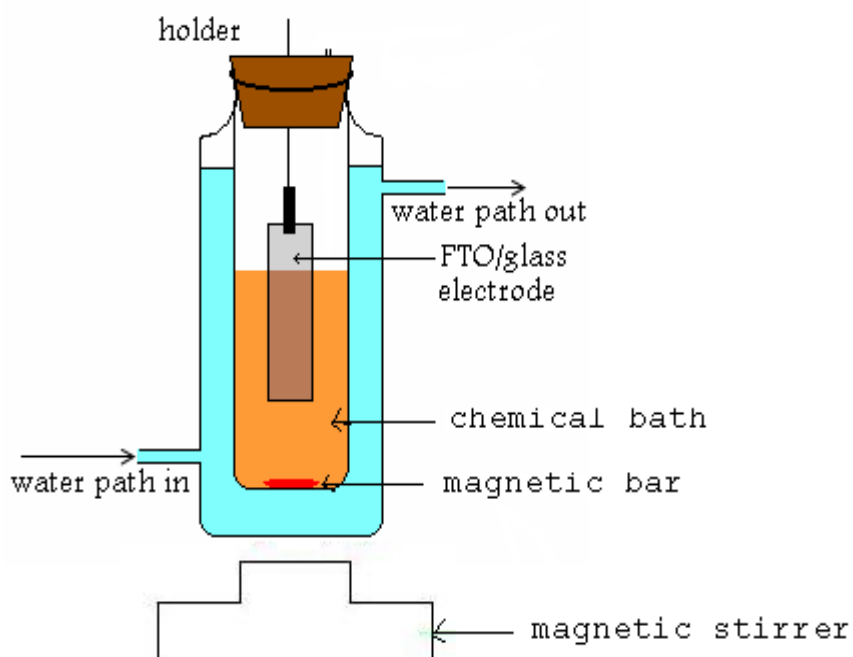


Figure (2.3): Experimental setup for solution growth of CBD-CuSe thin film.

2.2.3 Preparation of Electro-active (MP-Sil) Matrix

MP complex was prepared by vigorously refluxing tetrapyrrolyl porphyrin H_2TPyP (81.700 mg, 0.132 mmol) with excess manganese (II) sulphate (1.530 g, 0.91 mmol) in 60.0 mL of N,N-dimethylformamide (DMF) for

15 hours. The solution was concentrated by evaporating DMF under reduced pressure. Air was passed through the reaction mixture to oxidize Mn^{2+} to Mn^{3+} . The reaction mixture was then chromatographed over activated neutral alumina using DMF as an eluent. Eluate fractions with the characteristic absorption bands at 462, 569 and 620 nm were stored in the dark [57-61]. Commercial R.T.V. made polysiloxane paste (Sil) and tetra(-4-pyridyl)porphyrinatomanganese (III)sulfate (MP) complex, Figure (2.4), were used in preparing MP-Sil matrix to coat CuSe film electrode. MP solution was prepared by dissolving (0.010 g, 1.37×10^{-5} mol) in 1.0 mL methanol (CH_3OH). A dilute solution of Sil was prepared by dissolving 0.010 g of Sil in 20.0 mL dichloromethane (CH_2Cl_2). Three MP-Sil matrixes with different concentrations of MP were prepared by adding the MP solutions separately to the Sil solutions in 1:4 (v/v) ratios respectively. Figure (2.5 a) shows the Photoluminescence spectra of MP complex embedded in Sil polymer.

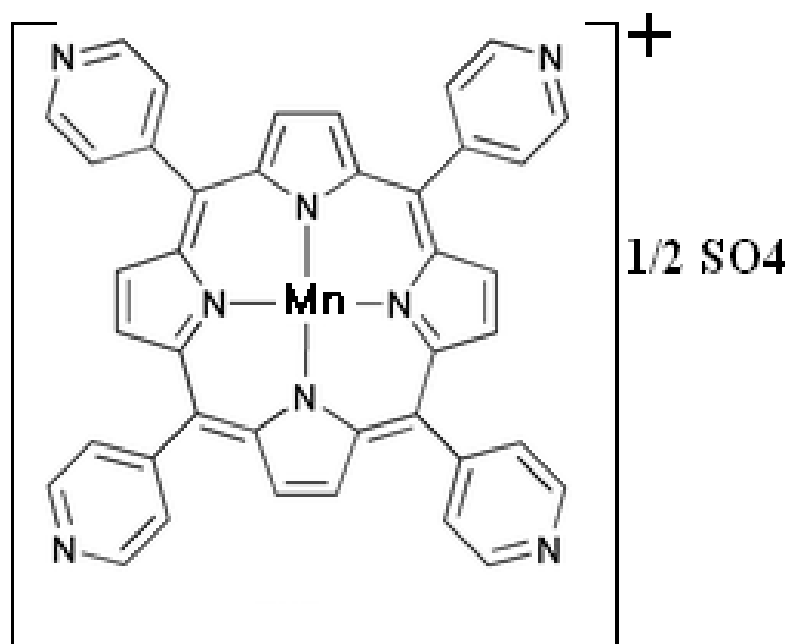


Figure (2.4): Tetra(-4-pyridyl)porphyrinatomanganese (III)sulfate (MP) complex.

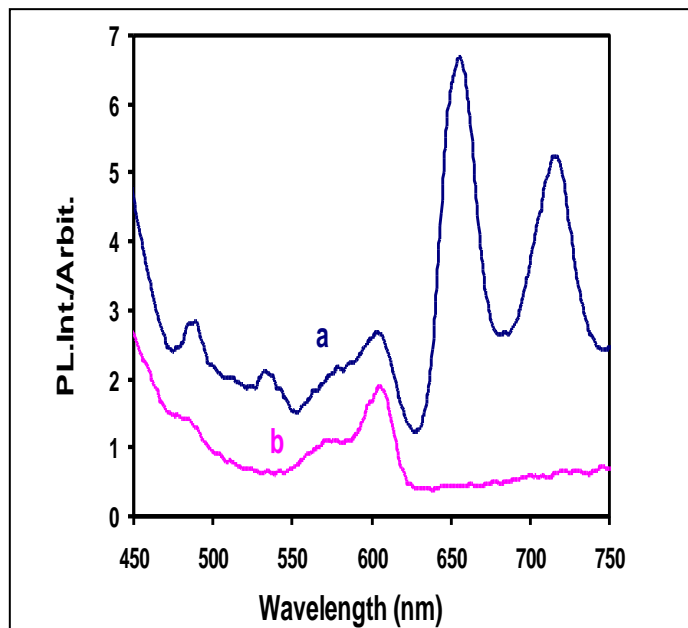


Figure (2.5): Photoluminescence spectra of: a) MP embedded in Sil polymer coated on FTO/Glass substrate, b) FTO/Glass substrate.

Figure (2.5 a), has bands at ~ 660 nm and ~ 720 nm (the same as the porphyrin). And it has bands at ~ 470 nm and ~ 540 nm, while the band at 540 nm confirms the presence of the Mn^{III} porphyrin species, the band at shorter wavelength 470 nm is attributed to the Mn^{II} porphyrin species [59, 63].

2.3 Modification of CuSe Thin Films

CuSe thin film modification involved annealing, cooling rate control and coating with (MP-Sil) matrix.

2.3.1 Annealing Process

Film annealing was fixed at temperature is 250°C , under N_2 atmosphere for 1 hour, by using a thermostated horizontal tube furnace. The prepared CuSe thin films were inserted in the middle of a glass cylinder for annealing. Figure (2.6), shows the annealing system.

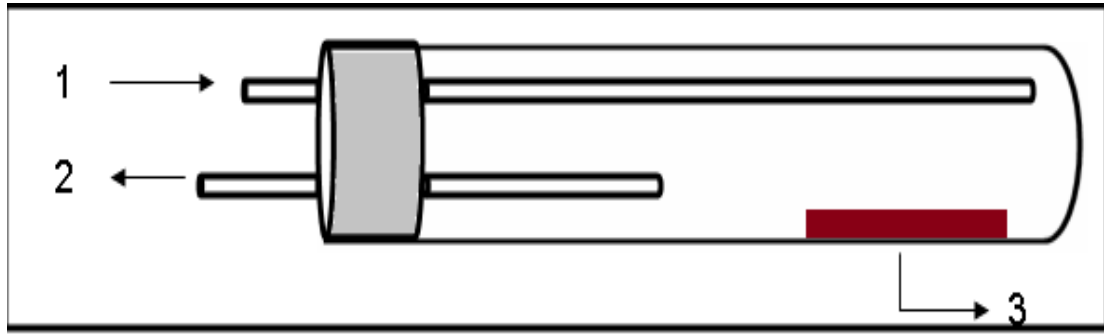


Figure (2.6): The annealing system, 1) nitrogen input, 2) nitrogen output, 3) CuSe thin film.

2.3.2 Cooling Process

2.3.2.1 Fast Cooling (Quenching)

After the films were annealed at 250°C for 1 hour, the furnace was shut down and the glass tube (which contained the CuSe thin films) was taken out of the tube furnace and left to cool to room temperature for 10-15 minutes under N₂ atmosphere.

2.3.2.2 Slow Cooling

After the films were annealed at 250°C for 1 hour, the furnace was shut down and left to cool slowly to room temperature under N₂ atmosphere. Slow cooling occurred in about 3 hours.

2.3.3 Coating with MP-Sil

CuSe thin films were coated by immersion in the (MP-Sil) solution for 3 seconds. The organic solvent mixture (CH₂Cl₂/ CH₃OH) was then allowed to evaporate off, leaving a transparent thin layer of (MP-Sil) matrices on the surfaces of CuSe thin films.

2.4 Film Characterization

2.4.1 Electronic Absorption Spectra

A Shimadzu UV-1601 spectrophotometer was used to measure solid state electronic absorption spectra for different thin films of CuSe. The wavelength of the incident photons was scanned in the range 200-800 nm.

2.4.2 Fluorescence Spectrometry

A Perkin-Elmer LS 50 luminescence spectrophotometer was used to measure the emission fluorescence spectra for different CuSe/FTO/Glass films. Emission photo luminescence spectra were measured to find the band gap of CuSe nano-particles using an excitation wavelength 383 nm. A cut-off filter (500 nm) was used to remove undesired reflected shorter wavelengths.

2.4.3 Atomic Force Microscopy (AFM)

The AFM measurements were done at Al-Quds University using a tapping mode-AFM system and the WSxM software designed by Nanotec Electronica (Madrid, Spain) to obtain and analyze the Data. Soft, non-conductive, rectangular, commercial Si_3N_4 cantilevers (NSG10, NT MDT Co., LTD.) with spring constants of 5.5-22.5 N/m and resonance frequencies from 190-325 kHz were employed. AFM was used to study the surface morphology of the prepared CuSe thin films.

2.4.4 X-Ray Diffraction (XRD)

XRD technique was used to give information about the crystallographic structure and chemical composition of our CuSe thin films prepared by different techniques. XRD measurements were kindly conducted in Jung-

Eun KIM, ISAA Environment Consulting Co., Ltd., 329-5, Chilgeum-Dong, Chungju-City, Chungbuk, 380-220 South Korea.

2.5 Photoelectrochemical Cell (PEC)

The PEC cell consisted of CuSe thin film electrode (as working electrode), and a platinum counter electrode connected to an internal reference electrode, all in electrolytic solution. $\text{K}_3\text{Fe}(\text{CN})_6/\text{K}_4\text{Fe}(\text{CN})_6/\text{LiClO}_4$ solution was used in this experiment as a redox couple (0.10 M $\text{K}_3\text{Fe}(\text{CN})_6$, 0.10 M $\text{K}_4\text{Fe}(\text{CN})_6$, 0.10 M LiClO_4). The solution was stirred at the beginning, but stirring was stopped as the PEC experiment started. High purity N_2 gas (99.999%) was bubbled through the solution for 5-10 minutes before each experiment, but was then kept to flow above the solution during the experiment to minimize air contamination.

A 50 Watt halogen spot lamp was used for illumination. The lamp has an intense converge of wide spectral range between 450-800 nm with high stability. The lamp was placed at a defined distance from the working electrode. The illumination power on the electrode was about (0.00196 W/cm^2) calculated by tungsten-halogen lamp spectrum.

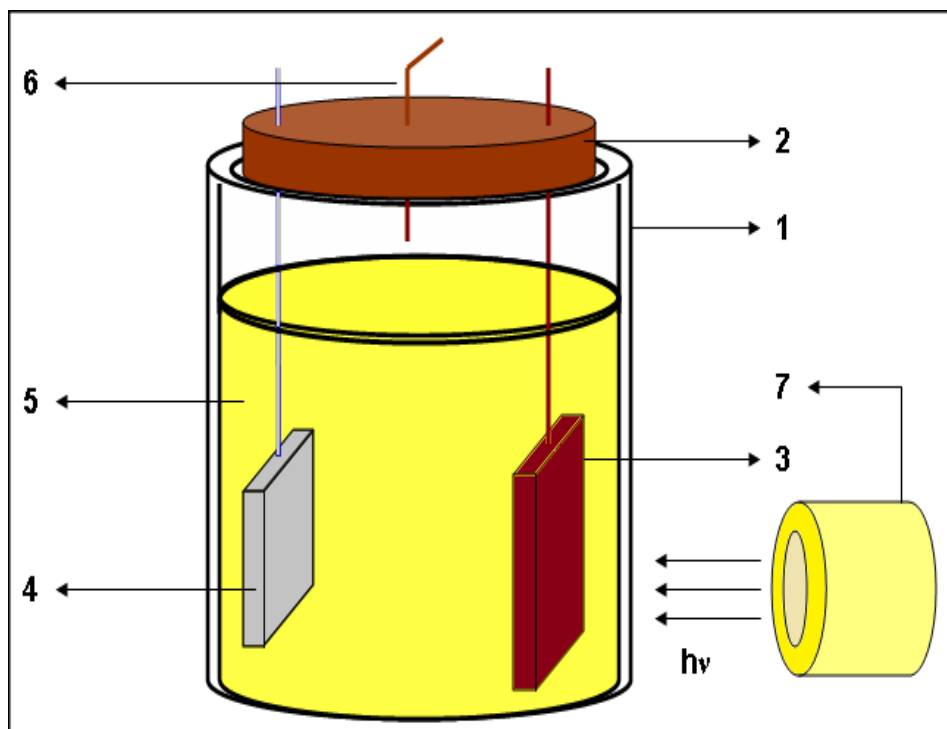


Figure (2.7): Two-electrode photo-electrochemical cell (PEC). 1) Beaker, 2) rubber seal, 3) CuSe working electrode, 4) platinum counter electrode and internal reference electrode 5) electrolytic solution, 6) nitrogen, 7) light source [57].

2.6 Current Density-Potential Plots

Plots of current vs. voltage (I - V) plots were measured using a computer controlled Princeton Applied Research (PAR) Model 263A Potentiostat/Galvanostat. The measured current (I) was converted into current density (J), by dividing the measured electric current (I) by area of the illuminated electrode (A).

The dark current experiments were conducted under complete dark using thick blanket cover. The photocurrent experiments were conducted, using the 50 Watt halogen spot lamp as described above. Experimental setup mentioned above, Figure (2.7), was used at room temperature under N_2

atmosphere, using $\text{K}_3\text{Fe}(\text{CN})_6$ (0.10M)/ $\text{K}_4\text{Fe}(\text{CN})_6$ (0.10M)/ LiClO_4 (0.10M) as redox couple.

The Potentiostat/Galvanostat had three electrodes. The counter electrode and the reference electrode were connected to the Platinum electrode, with internal reference used. The semiconductor electrode was incorporated as working electrode. The internal reference potential was calibrated vs. an Ag/AgCl reference, as shown in Figure (2.8).

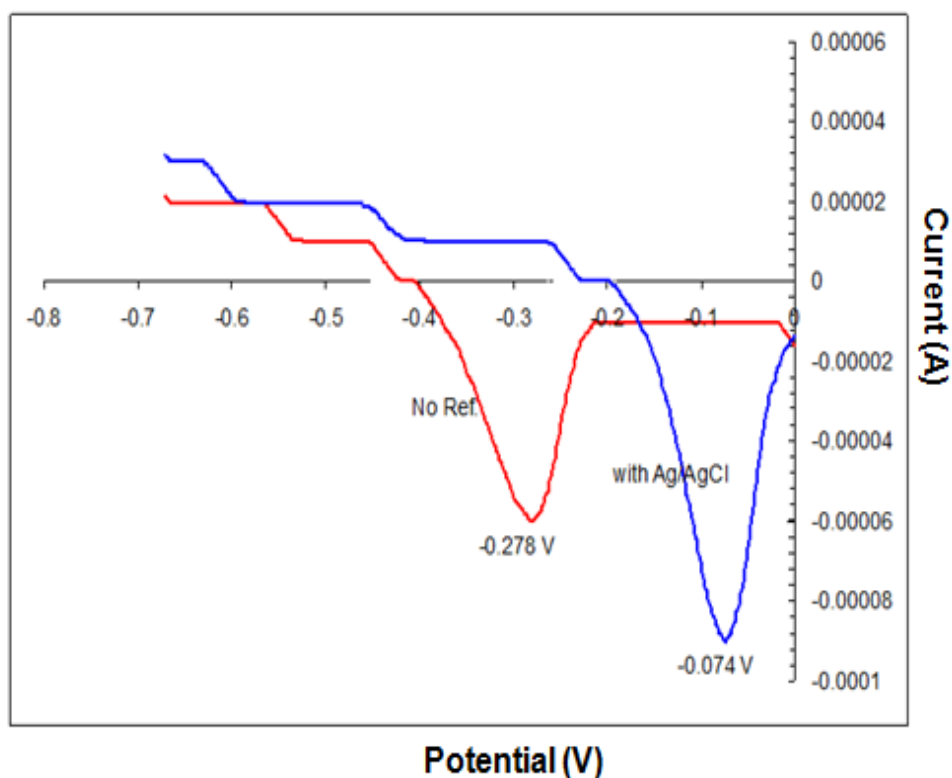


Figure (2.8): Reduction of copper ion in HCl electrolyte solution, on glassy carbon electrode.

As shown in the Figure (2.8), the internal reference electrode showed 0.204 V more negative than Ag/AgCl reference. This means that the internal reference of Potntiostat is equivalent to that of SHE. Thus all J - V plots

measured in this work are presented with reference to SHE, unless otherwise stated.

2.7 Electrode Stability Testing

A polarographic analyzer (Pol 150) and a polarographic stand (MDE 150) were used to study the electrode stability under PEC conditions as described formerly. The values of short circuit current (J_{sc}) were measured versus time by keeping the electrode under steady illumination (0.00196 W/cm^2) at applied potential 0.00 V (Ag/AgCl). The values of short circuit current density (J_{sc}) were obtained by dividing values of (I_{sc}) by the measured electrode area immersed in solution. All measurements were made at room temperature, under nitrogen atmosphere using $\text{K}_3\text{Fe}(\text{CN})_6/\text{K}_4\text{Fe}(\text{CN})_6/\text{LiClO}_4$ as redox couple.

Chapter Three

Results

Chapter Three

Results

CuSe thin films were prepared using electrochemical deposition (ECD), chemical bath deposition (CBD) and combined CBD/ECD preparation techniques. Different parameters were controlled to enhance the prepared films including such as deposition times (2, 4, and 6 hrs), annealing (at 250°C under nitrogen atmosphere for 1hr) and cooling rate (fast or slow cooling).

The main purpose of this work was to prepare CBD/ECD CuSe film electrodes with the highest PEC efficiency and stability. Effects of deposition time, annealing, cooling rate, and coating with MP-Sil matrix were all studied for different films, using AFM, XRD, PL spectra, electronic absorption spectra, *J-V* plots, efficiency, and stability testing. The CBD and CBD/ECD CuSe film electrodes deposited in 2 hrs, annealed at 250°C for 1 hr were studied after coating with MP-Sil matrix.

Part I

Naked CuSe Thin Film Electrodes

Characteristics of different prepared CuSe thin films, such as, electronic absorption, photoluminescence, AFM and XRD spectra are shown below.

3.1 Electronic Absorption Spectra

3.1.1 Effect of deposition time on CuSe thin film electrodes

The effect of deposition times on ECD, CBD and CBD/ECD-CuSe thin films was studied.

3.1.1.1 Effect of deposition time on ECD-CuSe thin film electrodes

In earlier studies, AL-Kerm prepared a new type of CuSe film by ECD technique and studied the effect of deposition time (5, 10 and 15 min) on their PEC characteristics. The 15 min deposition time gave best results [46]. The electronic absorption spectra for the CuSe thin films prepared by ECD here were investigated, Figure (3.1). The electronic absorption spectra results were consistent with Photoluminescence spectra results, with band gap value ~ 2.10 eV.

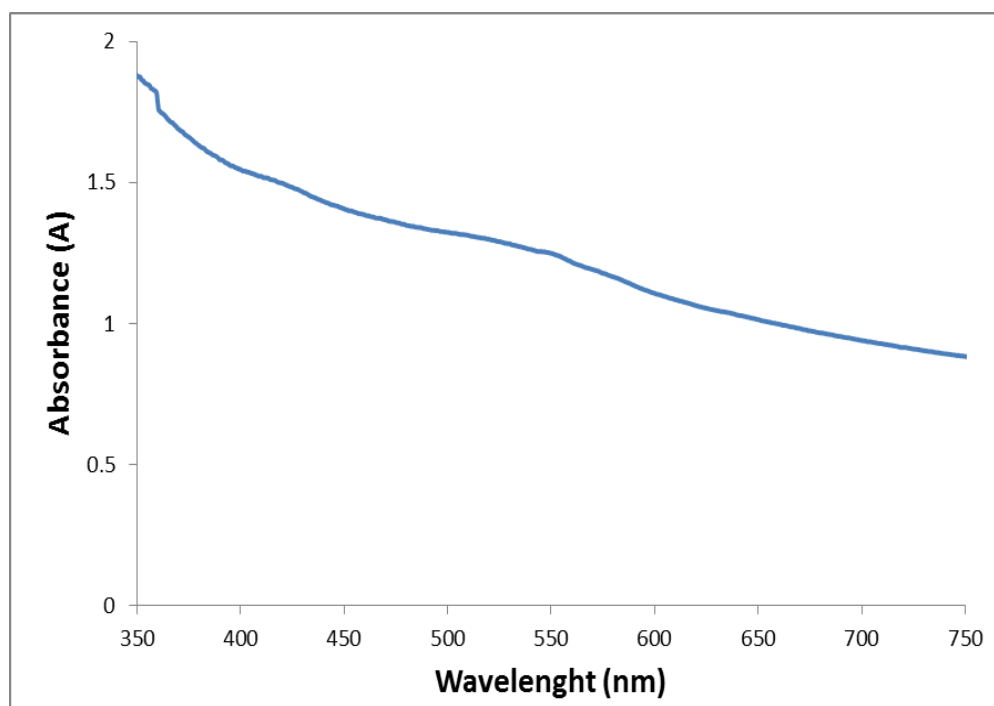


Figure (3.1): Electronic absorption spectra for ECD of the CuSe thin films deposited in 15 min.

3.1.1.2 Effect of deposition time on CBD-CuSe thin film electrodes

The effect of deposition times (2, 4 and 6 hrs) on the CuSe thin film spectra was studied. Electronic absorption spectra for the CuSe thin film electrodes prepared in different deposition times (2, 4 and 6 hrs.) were investigated,

Figure (3.2). The electronic absorption spectra results were consistent with Photoluminescence spectra results, with band gap value ~ 2.17 eV. Better absorption was observed for film deposited in 6 hours, due to its thickness.

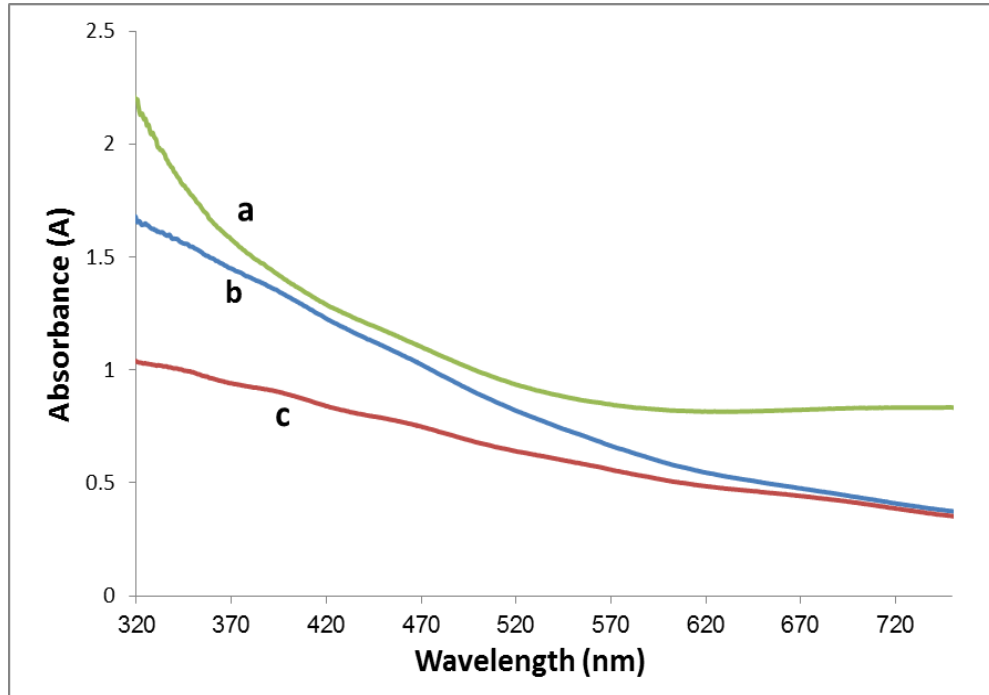


Figure (3.2): Electronic absorption spectra for CBD of CuSe thin films, deposited in different times, a) 2 hr, b) 4 hr and c) 6 hr.

3.1.1.3 Effect of deposition time on CBD/ECD-CuSe thin film electrodes

The electronic absorption spectra for the CuSe thin films prepared by CBD/ECD were investigated, Figure (3.3). The prepared films showed different absorption edge values, with band gap values in range of 2.00-2.25 eV. The band gap energy controls the light absorption characteristics of the semiconductors. A useful relationship between λ_{bg} and E_{bg} is [33]:

$$\lambda_{bg} = 1240/E_{bg}$$

Where λ_{bg} has units of nanometers (nm), while E_{bg} has units of electronvolts (eV). The film deposited in 6 hours shows absorption edge value about ~640 nm, with band gap ~2.00 eV, the film deposited in 4 hours shows absorption edge value about ~600 nm, with band gap ~2.06 eV, and the film deposited in 2 hours shows absorption edge value at about ~570 nm, with band gap ~2.17 eV. The film deposited in 6 hours shows Better absorption than others, due to it is higher thickness.

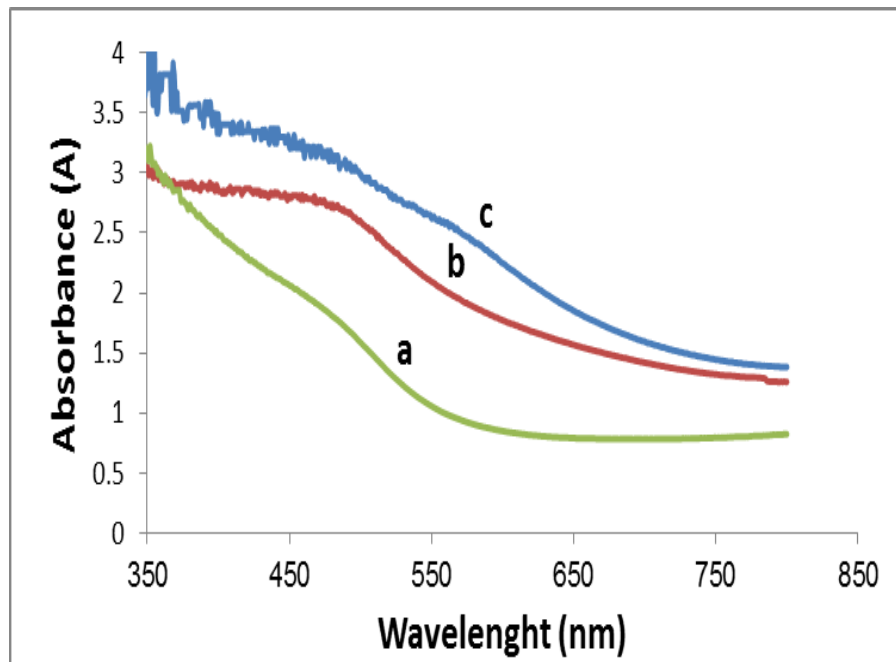


Figure (3.3): Electronic absorption spectra for the CBD/ECD of CuSe thin films, deposited in different times, a) 2 hr, b) 4 hr and c) 6 hr.

3.1.1.4 Comparison of CuSe thin film electrodes prepared by different techniques

The electronic absorption spectra for the CuSe thin films prepared by different techniques (ECD, CBD and CBD/ECD) were investigated, Figure (3.4). The prepared films show different absorption edges, with band gap values were in the range of 2.00- 2.25 eV. The film prepared by CBD/ECD

for 2 hr was consistent with Photoluminescence spectra results, with band gap ~ 2.17 eV, the film prepared by CBD for 2 hr was consistent with Photoluminescence spectra results, with band gap ~ 2.17 eV, and the film prepared by ECD for 15 min was consistent with Photoluminescence spectra results, with band gap ~ 2.10 eV.

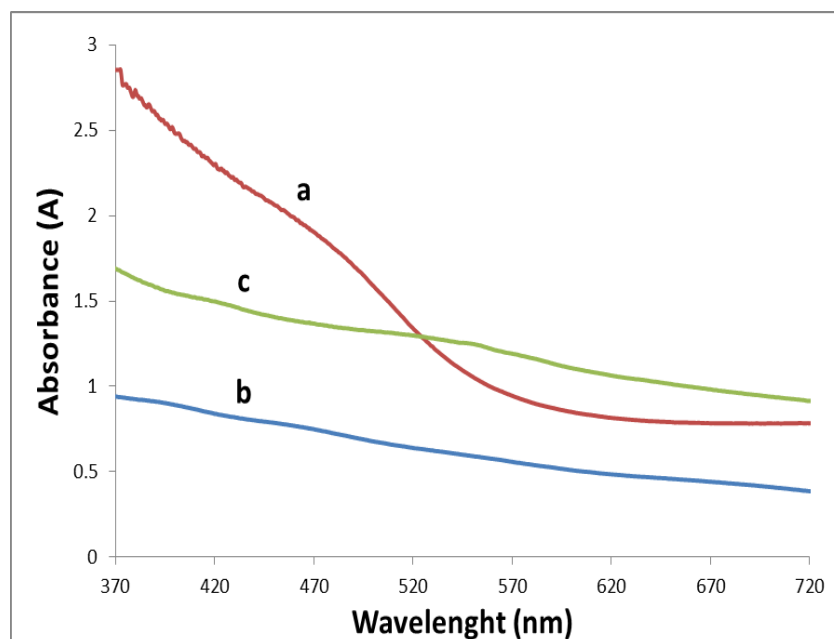


Figure (3.4): Electronic absorption spectra for CBD of the CuSe thin films, deposited in different techniques, a) CBD/ECD for 2 hr, b) CBD for 2 hr and c) ECD for 15 min.

3.1.2 Effect of cooling rate on the CuSe thin film electrodes

Effect of cooling rate (slow and fast cooling) on the CuSe thin film electrodes and annealed at temperature 250°C under nitrogen for 1 hr has been studied.

3.1.2.1 Effect of cooling rate on the CBD-CuSe thin film electrodes

Effect of cooling rate (slow and fast cooling) on the CBD-CuSe thin film electrodes deposited in 2 hrs and annealed at 250°C under nitrogen for 1 hr was studied. The results are shown below.

The electronic absorption spectra for the CuSe thin film electrodes deposited in 2 hrs, annealed at 250°C for 1 hr, cooled to room temperature by either fast or slow cooling were investigated, Figure (3.5). Absorption edge of ~ 570 nm was observed for both slowly and quickly cooled films. The quickly cooled film exhibit better absorption than slowly cooled counterpart.

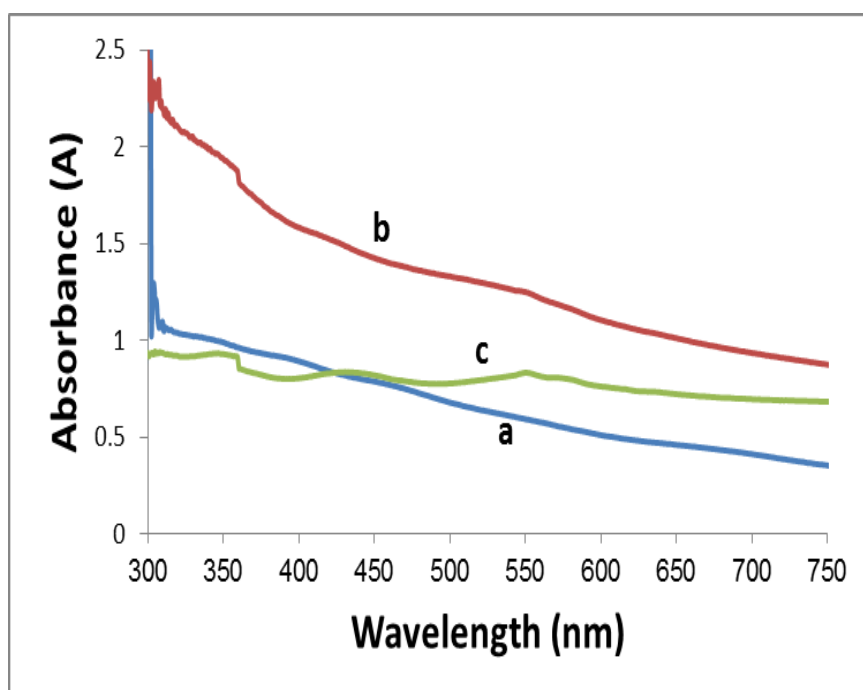


Figure (3.5): Electronic absorption spectra for CBD of the CuSe thin films deposited in 2 hr, a) non-annealed, b) annealed at 250°C for 1 hr, quickly cooled and c) annealed at 250°C for 1 hr, slowly cooled.

3.1.2.2 Effect of cooling rate on the CBD/ECD-CuSe thin film electrodes

The electronic absorption spectra for the CuSe thin films deposited in 2 hrs, annealed at 250°C for 1 hr, and cooled to room temperature by either slow or fast cooling were investigated, Figure (3.6). Absorption edge of ~570 nm was observed for both slowly and quickly cooled films. The

slowly cooled film exhibits better absorption than the quickly cooled counterpart. The non-annealed film shows better absorption than annealed film.

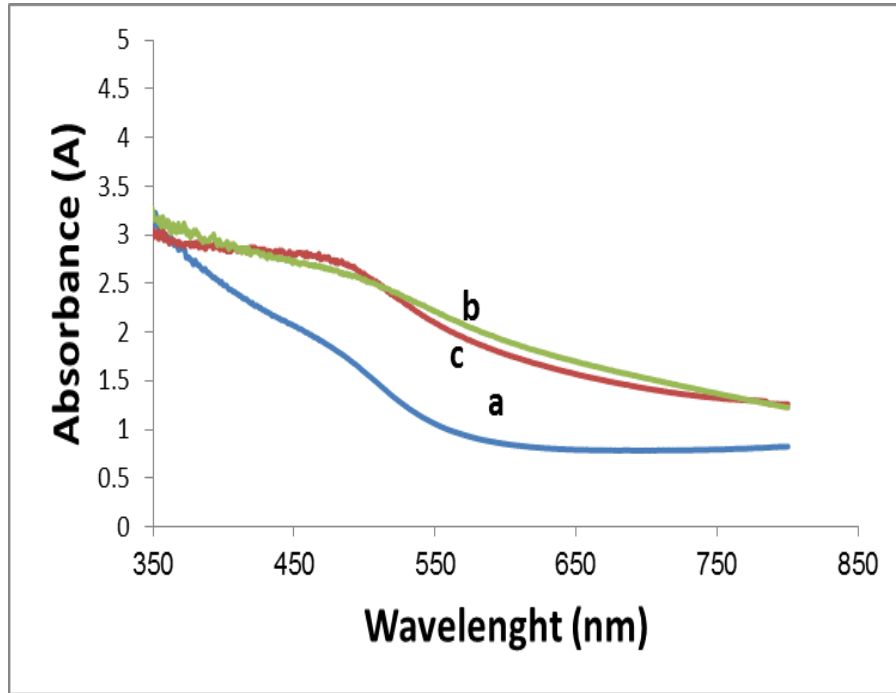


Figure (3.6): Electronic absorption spectra for CBD/ECD of the CuSe thin films deposited in 2 hr, a) non-annealed, b) annealed at 250°C for 1 hr, quickly cooled, and c) annealed at 250°C for 1 hr, slowly cooled.

CuSe thin films were prepared using different techniques (ECD, CBD and CBD/ECD). Effects of deposition time (2, 4, and 6 hr), annealing (at 250°C for 1 hr) and cooling rate (fast and slow cooling) were all studied for different films, using electronic absorption spectra.

3.2 Photoluminescence Spectra (PL)

3.2.1 Effect of deposition time on CuSe thin film electrodes

The effect of deposition time on ECD, CBD and CBD/ECD-CuSe thin films was studied.

3.2.1.1 Effect of deposition time on ECD-CuSe thin film electrodes

Photoluminescence spectra for CuSe thin film electrode, deposited by ECD in 15 min, were investigated, Figure (3.7). The systems were excited at wavelength 383 nm. The Figure shows many peaks, but the highest intensities appeared at wavelength ~590 nm, with band gap ~2.10 eV.

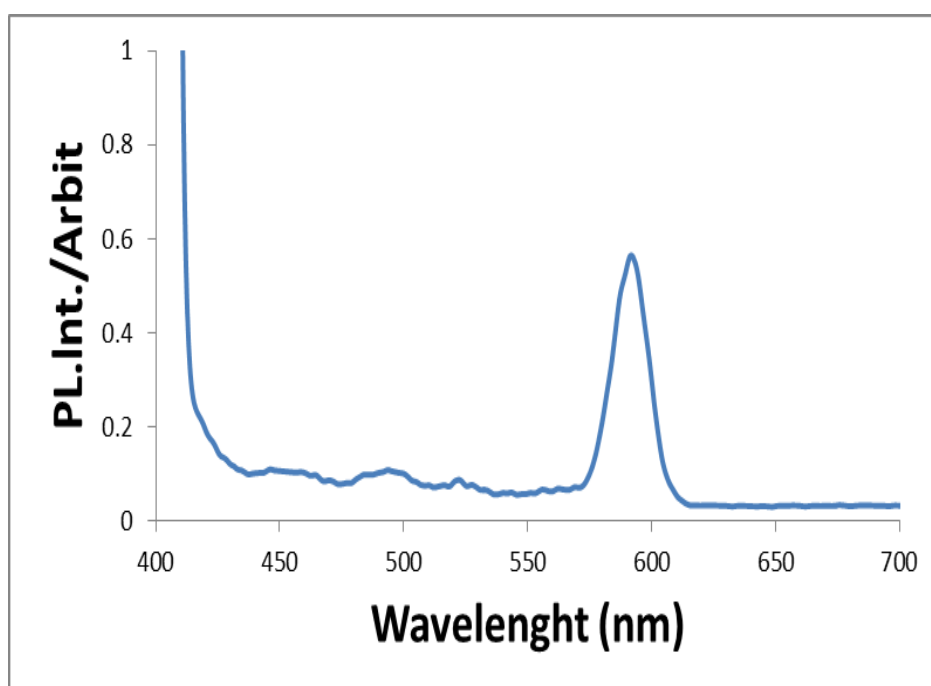


Figure (3.7): Photoluminescence spectra for ECD of CuSe thin film, deposited in 15 min.

3.2.1.2 Effect of deposition time on CBD-CuSe thin film electrodes

Photoluminescence spectra for CuSe thin film electrodes, deposited by CBD in different deposition times (2, 4 and 6 hrs.), were investigated, Figure (3.8). The systems were excited at wavelength 383 nm. The Figure shows many peaks, but the highest intensities appeared at wavelengths ~590 nm, and the band gap value was similar to that obtained from the electronic absorption spectra, $1240/590 = 2.10$ eV. All films prepared in

different deposition times show nearly same band gap values with different intensities. The intensity values for CuSe films prepared by CBD show, the film prepared in 2 hr gave higher intensity, then the film prepared in 4 hr. Finally, the film prepared in 6 hr gave lowest intensity.

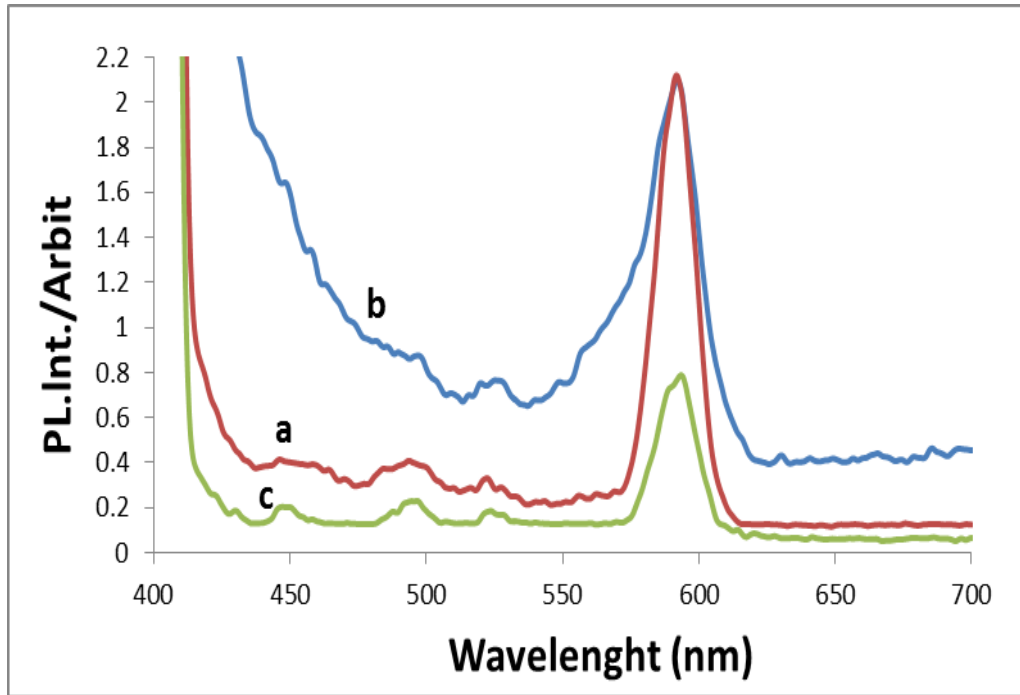


Figure (3.8): Photoluminescence spectra for CBD of CuSe thin films, deposited in different times, a) 2 hr, b) 4 hr and c) 6 hr.

3.2.1.3 Effect of deposition time on the CBD/ECD-CuSe thin film electrodes

The photoluminescence spectra for CuSe thin films prepared by CBD/ECD were investigated, Figure (3.9). The systems were excited at wavelength 383 nm. The Figure shows many peaks, but the highest intensities appeared at wavelength ~ 590 nm, showing a band gap $1240/590 = 2.10$ eV, which is consistent with electronic absorption spectra values. All films prepared in different deposition times show nearly same band gap with different

intensities. The intensity values for CuSe films prepared by CBD/ECD show that the film prepared in 2 hr gave higher intensity than the film prepared in 4 hr. Finally, the film prepared in 6 hr gave lowest intensity.

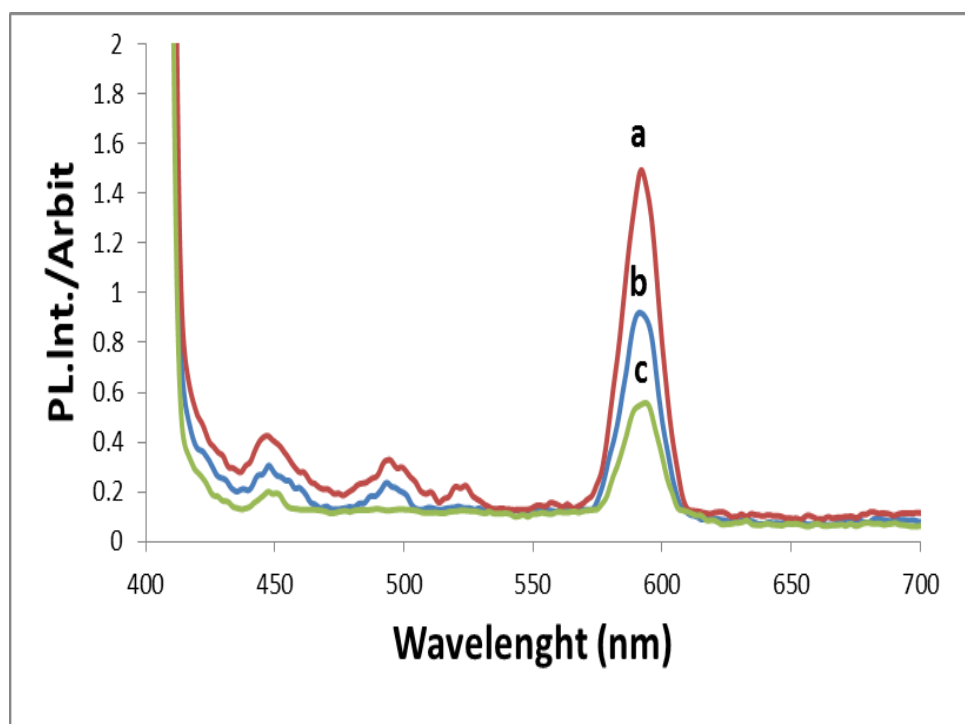


Figure (3.9): Photoluminescence spectra for CBD/ECD of CuSe thin films, deposited in different times, a) 2 hr, b) 4 hr and c) 6 hr.

3.2.1.4 Comparison of CuSe thin film electrodes prepared by different techniques

The photoluminescence spectra for CuSe thin films prepared by different techniques were investigated, Figure (3.10). The systems were excited at wavelength 383 nm. The Figure shows many peaks, but the highest intensities appeared at wavelength ~ 590 nm, showing a band gap $1240/590 = 2.10$ eV, which is consistent with electronic absorption spectra values. The film prepared by CBD for 2 hrs shows higher intensity than the other

films, and the film prepared by CBD/ECD for 2 hrs shows higher intensity than the film prepared by ECD for 15 min.

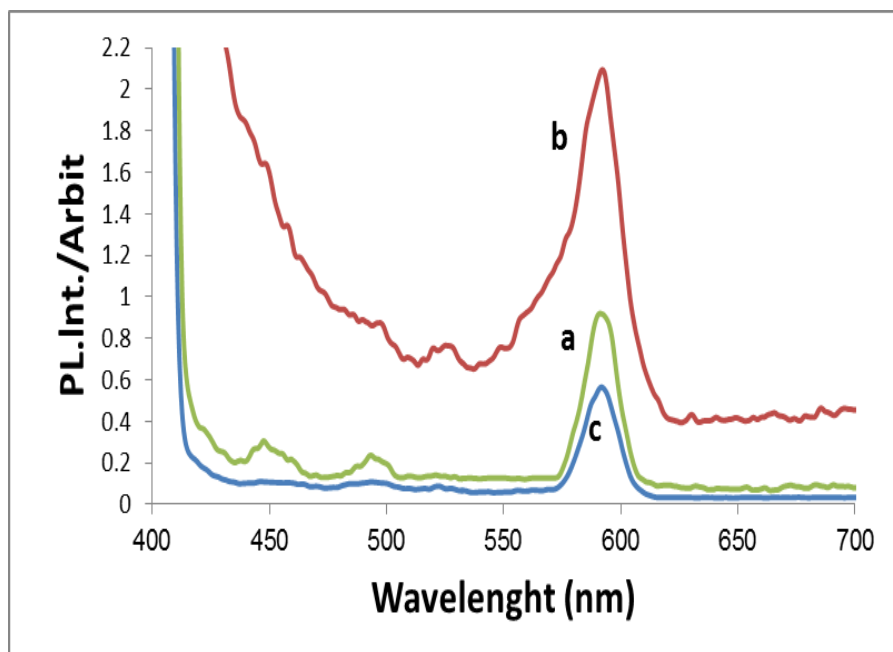


Figure (3.10): Photoluminescence spectra for CBD of CuSe thin films, deposited in different techniques, a) CBD/ECD for 2 hr, b) CBD for 2 hr, and c) ECD for 15 min.

3.2.2 Effect of cooling rate on CuSe thin film electrodes

Effect of cooling rate (slow and fast cooling) on the CuSe thin film electrodes and annealed at temperature 250°C under nitrogen for 1 hr has been studied.

3.2.2.1 Effect of cooling rate on the CBD-CuSe thin film electrodes

The photoluminescence spectra for CuSe thin films deposited in 2 hrs, annealed at 250°C for 1 hr, and cooled to room temperature by either slow or fast cooling, were investigated, Figure (3.11). The systems were excited at wavelength 383 nm. The Figure shows many peaks for each film, but the highest intensity appeared at wavelength ~590 nm, showing a band gap

$1240/590 = 2.10$ eV. The Figure shows that the non-annealed film exhibited higher PL intensity than annealed films. The film annealed at 250°C for 1 hr with fast cooling shows higher intensity than the film annealed at 250°C for 1 hr with slow cooling.

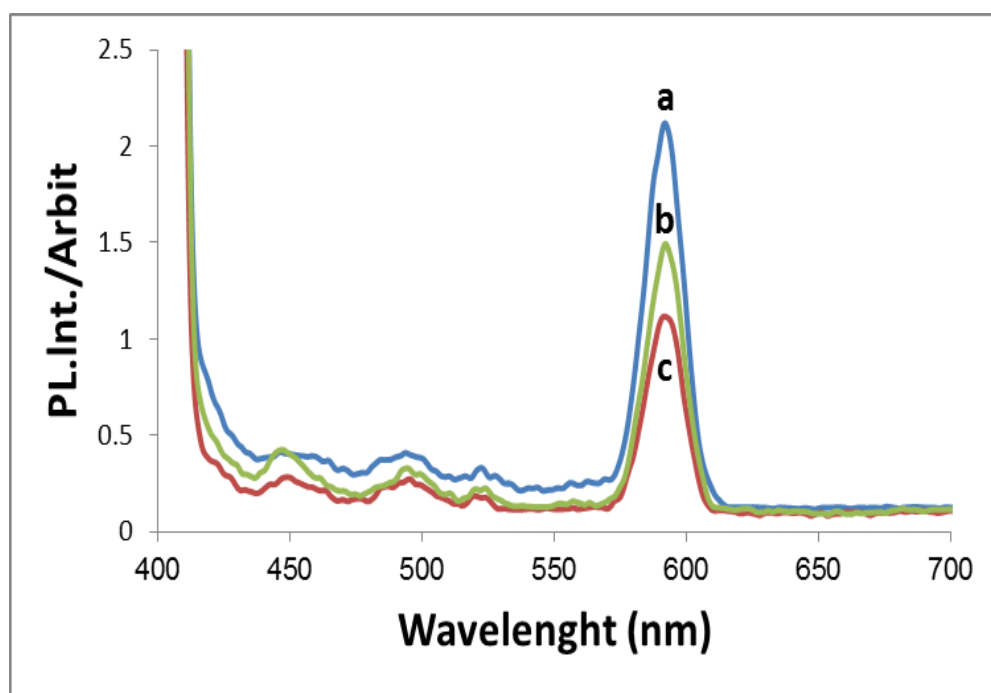


Figure (3.11): Photoluminescence spectra for CBD of CuSe thin films deposited in 2 hr: a) non-annealed, b) annealed at 250°C , for 1 hr, quickly cooled and c) annealed at 250°C , for 1 hr, slowly cooled.

3.2.2.2 Effect of cooling rate on CBD/ECD-CuSe thin film electrodes

The photoluminescence spectra for CuSe thin films deposited in 2 hrs, annealed at 250°C for 1 hr, and cooled to room temperature by either slow or fast cooling were investigated, Figure (3.12). The systems were excited at wavelength 383 nm. The Figure shows many peaks, but the highest intensities appeared at wavelength ~ 590 nm, showing a band gap $1240/590$

= 2.10 eV. The non-annealed film shows higher intensity than the annealed films. The film annealed at 250°C for 1 hr with fast cooling shows slightly higher intensity than the film annealed at 250°C for 1 hr with slow cooling.

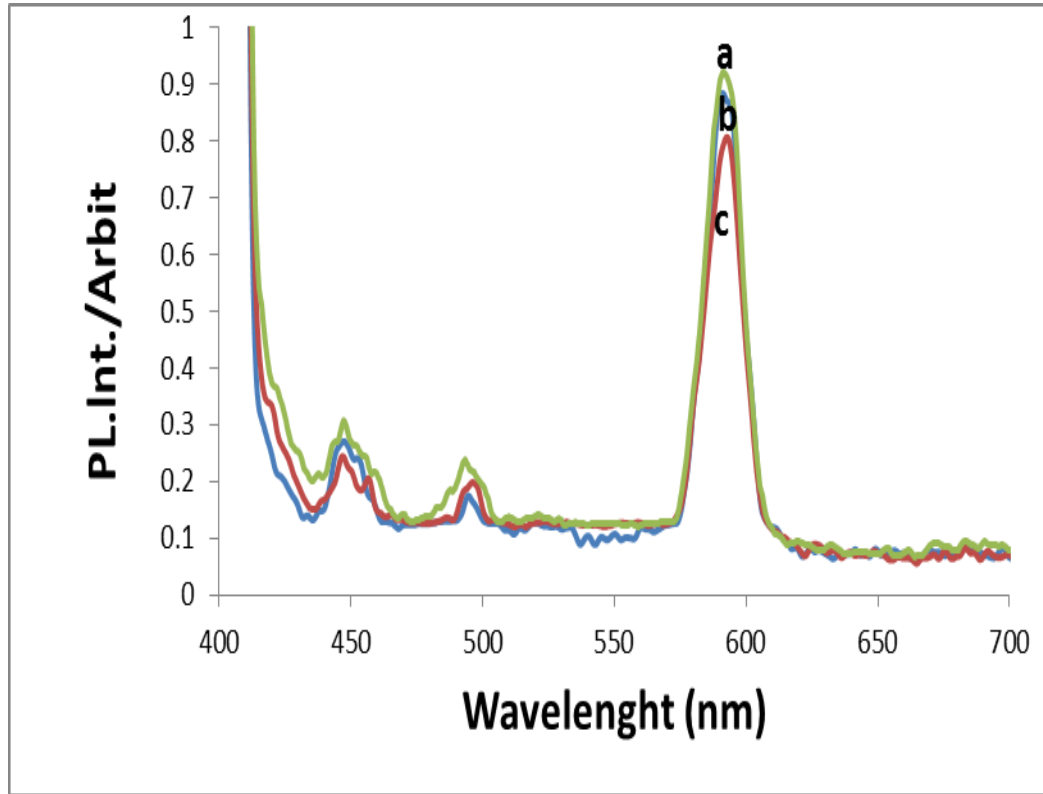


Figure (3.12): Photoluminescence spectra for CBD/ECD of CuSe thin films deposited in 2 hr: a) non-annealed, b) annealed at 250°C, for 1 hr, quickly cooled and c) annealed at 250°C, for 1 hr, slowly cooled.

3.3 Atomic Force Microscopy (AFM)

The surface morphology of CBD-CuSe and CBD/ECD-CuSe films deposited in 2 hr was studied using AFM. The CBD/ECD-CuSe film, annealed at 250°C under nitrogen for 1 hr and slowly cooled, was also studied.

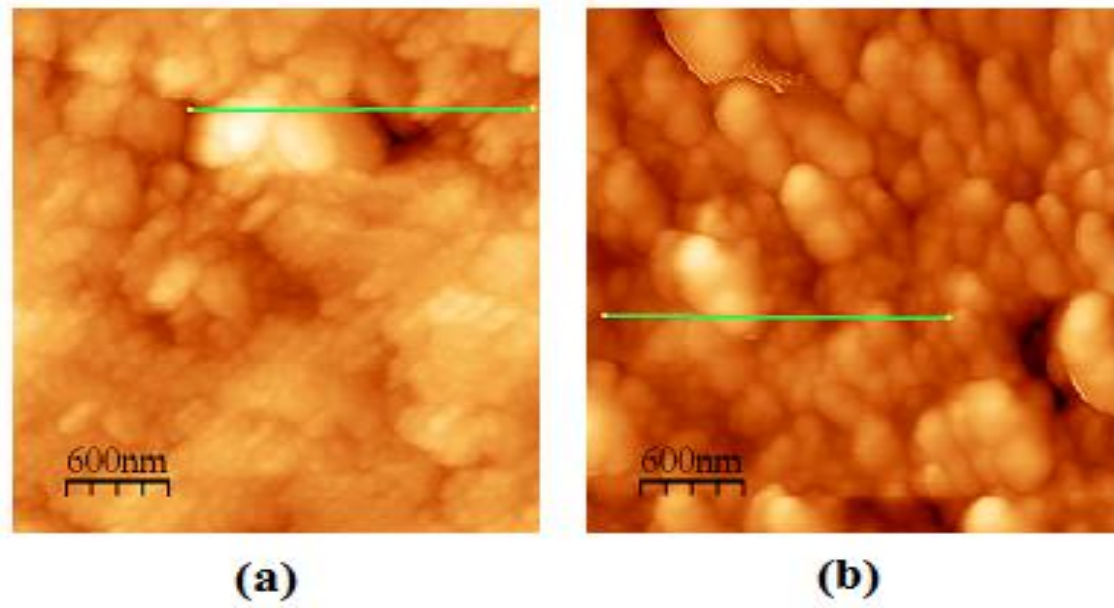


Figure (3.13): 2D AFM image for non-annealed CuSe thin films deposited in 2 hr, and prepared by different techniques: (a) by CBD/ECD, and (b) by CBD.

Figure (3.13), shows agglomerates of CuSe nano- particles with nearly 73 and 120 nm for the non-annealed films deposited in 2 hr by CBD/ECD and CBD respectively as 2D AFM images show. The film deposited by CBD/ECD had higher homogeneity with less dark islands, smoother surface and higher resolution than the film deposited by CBD. In earlier study, Al-Kerm studied a new type of CuSe film by ECD technique.

Values of root mean square (RMS) roughness were obtained from average surface roughness analysis, Figure (3.14). Films which were deposited in 2 hr by CBD and CBD/ECD exhibited RMS roughness of about ~150 and 100 nm respectively. As mentioned above, this indicates that the surface of the non-annealed film deposited in 2 hr by CBD/ECD shows better homogeneity, and its grains show more coalescence, than the non-annealed film deposited in 2 hr by CBD.

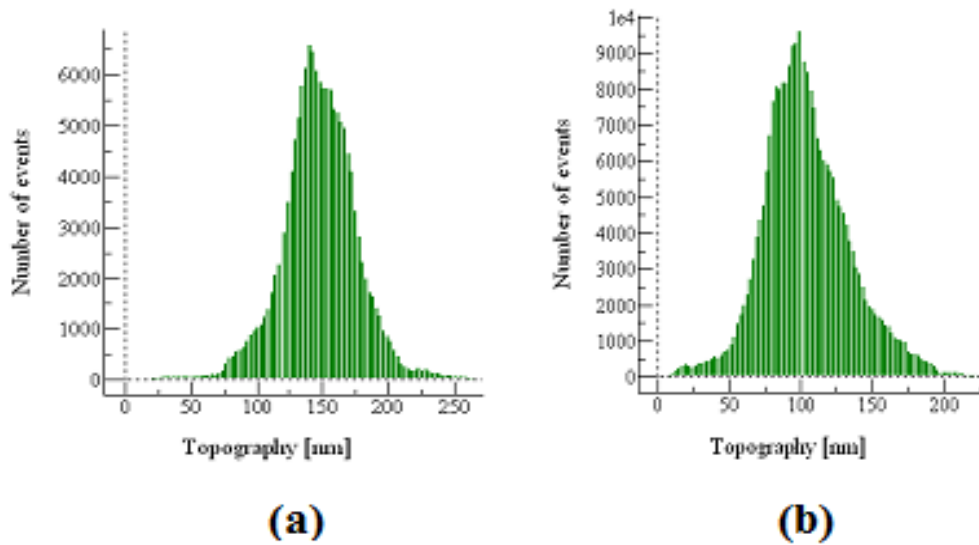


Figure (3.14): Average surface roughness analysis for non-annealed CuSe films deposited in 2 hr, prepared by different techniques: (a) by CBD, and (b) by CBD/ECD.

Figure (3.15), shows agglomerates of CBD/ECD-CuSe (deposited in 2 hr) nano- particles with nearly 73 and 250 nm for the non-annealed and annealed (at 250°C for 1 hr and slowly cooled) films respectively, as 2D AFM images show. The non-annealed film had higher homogeneity with little dark islands, smoother surface and higher resolution than the annealed film.

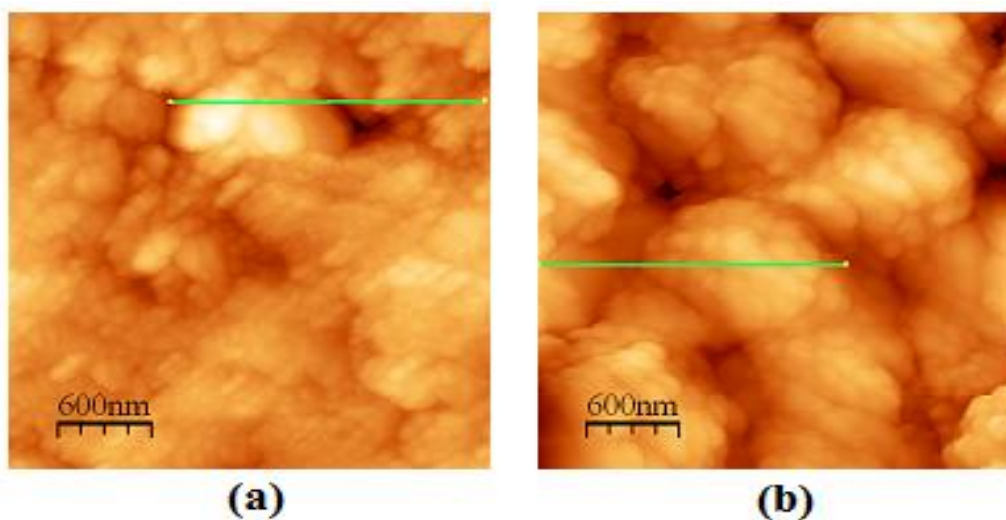


Figure (3.15): Effect of annealing on 2D AFM image for CBD/ECD-CuSe thin films deposited in 2 hr, (a) non-annealed, and (b) annealed (at 250°C for 1 hr and slowly cooled).

Values of root mean square (RMS) roughness were obtained from average surface roughness analysis, Figure (3.16). The CBD/ECD films (deposited in 2 hr) without and with annealing (at 250°C for 1 hr and slowly cooled) exhibited RMS roughness of about ~150 and 250 nm respectively. As mentioned above, this indicates that surface of the non-annealed film shows better homogeneity and the grains show more coalescence than the annealed film.

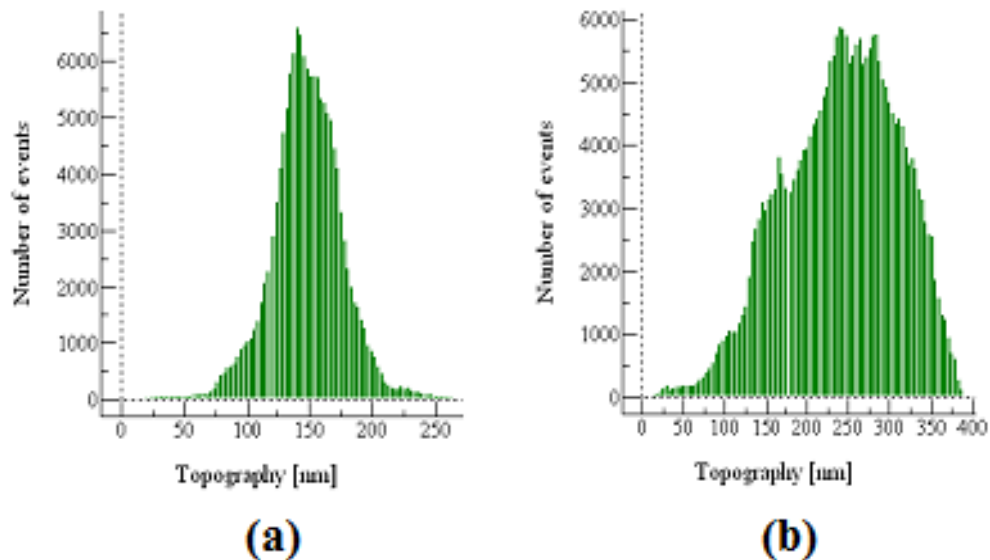


Figure (3.16): Effect of annealing on average surface roughness analysis for CBD/ECD-CuSe thin films deposited in 2 hr, (a) non-annealed, and (b) annealed (at 250°C for 1 hr and slowly cooled).

3.4 X-Ray Diffraction (XRD)

XRD measurements were obtained for CBD and CBD/ECD-CuSe thin film electrodes prepared in different duration times (2, 4 and 6 hr) and cooled by fast and slow cooling.

3.4.1 Effect of deposition time on CBD-CuSe thin film electrodes

XRD measurements were obtained for CBD-CuSe thin films deposited in different times (2, 4 and 6 hr). XRD patterns are shown in Figure (3.13). The average grain size of the CuSe was calculated using Debye-Scherrer's formula ($D = 0.9\lambda/\beta\cos\theta$). The average grain size for all CBD-CuSe (deposited in 2 hr) nano-particles was found to be ($\sim 27.00 \pm 0.01$ nm), the average grain size for CBD-CuSe (deposited in 4 hr) nano-particles was found to be ($\sim 31 \pm 0.01$ nm) and the average grain size for CBD-CuSe (deposited in 6 hr) nano-particles was found to be ($\sim 28 \pm 0.01$ nm). The film involved only cubic phase, [34, 65]. With no change in crystalline structure of CBD/ECD-CuSe films for both films deposited in (2 and 4 hr) and the film deposited in (6 hr) shows small change. Figure (3.17) shows that annealing CBD-CuSe film lowered the order in the film particles. This is evident from comparison of peak height ratios for the C(200) plane with the FTO reference peaks. The non-annealed CBD-CuSe film (deposited in 2 hr) showed higher ratio than other counterparts, and the CBD-CuSe film (deposited in 6 hr) showed higher ratio than CBD-CuSe film (deposited in 4 hr). Figure (3.17) summarizes these observations. Table (3.1) shows the positions of observed peaks and their significances.

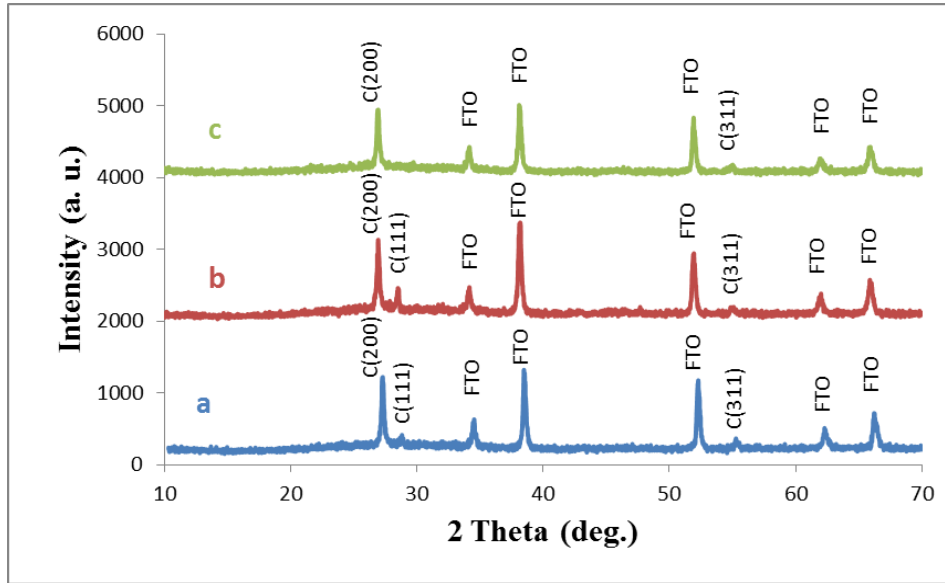


Figure (3.17): XRD spectra for CBD-CuSe thin films electrodes, deposited in different times, a) 2 hr, b) 4 hr and c) 6 hr.

Table (3.1): XRD measurements for CBD-CuSe thin films

Position of observed peak (2θ)	Cubic(C) (hkl)	References
(Deposited in 2 hr) 26.938	C(200)	[65]
28.441	C(111)	[34+65]
34.136	FTO	[64]
38.154	FTO	[64]
51.900	FTO	[64]
54.915	C(311)	[34+65]
61.937	FTO	[64]
65.875	FTO	[64]
(Deposited in 4 hr) 26.923	C(200)	[65]
28.480	C(111)	[34+65]
34.113	FTO	[64]
38.129	FTO	[64]
51.882	FTO	[64]
54.882	C(311)	[34+65]
61.905	FTO	[64]
65.858	FTO	[64]
(Deposited in 6 hr) 26.907	C(200)	[65]
34.109	FTO	[64]
38.121	FTO	[64]
51.888	FTO	[64]
54.910	C(311)	[34+65]
61.907	FTO	[64]
65.852	FTO	[64]

3.4.2 Effect of deposition time on CBD/ECD-CuSe thin film electrodes

XRD measurements were obtained for CBD/ECD-CuSe thin films deposited in different times (2, 4 and 6 hr). XRD data showed that there was more crystallinity and more ordering in cases of CBD/ECD-CuSe films than CBD-CuSe films. XRD patterns are shown in Figure (3.18) and Table (3.2). The average grain size of the CuSe was estimated using Debye-Scherrer's formula ($D = 0.9\lambda/\beta\cos\theta$). The average grain size for CBD/ECD-CuSe (deposited in 2 hr) nano-particles was found to be ($\sim 20.00 \pm 0.01$ nm), the average grain size for CBD/ECD-CuSe (deposited in 4 hr) nano-particles was found to be ($\sim 26.00 \pm 0.01$ nm) and the average grain size for CBD/ECD-CuSe (deposited in 6 hr) nano-particles was found to be ($\sim 29.70 \pm 0.01$ nm). The film involved only cubic phase with no change in crystalline structure of CBD/ECD-CuSe films deposited in (2, 4 and 6 hr). Figure (3.18) shows that annealing CBD-CuSe film lowered the order in the film particles. This is evident from comparison of peak height ratios for the C(200) plane with the FTO reference peaks. The non-annealed CBD-CuSe film (deposited in 6 hr) showed higher ratio than other counterparts, and the CBD-CuSe film (deposited in 4 hr) showed higher ratio than CBD-CuSe film (deposited in 2 hr). Figure (3.18 a, b & c) summarizes these observations.

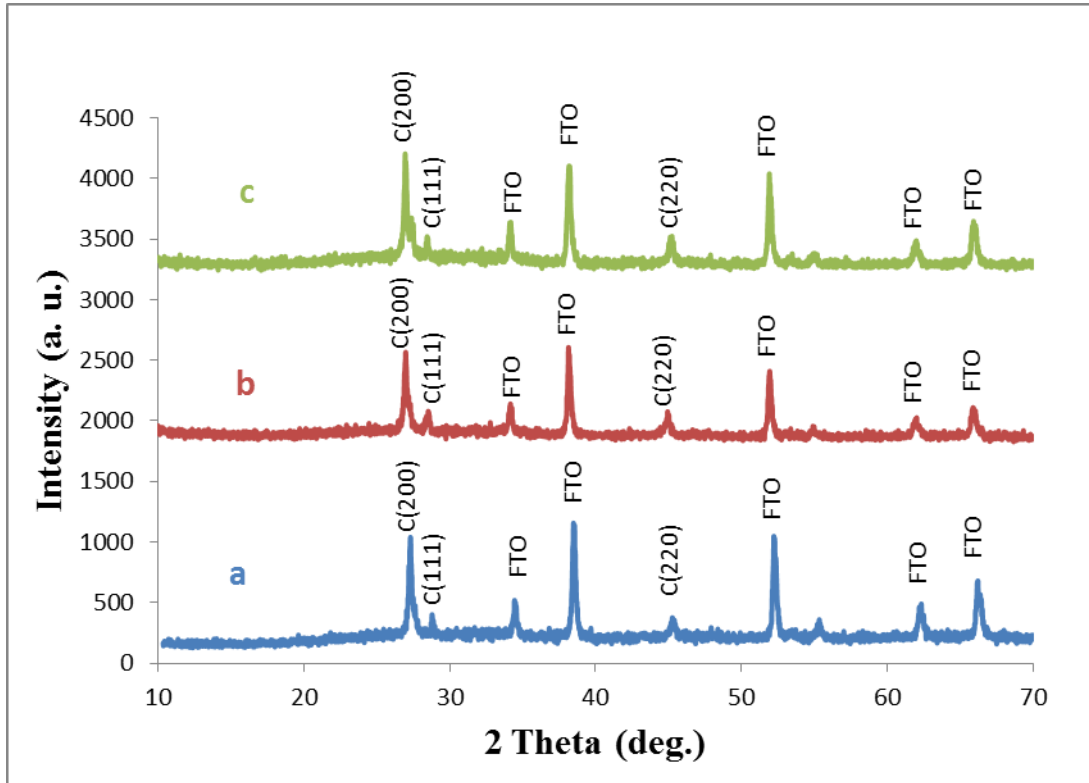


Figure (3.18): XRD spectra for CBD/ECD-CuSe thin films electrodes, deposited in different times, a) 2 hr, b) 4 hr and c) 6 hr.

Table (3.2): XRD measurements for CBD/ECD-CuSe thin films electrodes

Position of observed peak (2θ)	Cubic(C) (hkl)	References
(Deposited in 2 hr) 26.937	C(200)	[65]
28.452	C(111)	[34+65]
34.111	FTO	[64]
38.149	FTO	[64]
44.921	C(220)	[34+65]
51.900	FTO	[64]
61.902	FTO	[64]
65.877	FTO	[64]
(Deposited in 4 hr) 26.964	C(200)	[65]
28.474	C(111)	[34+65]
34.129	FTO	[64]
38.158	FTO	[64]
44.898	C(220)	[34+65]
51.908	FTO	[64]
61.908	FTO	[64]

65.874	FTO	[64]
(Deposited in 6 hr) 26.946	C(200)	[65]
28.439	C(111)	[34+65]
34.126	FTO	[64]
38.156	FTO	[64]
45.151	C(220)	[34+65]
51.907	FTO	[64]
61.912	FTO	[64]
65.897	FTO	[64]

3.4.3 Effect of cooling rate on CBD/ECD-CuSe thin film electrodes

The XRD patterns for CuSe thin films deposited in 2 hrs, annealed at 250°C for 1 hr, and cooled to room temperature by either slow or fast cooling were investigated, Figure (3.19). The average grain size of the CuSe was estimated using Debye-Scherrer's formula ($D = 0.9\lambda/\beta\cos\theta$). The average grain size for quickly cooled CuSe nano-particles was ($\sim 57.00 \pm 0.01$ nm), and for slowly cooled CuSe, it was ($\sim 39 \pm 0.01$ nm), and the average grain size of non-annealed CBD/ECD-CuSe film is smaller than the average grain size of annealed CBD/ECD-CuSe film (at 250°C for 1 hr). As shown in Figure (3.19 b). Both films involved cubic phase only, with no change in crystal structure of CBD/ECD-CuSe films by cooling rate under N₂ atmosphere. Figure (3.19) shows that annealing CBD/ECD-CuSe film (at 250°C for 1 hr) enhanced the ordering in the film particles. This is evident from comparison of peak height ratios for the C(200) plane with the FTO reference peaks. The annealed CBD/ECD-CuSe film (at 250°C for 1 hr with fast cooling) showed higher ratio than annealed CBD/ECD-CuSe film (at 250°C for 1 hr with slow cooling). Figure (3.19) summarizes these observations.

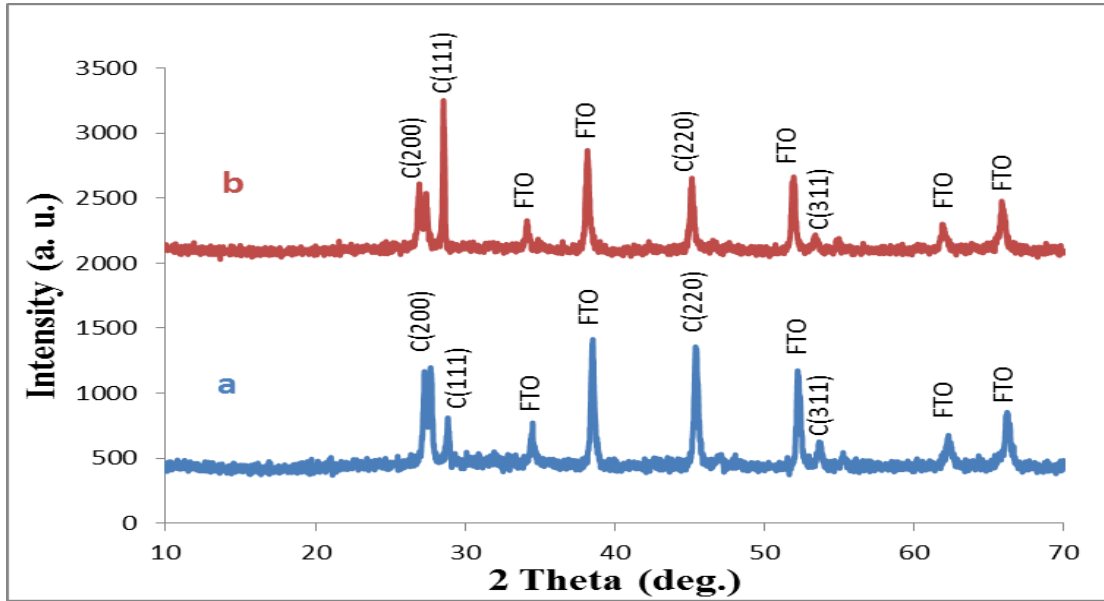


Figure (3.19): XRD spectra for CBD/ECD of CuSe thin films deposited in 2 hr: a) annealed at 250°C, for 1 hr, quickly cooled and b) annealed at 250°C, for 1 hr, slowly cooled.

Table (3.3): XRD results for annealed CBD/ECD-CuSe thin film electrodes

Position of observed peak (2 θ)	Cubic(C) (hkl)	References
(Quickly cooled) 27.162	C(200)	[65]
28.486	C(111)	[34+65]
34.121	FTO	[64]
38.153	FTO	[64]
45.066	C(220)	[34+65]
51.899	FTO	[64]
53.310	C(311)	[34+65]
61.919	FTO	[64]
65.855	FTO	[64]
(Slowly cooled) 27.098	C(200)	[65]
28.550	C(111)	[34+65]
34.128	FTO	[64]
38.153	FTO	[64]
45.124	C(220)	[34+65]
51.902	FTO	[64]
53.394	C(311)	[34+65]
61.924	FTO	[64]
65.865	FTO	[64]

3.5 PEC Studies

PEC studies were investigated for ECD, CBD and CBD/ECD-CuSe thin film electrodes before annealing and after annealing with control in cooling rate.

3.5.1 Effect of deposition time on the CuSe thin film electrodes

3.5.1.1 Photo J - V plots measured for ECD-CuSe thin film electrodes

Photo J - V plots were measured for CuSe thin film electrodes prepared by ECD deposited in 15 min, Figure (3.20).

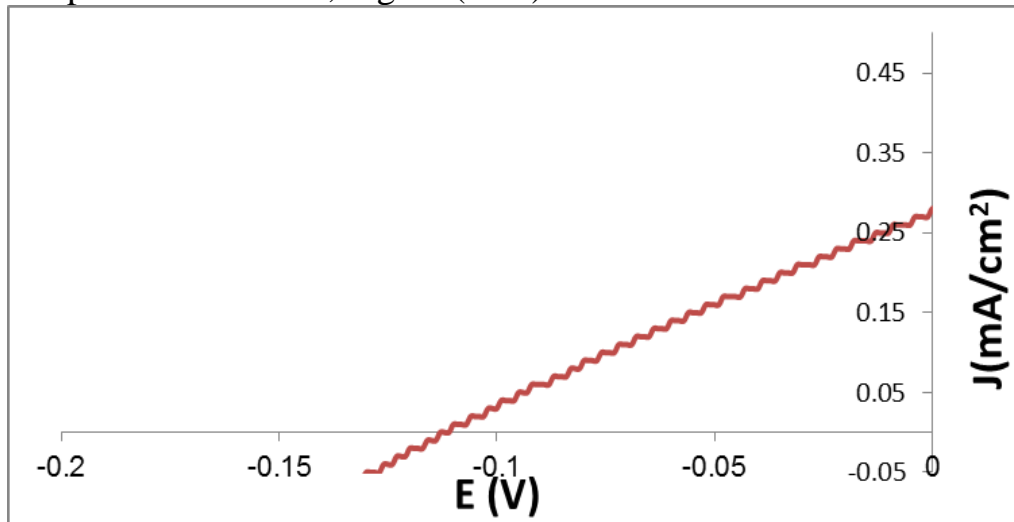


Figure (3.20): Photo J - V plots for ECD of CuSe thin films, deposited in 15 min.

Table (3.4): The PEC characteristics of ECD-CuSe thin film electrode deposited in 15 min

description	V_{oc} (V)	J_{sc} (mA/cm ²)	* η %	** FF %
15 min	-0.113	0.28	0.42	26.54

The V_{oc} value for the films deposited in 15 min is (-0.113 V) and the J_{sc} value is (0.28 mA/cm²) with percentage conversion efficiency (η % ~0.42).

Table (3.4) summarizes PEC characteristics for each film electrode.

* η (%) = [(maximum observed power density) / (reach-in power density)] \times 100%.

** FF = [(maximum observed power density) / $J_{sc} \times V_{oc}$] \times 100%.

3.5.1.2 Photo J - V plots measured for CBD-CuSe thin film electrodes

Photo J - V plots were measured for CBD-CuSe thin film electrodes prepared in different deposition times (2, 4, and 6 hr), Figure (3.21).

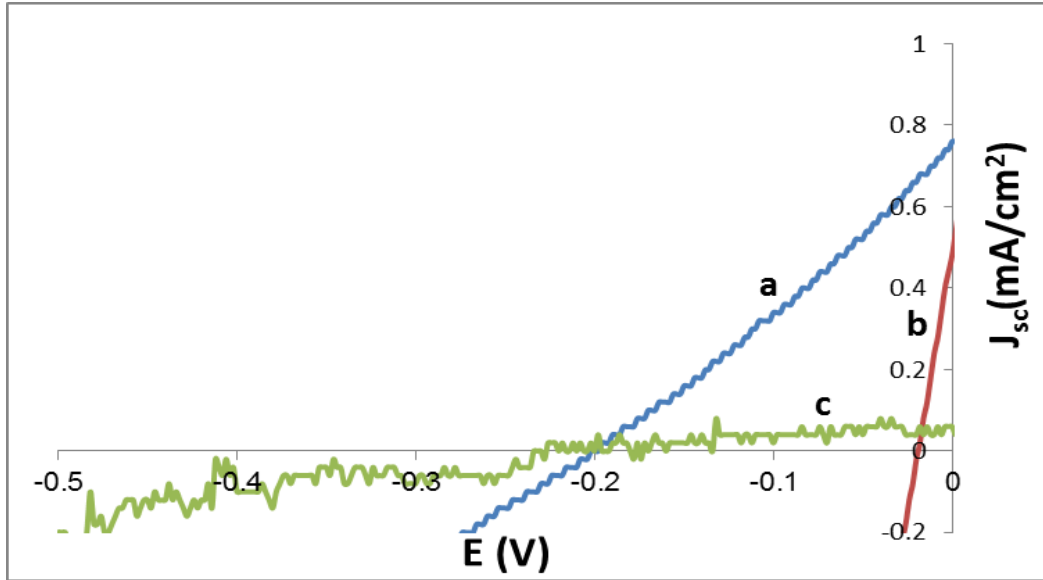


Figure (3.21): Photo J - V plots for CBD of CuSe thin films, deposited in different times, a) 2 hr, b) 4 hr and c) 6 hr.

Table (3.5): Effect of deposition time on PEC characteristics of CBD-CuSe thin film electrodes

Sample	description	V_{oc} (V)	J_{sc} (mA/cm ²)	* η %	** FF %
a	2 hr	-0.21	0.76	1.83	22.52
b	4 hr	-0.02	0.48	0.13	26.25
c	6 hr	-----	0.06	-----	-----

The V_{oc} values for the films deposited in 2 and 6 hrs were close to each other. But the V_{oc} value for film deposited in 4 hrs is different. The film deposited in 2 hr showed higher J_{sc} than other counterparts, and gave highest percentage conversion efficiency (η % \sim 1.83). Table (3.5) summarizes PEC characteristics for each film electrode. The Table shows

* η (%) = [(maximum observed power density) / (reach-in power density)] \times 100%.

** FF = [(maximum observed power density) / $J_{sc} \times V_{oc}$] \times 100%.

that 2 hr deposition time gives better values than films deposited in 4 and 6 hrs.

3.5.1.3 Dark J - V plots measured for CBD-CuSe thin film electrodes

Dark J - V plots were investigated for CBD-CuSe thin film electrodes deposited in different times, Figure (3.22).

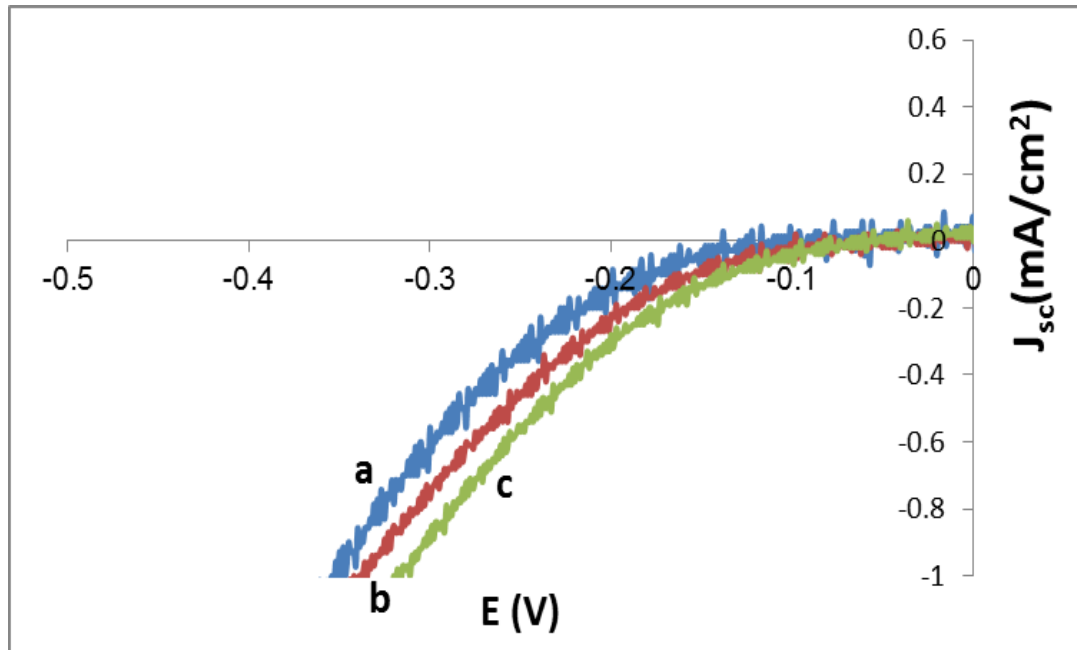


Figure (3.22): Dark J - V plots for CBD of CuSe thin films, deposited in different times, a) 2 hr, b) 4 hr and c) 6 hr.

The prepared film deposited in 2 hr showed higher, V_{onset} negative value than other counterparts. The film deposited in 4 hr showed higher, V_{onset} negative value than film deposited in 6 hr.

3.5.1.4 Photo J - V plots measured for CBD/ECD-CuSe thin film electrodes

Photo J - V plots were measured for CuSe thin film electrodes prepared by CBD/ECD in different times (2, 4 and 6 hrs), Figure (3.23).

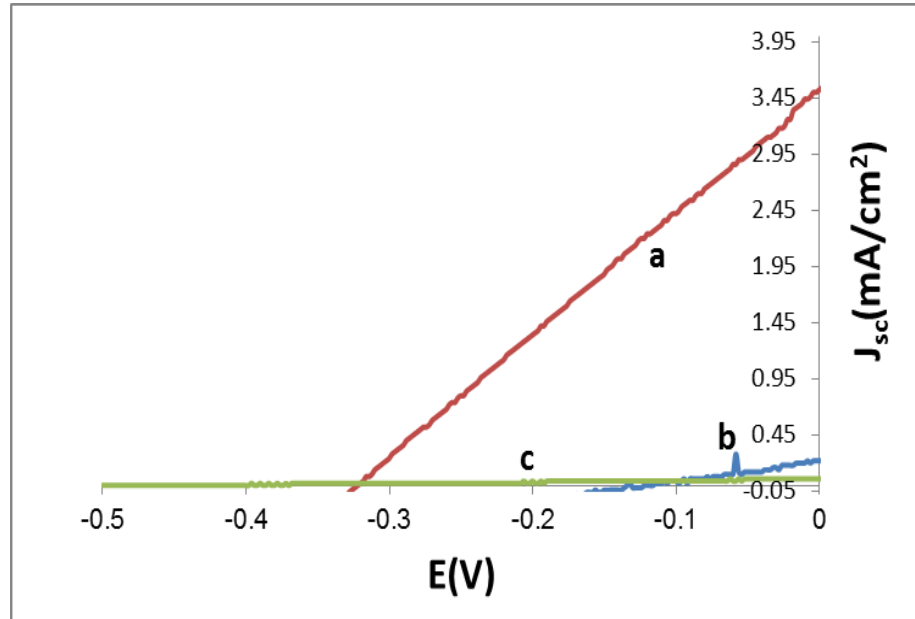


Figure (3.23): Photo J - V plots for CBD/ECD of CuSe thin films, deposited in different times, a) 2 hr, b) 4 hr and c) 6 hr.

Table (3.6): Effect of deposition time on PEC characteristics of CBD/ECD-CuSe thin film electrodes

Sample	description	V_{oc} (V)	J_{sc} (mA/cm ²)	* η %	** FF %
a	2 hr	-0.32	3.52	14.6	25.41
b	4 hr	-0.13	0.22	0.89	61.15
c	6 hr	-----	0.06	0.41	36.08

The film deposited in 2 hr showed higher J_{sc} than other counterparts, and gave highest percentage conversion efficiency (η % \sim 14.6). Table (3.6) summarizes PEC characteristics for each film electrode. The Table shows that 2 hr deposition time gives better values than films deposited in 4 hr and 6 hr.

* η (%) = [(maximum observed power density)/(reach-in power density)] \times 100%.

** FF = [(maximum observed power density)/ $J_{sc} \times V_{oc}$] \times 100%.

3.5.1.5 Dark J - V plots measured for CBD/ECD-CuSe thin film electrodes

Dark J - V Plots were investigated for CBD/ECD-CuSe thin film electrodes deposited in different times (2, 4 and 6 hr), Figure (3.24).

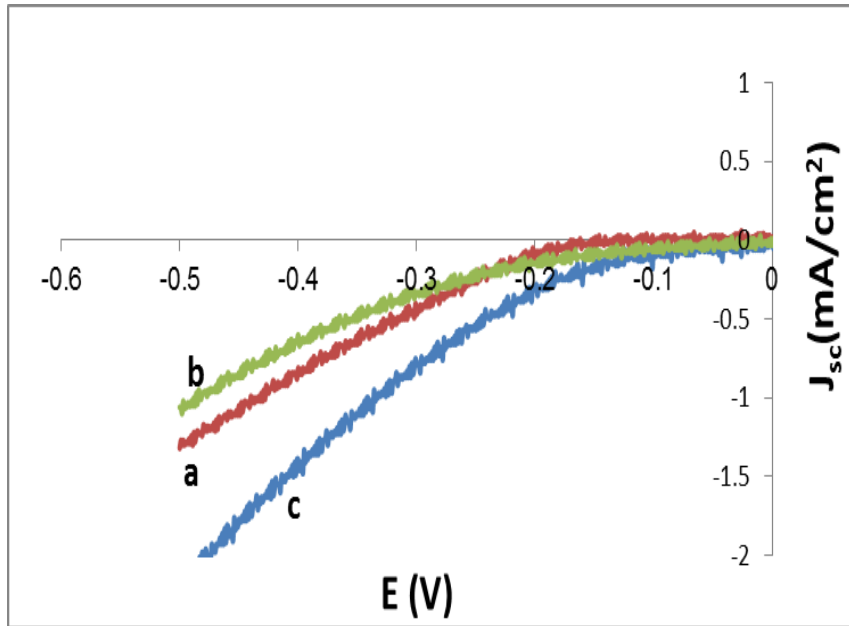


Figure (3.24): Dark J - V plots for CBD/ECD of CuSe thin films, deposited in different times, a) 2 hr, b) 4 hr and c) 6 hr.

The prepared film deposited in 2 hr showed higher, V_{onset} negative value than other counterparts. The film deposited in 4 hr showed higher, V_{onset} negative value than film deposited in 6 hr.

3.5.1.6 Photo J - V plots measured for CuSe thin film electrodes prepared by different techniques

Photo J - V plots were measured for CuSe thin film electrodes prepared by different techniques (ECD, CBD and CBD/ECD), Figure (3.25).

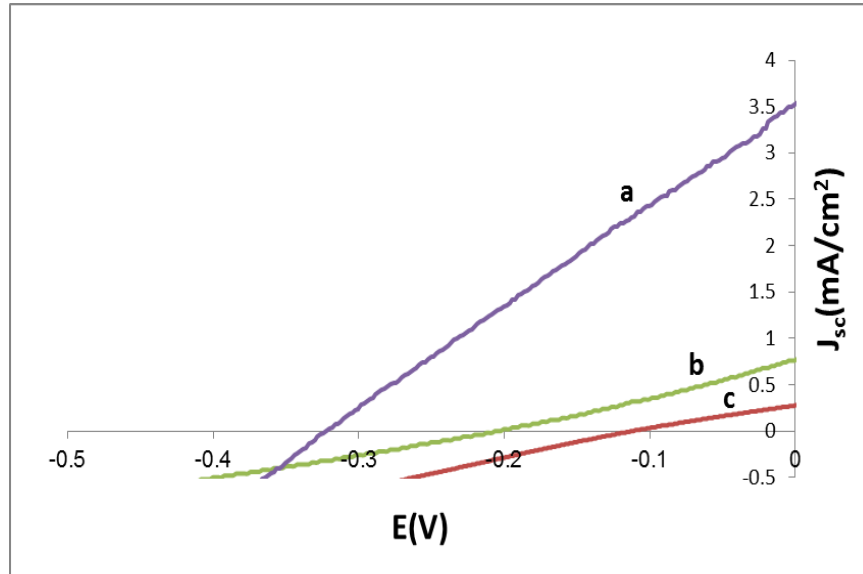


Figure (3.25): Photo J - V plots for CuSe thin films, deposited in different techniques, a) CBD/ECD for 2 hr, b) CBD for 2 hr and c) ECD for 15 min.

Table (3.7): Comparison of CuSe thin film electrodes prepared by different techniques

Sample	description	V_{oc} (V)	J_{sc} (mA/cm ²)	* η %	**FF %
a	CBD/ECD for 2 hr	-0.32	3.52	14.6	25.41
b	CBD for 2 hr	-0.20	0.76	1.83	22.5
c	ECD for 15 min	-0.11	0.28	0.42	26.5

The V_{oc} values for films prepared by different techniques, ECD (15 min), CBD (2 hr) and CBE/ECD (2 hr) were -0.11, -0.20 and -0.32V respectively. The film prepared by CBD/ECD in 2 hr showed higher J_{sc} and gave higher percentage conversion efficiency (η % \sim 14.6). Table (3.7) summarizes PEC values. The film prepared by CBD/ECD in 2 hrs shows better PEC characteristics than other two films. The film prepared by CBE/ECD (deposited in 2 hr) gave percentage conversion efficiency (η % \sim 14.6), and this result has not been obtained before.

* η (%) = [(maximum observed power density)/(reach-in power density)] \times 100%.

**FF = [(maximum observed power density)/ $J_{sc} \times V_{oc}$] \times 100%.

3.5.2 Effect of cooling rate on the CuSe thin film electrodes

Effect of cooling rate (slow and fast cooling) on the CuSe thin film electrodes deposited in 2 hrs and annealed at 250°C under nitrogen for 1 hr was studied. The results are shown below.

3.5.2.1 Photo J - V plots measured for CBD-CuSe thin film electrodes

Photo J - V plots were measured for CuSe thin film electrodes deposited in 2 hrs, annealed at 250°C for 1 hr, cooled to room temperature by either slow or fast cooling, Figure (3.26). The PEC characteristics for each film are summarized in Table (3.4).

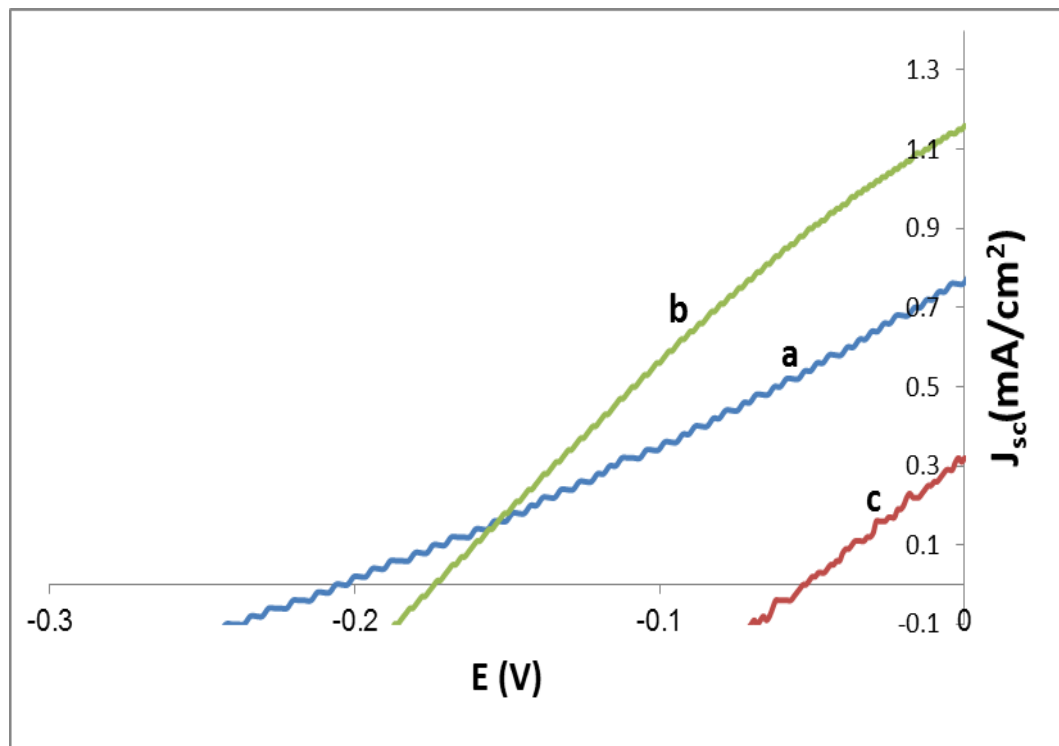


Figure (3.26): Photo J - V plots for CBD of CuSe thin films, deposited in 2 hr, a) non-annealed b) annealed at 250°C, 1 hr with fast cooling and c) annealed at 250°C, 1 hr with slow cooling.

Table (3.8): Effect of annealing on PEC characteristics of CBD-CuSe thin film electrodes

Sample	description	V_{oc} (V)	J_{sc} (mA/cm ²)	* η %	** FF %
a	Non-annealed	-0.20	0.76	1.83	22.52
b	Fast cooling	-0.17	1.16	2.94	29.23
c	Slow cooling	-0.05	0.32	0.23	29.00

The quickly cooled film showed higher J_{sc} and higher V_{oc} values than the slowly cooled one, and gave higher percentage conversion efficiency (η % ~2.94), Table (3.8).

3.5.2.2 Photo J - V plots measured for CBD/ECD-CuSe thin film electrodes

Photo J - V plots were measured for CuSe thin film electrodes deposited in 2 hrs, annealed at 250°C for 1 hr, and cooled to room temperature by either slow or fast cooling, Figure (3.27).

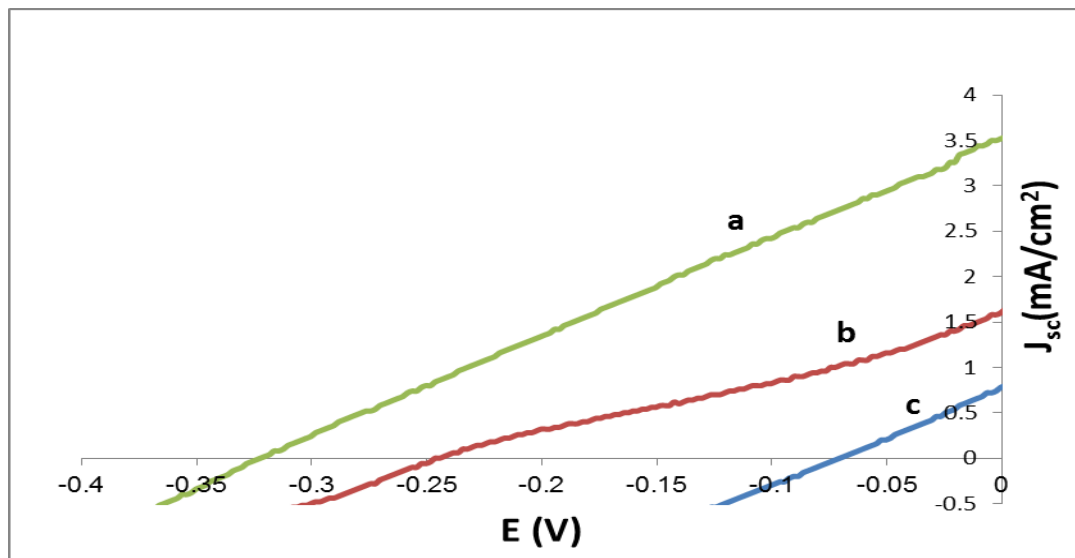


Figure (3.27): Photo J - V plots for CBD/ECD of CuSe thin films, deposited in 2 hr, a) non-annealed b) annealed at 250°C, 1 hr with fast cooling and c) annealed at 250°C, 1 hr with slow cooling.

* η (%) = [(maximum observed power density)/(reach-in power density)] \times 100%.

** FF = [(maximum observed power density)/ $J_{sc} \times V_{oc}$] \times 100%.

Table (3.9): Effect of annealing on PEC characteristics of CBD/ECD-CuSe thin film electrodes

Sample	Description	V_{oc} (V)	J_{sc} (mA/cm ²)	* η %	** FF %
a	Non-annealed	-0.32	3.52	14.6	25.41
b	Fast cooling	-0.24	1.60	4.51	23.04
c	Slow cooling	-0.07	0.82	0.76	26.02

The non-annealed film showed higher J_{sc} and higher V_{oc} values than the annealed one, and gave higher percentage conversion efficiency (η % ~14.6). The quickly cooled film showed higher J_{sc} and higher V_{oc} values than the slowly cooled one, and gave higher percentage conversion efficiency (η % ~4.51), Table (3.9).

3.6 Stability of the CuSe thin film electrodes

We have studied the stability on the best thin film gave the efficiency conversion. The stability under PEC conditions was investigated for CBD/ECD-CuSe thin film electrodes deposited in 2 hr, Figure (3.28). The value of J_{sc} vs. time was measured at 0.0 V applied potential with respect of Ag/AgCl electrode.

* η (%) = [(maximum observed power density)/(reach-in power density)] \times 100%.

** FF = [(maximum observed power density)/ $J_{sc} \times V_{oc}$] \times 100%.

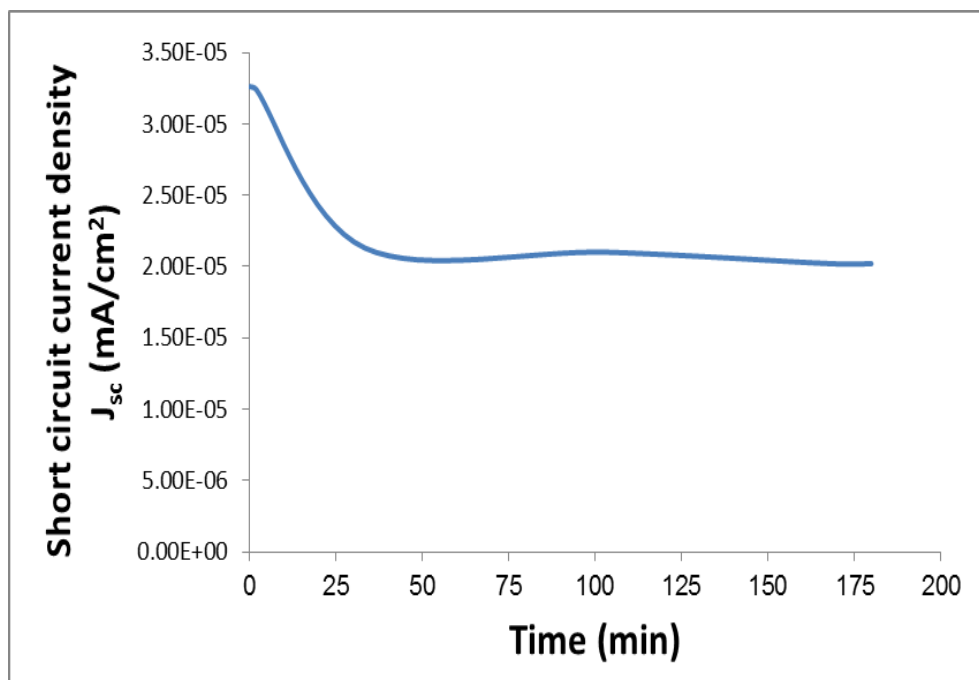


Figure (3.28): Short circuit current density vs. time measured for CBD/ECD of CuSe thin film electrodes, deposited in 2 hrs. The measurement was conducted in aqueous $K_3Fe(CN)_6/K_4Fe(CN)_6/LiClO_4$ redox system at room temperature.

Prepared film by CBD/ECD deposited in 2 hrs showed soundly good stability with steady value for 180 minute. This indicates the relative stability of CuSe thin films deposited by CBD/ECD in 2 hrs under PEC conditions.

Part II

Coating with MP-Sil

Characteristics of CBD and CBD/ECD-CuSe thin film electrodes deposited in 2 hrs and coated with MP-Sil matrix have been studied.

3.7 Electronic Absorption Spectra

3.7.1 Effect of coating with MP-Sil matrix on CBD-CuSe thin film electrodes

The electronic absorption spectra for CuSe thin film electrodes coated by MP-Sil matrix was investigated, Figure (3.29). The band gap values in the range of around ~ 2.1 - 2.3 eV were observed. Figure (3.29 b), shows small bands at ~ 450 nm, ~ 550 nm and ~ 570 nm which confirm the presence of the metalloporphyrin (MP). The coating didn't affect the spectra of naked films.

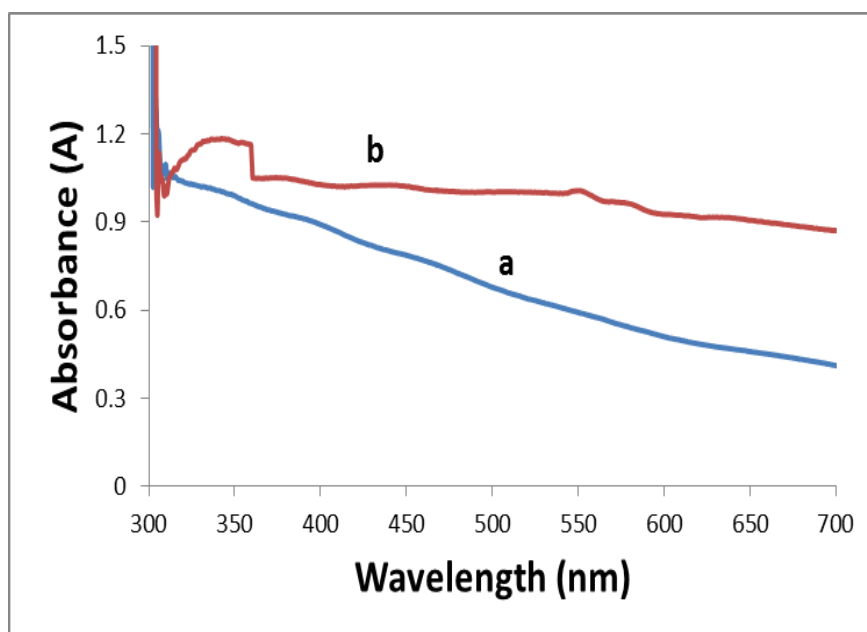


Figure (3.29): Electronic absorption spectra for CBD of CuSe thin films, deposited on FTO in 2 hr, a) naked, b) coated.

3.7.2 Effect of coating with MP-Sil matrix on CBD/ECD-CuSe thin film electrodes

The electronic absorption spectra for CuSe thin film electrodes coated by MP-Sil matrix was investigated, Figure (3.30). The prepared films show the same absorption edges values ~ 570 nm, with band gaps values in the range of ~ 2.1 - 2.3 eV were observed. The coating didn't affect the spectra of naked films.

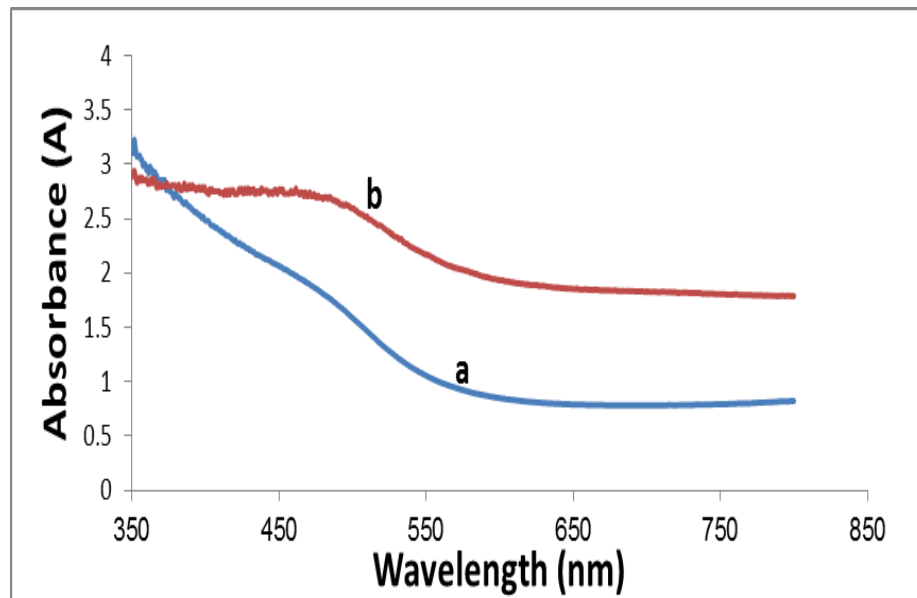


Figure (3.30): Electronic absorption spectra for CBD/ECD CuSe thin films, deposited in 2 hr, a) naked, b) coated.

3.8 Photoluminescence Spectra (PL)

3.8.1 Effect of coating with MP-Sil matrix on CBD-CuSe thin film electrodes

The photoluminescence spectra for CuSe thin film electrodes, naked and coated were investigated, Figure (3.31). The systems were excited at wavelength 383 nm. The Figure shows many peaks for each film, but the

highest intensities appeared at wavelengths ~ 590 nm, band gap value is consistent with PL spectra values, showing a band gap $1240/590 = 2.10$ eV. The naked film showed higher PL intensity than coated film.

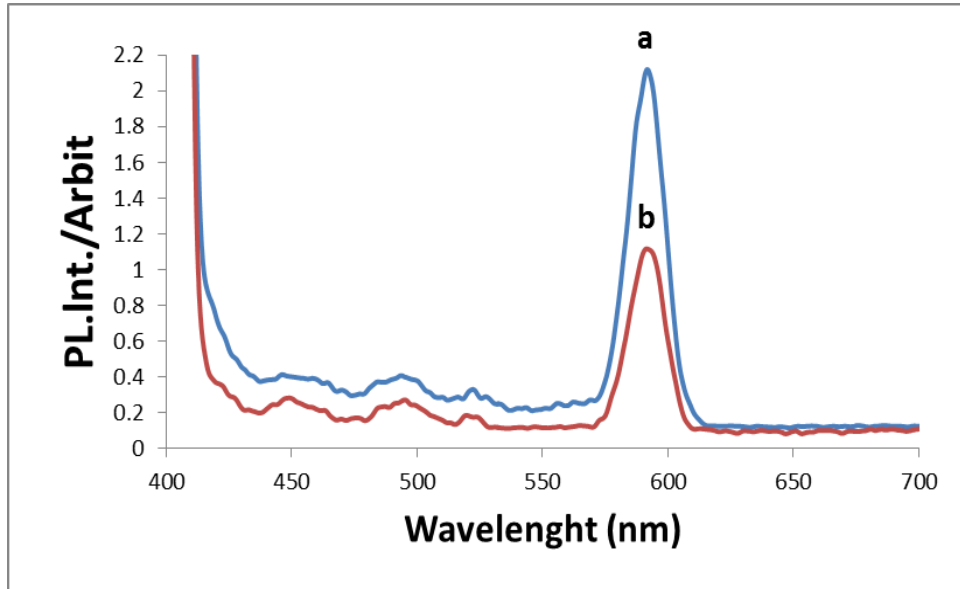


Figure (3.31): Photoluminescence spectra for CBD of CuSe thin films, deposited in 2hr, a) naked, b) coated.

3.8.2 Effect of coating with MP-Sil matrix on CBD/ECD-CuSe thin film electrodes

The photoluminescence spectra for CuSe thin film electrodes, naked and coated were investigated, Figure (3.32). The systems were excited at wavelength 383 nm. The Figure shows many peaks for each film, but the highest intensities appeared at wavelengths ~ 590 nm, the band gap is similar with PL spectra values, showing a band gap $1240/590 = 2.10$ eV. The naked film showed slightly higher PL intensity than the coated film.

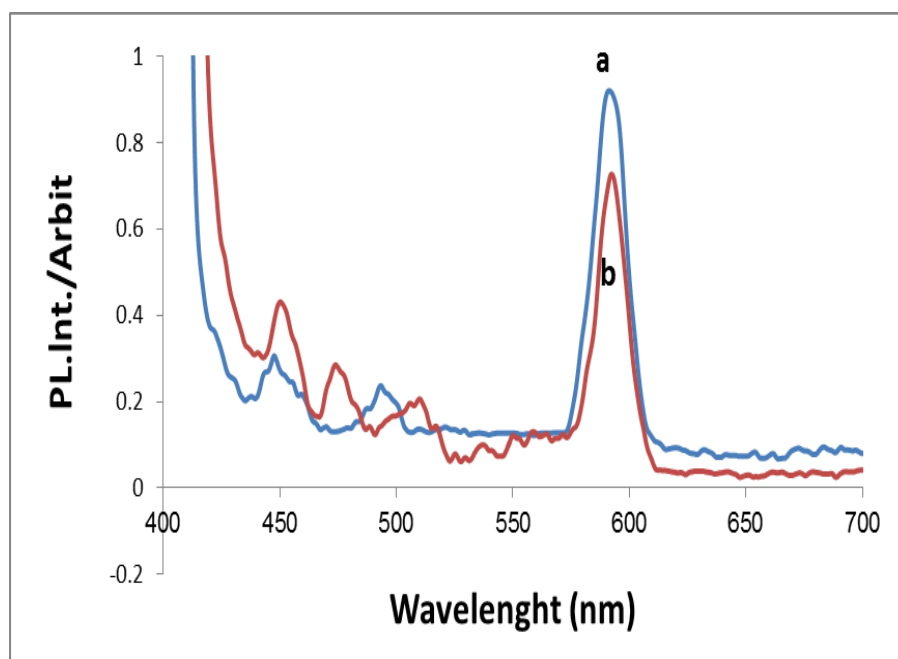


Figure (3.32): Photoluminescence spectra for CBD/ECD of CuSe thin films, deposited in 2 hr: a) naked, b) coated.

3.9 PEC Studies

Effect of coating CuSe thin film deposited in 2 hrs and coated with MP-Sil matrix has been studied.

3.9.1 Photo J - V plots measured for coated CBD-CuSe thin film electrodes

Photo J - V plots were measured for CuSe thin film electrodes coated with MP-Sil, Figure (3.33). The results are summarized in Table (3.6).

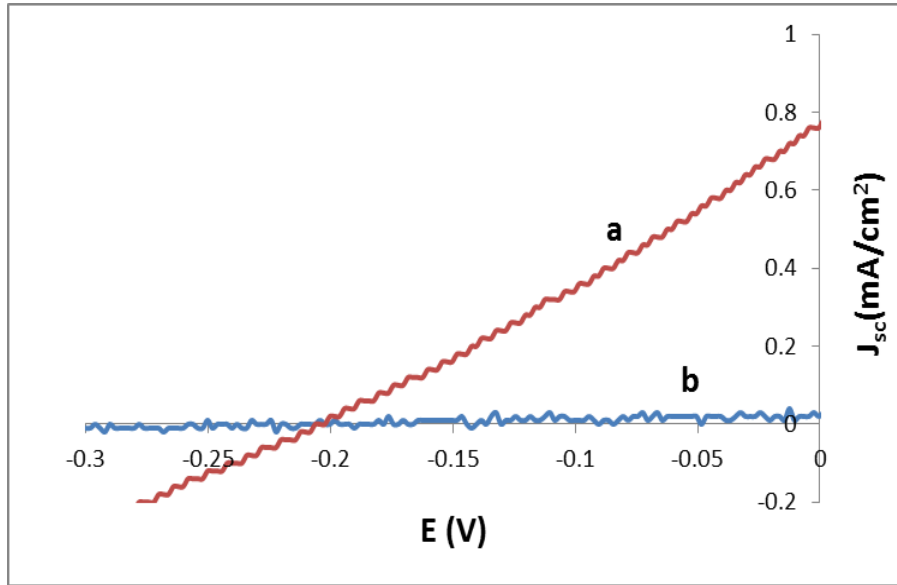


Figure (3.33): Photo J - V plots for CBD of CuSe thin films, deposited in 2 hr, a) naked, b) coated.

Table (3.10): Effect of coating with MP-Sil matrix on PEC characteristics of CBD-CuSe thin film electrodes

Sample	Description	V_{oc} (V)	J_{sc} (mA/cm ²)	* η %	** FF %
a	Naked	-0.21	0.76	1.83	22.52
b	Coated	-0.26	0.03	0.17	73.55

The V_{oc} values for naked and coated films were close to each other. The naked film showed higher J_{sc} than the coated film, and gave higher percentage conversion efficiency (η % \sim 1.83), Table (3.10).

3.9.2 Photo J - V plots measured for coated CBD/ECD-CuSe thin film electrodes

Photo J - V plots were measured for CuSe thin film electrodes coated with MP-Sil, Figure (3.34). The results are summarized in Table (3.7).

* η (%) = [(maximum observed power density)/(reach-in power density)] \times 100%.

** FF = [(maximum observed power density)/ $J_{sc} \times V_{oc}$] \times 100%.

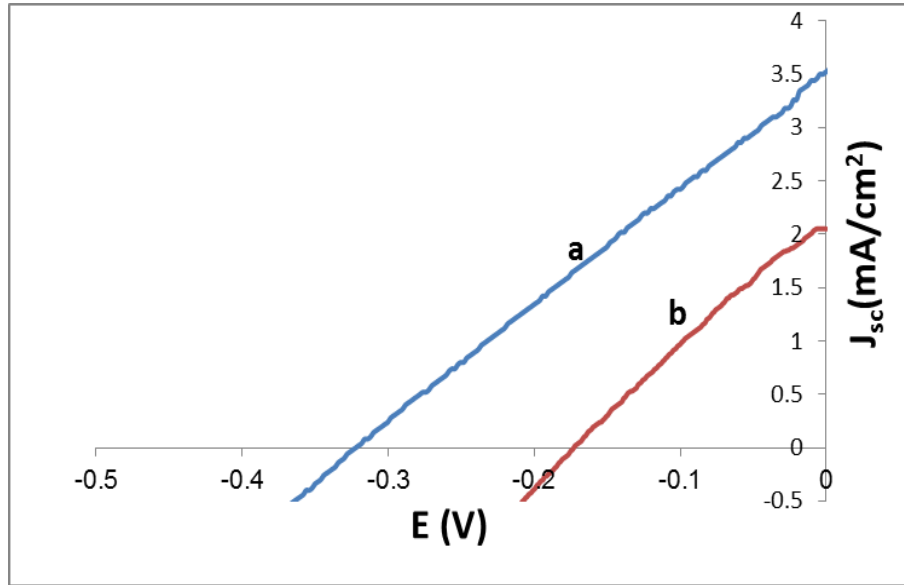


Figure (3.34): Photo J - V plots for CBD/ECD of CuSe thin films, deposited in 2 hr, a) naked, b) coated.

Table (3.11): Effect of coating with MP-Sil matrix on PEC characteristics of CBD/ECD-CuSe thin film electrodes

Sample	Description	V_{oc} (V)	J_{sc} (mA/cm ²)	* η %	**FF %
a	Naked	-0.32	3.52	14.6	25.41
b	Coated	-0.17	2.05	5.04	28.37

Naked film showed higher V_{oc} and higher J_{sc} than coated film. The naked film gave higher percentage conversion efficiency (η % ~14.6), than coated film, Table (3.11). The coated CBD/ECD-CuSe gave higher percentage conversion efficiency (η % ~5.04) than both of the coated CBD-CuSe (η % ~0.17) and ECD-CuSe (η % ~0.42) films.

* η (%) = [(maximum observed power density)/(reach-in power density)] \times 100%.

**FF = [(maximum observed power density)/ $J_{sc} \times V_{oc}$] \times 100%.

Chapter Four

Discussion

Chapter Four

Discussion

Many methods were used to enhance the semiconductor thin film electrode PEC characteristics including: Controlling deposition time, annealing temperature and cooling rate. In this work, we experimented such concepts to enhance PEC characteristics of CuSe thin films. Moreover, we used a new combined technique of ECD followed by CBD to give CBD/ECD film for the same purpose. To our knowledge, such technique has not been used to enhance PEC characteristics of CuSe film electrodes.

In this chapter, we discuss the results, and highlight the advantages of combined CBD/ECD preparation, annealing and cooling rate on CuSe thin film characteristics including XRD patterns, electronic absorption spectra, PL spectra and PEC properties.

As we look around, many things we see are solid substance. A solid is a material which has definite volume and shape. Solids which have regular order of their constituent components (atoms, molecules or ions) are called crystalline solids. These components are present at fixed positions. The properties of the solid depend on the nature of the constituents and on their arrangements which hold the constituent particles together in tight arrangement [66].

As discussed in Section (1.10), solid CuSe may exist in hexagonal (hcp) or cubic (fcc) crystal structures [37]. The face centered cubic (fcc) structure is known to be more stable [65]. The prepared CuSe solid may be cubic,

hexagonal or both. XRD can help confirm the real structure, by comparison with earlier reports.

Part I

4.1 Naked CuSe thin film electrodes

4.1.1 ECD-CuSe thin film electrodes

AL-Kerm prepared a new type of CuSe film by ECD technique and studied the effect of deposition time (5, 10 and 15 min) on its characteristics and PEC properties. The 15 min deposition time gave the best results. All AFM, photoluminescence and electronic absorption spectra showed better result for film deposited in 15 min than other two counterparts [46]. All measurements (electronic absorption spectra, PL spectra and PEC study) were repeated here for the 15 min ECD-CuSe thin films, Figures (3.1, 3.7 and 3.20). The goal was to reconfirm earlier study. Our results were consistent with earlier results.

4.1.2 CBD-CuSe thin film electrodes

CBD-CuSe thin films were reported earlier, and their characteristics were studied [34]. Unfortunately no work was made to study PEC characteristics of such film electrodes, to the best of our knowledge.

Effect of deposition time on the CuSe thin film deposited in (2, 4 and 6 hr) has been studied, Figures (3.2, 3.8, 3.21 and 3.22). The deposition time didn't significantly affect position of photoluminescence emission band. This is because longer deposition time increases film thickness, with no effect on particles size and structure. The deposition time significantly

affect intensity of photoluminescence; this is because longer deposition time increases the disorder between the particles.

Electronic absorption spectra were slightly enhanced by increasing deposition time and the spectrum for 6 hr deposition time showed more curved plot than other two counterparts, Figure (3.2). This is because longer deposition time increases film thickness which in turn increases absorbance. For PEC study, the 2 hr time gave higher PEC characteristics than other two counterparts, Figure (3.21 and 3.22). In general, the change in deposition time slightly affected the film characteristics, since it affects the thickness of the films though not the structure of crystal. This is due to suitable thickness and longer deposition time increases the disorder between the particles.

Comparison between XRD spectra for non-annealed CBD-CuSe films deposited in (2, 4 and 6 hr) was studied, Figures (3.13). In general, in this study the CuSe films prepared by CBD in different times (2, 4 and 6 hr) did have difference in crystallite sizes. The crystallite size for CBD-CuSe films have comparable XRD intensities with preferential orientation in the C(200), C(111) and C(311) planes, Figure (3.13). This is acceptable as the CBD-CuSe is expected to be relatively uniform and crystalline. This because without change in the structure disorder and with a small change on particle size. The non-annealed CBD-CuSe film (deposited in 2 hr) showed higher signal ratio than other counterparts. This means that the CBD-CuSe film (deposited in 2 hr) has higher crystallinity and uniformity than other counterparts [62].

The effect of annealing on CuSe thin film electrode characteristics was studied. Annealing may reduce defects, remove surface roughness and consequently enhance SC characteristics. Since there is no perfect crystal, so all semiconductors contain vacancies or defects. Through heating, the semiconductors defect concentration increases, normally first at crystal surface. These defects gradually spread throughout the crystal (from surface into the bulk). On cooling the vacancy concentration is lowered by diffusion to grain boundaries or dislocations. The rate at which vacancies move from point to point in the lattice decreases exponentially with decreasing temperature. In general, annealing CuSe thin films improves their photo $J-V$ plots, conversion efficiency by improving the crystal homogeneity and structure [46, 58 and 61-63].

In this study, effect of annealing on CBD-CuSe thin film electrode deposited in 2 hr and annealed at 250°C for 1 hr has been studied, Figures (3.5, 3.11 and 3.26). Effect of annealing didn't significantly affected position of photoluminescence emission band, but significantly affect intensity of PL (the non-annealed gave higher intensity than annealed). This is because annealing caused a small disorder in the particles which was not repaired. Electronic absorption spectra were slightly affected by annealing, and the annealed film exhibited slightly better absorption than non-annealed, Figure (3.5).

PEC study was made, Figure (3.26). In general, annealing CuSe thin films improves their PEC characteristics. The fast cooling showed better result

than non-annealed, but the annealing for long time reduced the efficiency. Accordingly, slow cooling reduced the efficiency conversion.

Many semiconductor crystal parameters are affected by cooling rates (fast and slow cooling). Examples of such parameters are: Composition, uniformity, film thickness, and PL properties. The dislocation density and concentration of structural defects also depend on the cooling rate SC crystals [67]. So cooling rate, slow or fast, affects the crystal. Both fast cooling and slow cooling may improve the properties, and may worsen them.

As far as we know, effect of cooling rate of CBD-CuSe thin film electrodes on their characteristics has been studied here for the first time. In this study, effect of cooling rate on CBD-CuSe thin film electrode deposited in 2 hr and annealed (at 250°C for 1 hr) has been studied here, Figures (3.5, 3.11 and 3.26). For PL spectra, the cooling rate didn't significantly affect position of PL emission band but slightly affect intensity of PL (the quickly cooled gave higher intensity than slowly cooled) and electronic absorption spectra (the quickly cooled gave better absorption than slowly cooled) and all PEC study showed better result for quickly cooled film than slowly cooled film, Figure (3.26). In general, annealing of CuSe thin films improves their PEC studies, the fast cooling showed better result than non-annealed, but the annealing for long time is reduced the efficiency. Accordingly, slow cooling reduced the efficiency conversion.

4.1.3 CBD/ECD-CuSe thin film electrodes

CBD/ECD-CuSe thin films didn't reported earlier. Unfortunately no work was made to study characteristics of such film electrodes, to the best of our knowledge.

Effect of deposition time on CBD/ECD-CuSe thin film deposited in (2, 4 and 6 hr) has been studied, Figures (3.3, 3.9, 3.23 and 3.24). The deposition time didn't significantly affect position of photoluminescence emission band, Figures (3.9). This is because longer deposition time increases film thickness, with no effect on structure. The deposition time significantly affect intensity of photoluminescence; this is because longer deposition time increases the disorder between the particles. Electronic absorption spectra were enhanced by increasing deposition time and the spectrum for 6 hr deposition time showed more curved plot than other two counterparts, Figure (3.3), this is because longer deposition time increases film thickness which in turn increases absorbance. For PEC study, the 2 hr time gave higher PEC characteristics than other two counterparts, Figure (3.23 and 3.24). In general, the change in deposition time affected the film characteristics, since it affects the surfaces of the films though not the particle size and structure of crystal. This is due to suitable thickness and longer deposition time increases the disorder between the particles. Moreover, the CBD/ECD-CuSe film deposited in 2 hr gave very high efficiency conversion (η % ~14.6). This is an important finding that has not been reported earlier. For example, the CBD/ECD-CdS gave efficiency conversion (η % ~0.29 %) [62], CBD-CdSe gave efficiency conversion (η % ~0.28 %) [63] and ECD-CuSe gave efficiency conversion (η % ~13.4 %) [46].

Comparison between XRD spectra for non-annealed CBD/ECD-CuSe films deposited in (2, 4 and 6 hr) was studied. Spectra for different CBD/ECD-CuSe films deposited in (2, 4 and 6 hr) were studied, Figure (3.17). In general, in this study the CuSe films prepared by CBD did affect in the

crystallite size and without change in the structure disorder. The crystallite size for CBD/ECD-CuSe films which have comparable intensities with preferential orientation in the C(200), C(111) and C(311) directions, Figure (3.17). This is acceptable as the CBD/ECD-CuSe is expected to be relatively uniform and crystalline. Thus may do not change their disorder, but affect in particle size. The non-annealed CBD/ECD-CuSe film (deposited in 6 hr) showed higher ratio than other counterparts. This means that the CBD/ECD-CuSe film (deposited in 6 hr) has higher crystallinity and uniformity than others [62].

In general, annealing CuSe thin films improves the photo $J-V$ plots, conversion efficiency, and annealing the semiconductors was reported to enhance the crystal homogeneity, structure and PEC performance [46, 58 and 61-63]. In this study, effect of annealing temperature on CBD/ECD-CuSe thin film electrode deposited in 2 hr and annealed at 250°C for 1 hr has been studied here, Figures (3.6, 3.12 and 3.27). Effect of annealing didn't significantly affect position of photoluminescence emission band, but significantly affect intensity of PL (the non-annealed gave higher intensity than annealed). This is because annealing causes a small disorder on the particles surface. Electronic absorption spectra were slightly affected by annealing and the annealed film exhibit slightly better absorption than non-annealed, All PEC study, showed better result for non-annealed film than annealed film, Figure (3.27). This is because annealing may damage the ECD-CuSe layer, this reduces conversion efficiency of the film

electrode. Moreover, the annealed temperature is not high enough to make a difference in the nano-particle size; this reduces the efficiency of the film. As far as we know, effect of cooling rate of CBD/ECD-CuSe thin film electrodes on their characteristics has been studied here for the first time. In this study, effect of cooling rate on CBD/ECD-CuSe thin film electrode deposited in 2 hr and annealed at 250°C for 1 hr has been studied here, Figures (3.6, 3.12 and 3.27). For PL spectra, the cooling rate didn't significantly affect position of PL emission band but slightly affect intensity of PL (the quickly cooled gave higher intensity than slowly cooled), electronic absorption spectra (the quickly cooled gave slightly better absorption than slowly cooled) and all PEC study showed better result for quickly cooled film than slowly cooled film, Figure (3.27). In general, annealing of CuSe thin films improves their PEC study, the fast cooling showed better result than non-annealed one, but the annealing for long time is reduced the efficiency. Accordingly, slow cooling reduced the efficiency conversion.

For AFM, the non-annealed CBD/ECD-CuSe films showed better surface morphology than annealed CBD/ECD-CuSe films (at 250°C for 1 hr, slow cooling), Figure (3.15 and 3.16). This is because the non-annealed CBD/ECD-CuSe more uniform and continuous surface than other counterpart.

Comparison between XRD spectra for annealed CBD/ECD-CuSe films (deposited in 2 hr) with fast and slow cooling was studied, Figures (3.19). Cooling rate enhanced the crystallite size in CBD/ECD-CuSe films with

slowly cooling and fast cooling. The crystallite size was enhanced from ~39 nm to ~57 nm for slow cooled and fast cooled of CBD/ECD respectively, Figures (3.19). The increase in crystallite sizes for CBD/ECD-CuSe particles is due to increasing of disorder in the crystallites. The annealed CBD/ECD-CuSe film (fast cooling) showed higher ratio than annealed CBD/ECD-CuSe film (slow cooling). This means that the CBD/ECD-CuSe film (with fast cooling) has higher crystallinity and uniformity than other [62]. It is also assumed that annealing homogenize the two CuSe layers prepared successively by ECD and CBD.

4.1.4 Comparison between different preparation techniques: ECD (15 min), CBD (2 hr) and CBD/ECD (2 hr)

The electronic absorption spectra and PL intensity value for non-annealed CBD/ECD-CuSe film was higher than those for both non-annealed ECD-CuSe and CBD-CuSe counterparts, Figures (3.4, 3.10 and 3.25). This may be attributed to the fact that CBD/ECD-CuSe consists of two distinct layers, because there is a layer of ECD ranked, this helped arrange a layer of CBD as well, thereby creating two layers regularly.

For AFM, the non-annealed CBD/ECD-CuSe films showed better surface morphology than CBD-CuSe non-annealed films, Figure (3.13 and 3.14). This is because the CBD/ECD-CuSe films more uniform and continuous surface than CBD-CuSe films, and CBD/ECD-CuSe consists of two distinct layers.

For PEC study, the non-annealed CBD/ECD-CuSe films showed better photo *J-V* plots and higher conversion efficiency than either ECD-CuSe or

CBD-CuSe non-annealed films, Figure (3.25). This may be attributed to the fact that CBD/ECD technique is expected to give a film that has good contact, suitable thickness and CBD/ECD-CuSe consists of two distinct layers with higher thickness than CBD-CuSe and ECD-CuSe films.

Part II

4.2 Coating with MP-Sil

The CuSe thin films prepared by CBD and CBD/ECD deposited in 2 hrs and coated with MP-Sil matrix has been studied, Figures (3.29- 3.34).

Coating is a double-edged sword. It may improve the properties, and may worsen them. The coating of electrodes with MP matrix improved the conversion efficiencies of the film electrodes, by two ways: Firstly, The MP involves Mn^{+2}/Mn^{+3} ions, which may catalyze hole transfer from thin film to electrolyte. Fast removal of holes from accumulation region protects the film surface from corrosion. Secondly, The MP matrix coating may physically protect thin film layer from oxygen and water molecules [46]. In this work coating of electrodes with MP reduced the conversion efficiencies of electrodes; this is possibly due to two reasons. Firstly, the polymer layer may behave as resistance and slow down the charge transfer process between the electrode surface and the electrolyte. Secondly, the coating of film surface with MP matrix may screen light from reaching the electrode surface [58]. In this study, it was found that the coating of CuSe electrodes with MP-Sil reduced the conversion efficiencies of electrodes.

4.2.1 CBD-CuSe thin film electrodes

Effect of CBD-CuSe thin film electrodes deposited in 2 hrs and coated with MP-Sil matrix has been studied, Figures (3.29, 3.31 and 3.33).

The coating with MP-Sil didn't significantly affect position of photoluminescence emission band, Figures (3.31). This is because no effect on particles size and structure. The coating with MP-Sil significantly affect intensity of photoluminescence (the naked film showed higher PL intensity than the coated film); this is because the coating of film surface with MP matrix may screen light of excitation from reaching electrode surface, and may screen emitted light from reaching detector. Electronic absorption spectra, Figure (3.29 b), showed that the coated has a small bands at ~ 450, ~ 550 nm and ~ 570 nm. This are confirm the presence of the metalloporphyrin (MP). But, electronic absorption spectra for naked films are not affected by coating, Figure (3.29 a). This is natural, as coating occurs only on the surface and does not affect crystallite properties.

It is known that the photo $J-V$ plots for SC electrodes are improved by MP-Sil coating compared to uncoated counterparts [61]. In this study, it was found that the coating of CuSe electrodes with MP-Sil reduced the conversion efficiencies of electrodes, Figures (3.33). This is possibly due to two reasons. Firstly, the polymer layer may behave as resistance and slow down the charge transfer process between the electrode surface and the electrolyte. Secondly, the coating of film surface with MP-Sil may screen light to reach the surface. Practical work and measurements showed that the coating layer lowered the light intensity for CBD-CuSe thin films. We

have noticed that the properties of small band gap semiconductors are improved by coating (for example: CdSe) [63]. On the other hand, the properties wide band gap semiconductors are not improved by coating (for example: CdS) [62].

4.2.2 CBD/ECD-CuSe thin film electrodes

Effect of CBD/ECD-CuSe thin film electrodes deposited in 2 hrs and coated with MP-Sil matrix has been studied, Figures (3.30, 3.32 and 3.34). The coating with MP-Sil didn't significantly affect position of photoluminescence emission band, Figures (3.32). This is because no effect on particles size and structure. The coating with MP-Sil slightly affect intensity of photoluminescence (the naked film showed higher PL intensity than the coated film); this is because the coating of film surface with MP matrix may screen light of excitation from reaching electrode surface, and may screen emitted light from reaching detector.

Electronic absorption spectra did not affect between coated and naked films, Figure (3.30). This is because coating occurs only on the surface and does not affect crystallite properties.

For PEC study, the naked film showed higher PEC properties than coated one. It was found that the coating of CuSe electrodes with MP-Sil reduced the conversion efficiencies of electrodes, Figures (3.34). This is possibly due to two reasons. Firstly, the polymer layer may behave as resistance and slow down the charge transfer process between the electrode surface and the electrolyte. Secondly, the coating of film surface with MP-Sil may screen light to reach the surface, thereby to reduce the efficiency of the film.

Conclusions

- CuSe thin films were prepared by three different techniques, including electrochemical deposition (ECD), chemical bath deposition (CBD) and combined CBD/ECD techniques. All films showed PEC behaviors.
- CBD/ECD-CuSe thin films showed higher efficiency in PEC systems than its CBD-CuSe and ECD-CuSe films counterparts. It has been obtained on the efficiency of up to almost (η % \sim 14.6), and this is an important finding that has not been reported earlier.
- Non-annealed CBD/ECD-CuSe and CBD-CuSe thin films showed higher conversion efficiency in PEC systems than its annealed.
- CBD/ECD films showed soundly good stability with steady values of J_{sc} versus time.
- Annealing and slow cooling process showed enhanced characteristics for different prepared CuSe thin films, such as, AFM, XRD spectra.
- Enhancement of PEC conversion efficiency and stability of different CuSe films are consistent with enhancements in XRD, PL spectra and AFM characteristics of the films.

Suggestions for Further Work

For future work, we recommend doing the following:

- 1) Prepare CuSe thin films using ECD followed by CBD, with multi deposition steps.
- 2) Use annealing at different temperatures to improve the PEC characteristics.
- 3) Study the effect of cooling rates of different annealed films, at different temperatures, on their PEC characteristics.
- 4) Modify the CuSe films with new coating material and different electro-active polymers.
- 5) Apply different PEC cells using different experimental conditions and different redox couples to enhance electrode efficiency and stability.
- 6) Effect of thickness of different prepared CuSe thin films.

References

- [1] Future energy: how to secure energy after depletion of resources?
<http://www.futureenergia.org/ww/en/pub/futureenergia/chats/oil.htm>
 (Accessed on 2014, February, 20).
- [2] Renewable Energy Network for News, Information & Companies,
<http://www.renewableenergyworld.com/rea/tech/solar-energy>
 (Accessed on 2014, February, 20).
- [3] Wallace, J. M., Hobbs, P. V., "Atmospheric Science: An introductory Survey", ed. Academic Press, New York, (1977), 54.
- [4] <http://www.fi.edu/PECO/solar-guide-family.pdf> (Accessed on 2014, February, 20).
- [5] MaryeAudet, Why Is Solar Energy Important?
http://greenliving.lovetoknow.com/Why_Is_Solar_Energy_Important
 (Accessed on 2014, February, 22).
- [6] http://www.chm.bris.ac.uk/webprojects2003/ledlie/advantages_of_solar_energy.htm (Accessed on 2014, February, 22).
- [7] Semiconductor, <http://en.wikipedia.org/wiki/Semiconductor> (Accessed on 2014, February, 22).
- [8] S. Chandra, "**Photo-electrochemical solar cell**", Gordon and Breach Science Publisher, New York, (1986), p. 162-183.
- [9] <http://www.elmhurst.edu/~ksagarin/color/figdis12-7.gif> (Accessed on 2014, February, 23).
- [10] K. W. Frese, Jr., in "**Semiconductor Electrodes**", ed. H.O Finklea, Elsevier, Amsterdam, (1988), p. 373.

- [11] B. Finnstr M., in "**Solar Energy Photochemical Processes Available for Energy Conversion**", 14, eds. S. Clae ssonand B. Holmstr M., National Swedish., Board for Energy Source Development (1982).
- [12] <http://butane.chem.uiuc.edu/pshapley/GenChem2/C4/bands.png> Accessed on 2014, February, 24.
- [13] L.Hollman, J. P. Hallais and J. C. Price, in "**Current Topics in Materials and Science**", E. Kaldis, North Holland Publ. Co. **Vol.5**, ed.(1980), p. 1.
- [14] **Band gap**, http://en.wikipedia.org/wiki/Band_gap (Accessed on 2014, February, 25).
- [15] http://chemwiki.ucdavis.edu/@api/deki/files/8951/chemwiki_picture_2.jpg (Accessed on 2014, February, 27).
- [16] A. Floyd, "**Electronic Devices**", Electronic Devices Fourth Edition, Published by Prentice Hall (2001), p. 78-90.
- [17] Bart J. Van Zeghbroeck, **Doped Semiconductors**, <http://ecee.colorado.edu/~bart/book/extrinsi.htm> (Accessed on 2014, February, 29).
- [18] http://www.optiqueingenieur.org/en/courses/OPI_ang_M05_C02/co/Contenu_04.html (Accessed on 2014, February, 29).
- [19] K. W. Frese, Jr., in "**Semiconductor Electrodes**", ed. H.O Finklea, Elsevier, Amsterdam, (1988), p. 373.
- [20] B. Finnstr M., in "**Solar Energy Photochemical Processes Available for Energy Conversion**", 14, eds. S. Clae ssonand B. Holmstr M., National Swedish., Board for Energy Source Development (1982).

- [21] [http://www.quarkology.com/12-physics/94-ideas implementation/94C-Semiconductors.html](http://www.quarkology.com/12-physics/94-ideas%20implementation/94C-Semiconductors.html) (Accessed on 2014, February, 29).
- [22] T. Watanabe, A. Fujishima, K. Honda, **photoelectrolysis of water and Sensitization of Semiconductors, in "Energy Resources through Photochemistry and Catalysis"**, ed. M. Gratzel, Academic Press, N.Y., (1983), p. 350-371.
- [23] **Fermi Level,**
<http://hyperphysics.phy-astr.gsu.edu/hbase/solids/fermi.html>
 (Accessed on 2014, June, 10).
- [24] Simon Connell, **Fermi statistics, charge carrier concentrations, dopants,**
http://psi.phys.wits.ac.za/teaching/Connell/phys284/2005/lecture07/lecture_07/node6.html (Accessed on 2014, June, 10).
- [25] **Alternative Energy: Solar Energy,**
<http://esa21.kennesaw.edu/activities/solar/solaractivity.pdf>
 (Accessed on 2014, March, 05).
- [26] **Introduction to photovoltaic solar energy,** M. Zeman, Delft University of Technology, p. 8.
- [27] **The basics of solids and solutions,** <http://www.porous-35.com/electrochemistry-semiconductors-2.html> (Accessed on 2014, March, 02).
- [28] B. Finnström, in **"Solar Energy Photochemical Processes Available for Energy Conversion"**, vol. 14, eds. S. Claesson and B. Holmström,

National Swedish. Board for Energy Source Development (1982), p. 56-64.

- [29] B. Finnstr M., in **"Solar Energy Photochemical Processes Available for Energy Conversion"**, 14, eds. S. Clae ssonand B. Holmstr M., National Swedish., Board for Energy Source Development (1982).
- [30] Carlo Alberto Bignozzi, Stefano Caramori, Vito Cristino, Roberto Argazzi, Laura Meda and Alessandra Tacca, **Nanostructured photoelectrodes based on WO₃: applications to photooxidation of aqueous electrolytes**, *Chemical Society Reviews*, Issue 6, 2013.
- [31] **Photonic Semiconductor Devices 355**,
<http://www.toolingu.com/definition-460355-34913-dark-current.html>
(Accessed on 2014, March, 07).
- [32] H. O. Finklea, in **"Semiconductor Electrodes"**, ed., Elsevier, Amsterdam, (1988), p. 18-22.
- [33] H. O. Fink lea, in **"Semiconductor Electrodes"**, ed., Elsevier, Amsterdam, (1988), p. 1-42.
- [34] A. Mamun, A. Islam, **"Characterization of copper selenide thin films deposited by chemical bath deposition technique"**, *Applied Surface Science*, **238** (2004)184-188.
- [35] **Thin film solar cell**,
http://en.wikipedia.org/wiki/Thin_film_solar_cell
(Accessed on 2014, March, 11).

- [36] D. Xu, Y. Xu, D. Chen, G. Guo, L. Gui, Y. Tang, "**Preparation of CdS single-crystal nanowires by electrochemically induced deposition**", *Advanced Materials*, **12** (2000) 520-522.
- [37] S. Ambade, R. Mane, S. Kale, S. Sonawane, A. Shaikh, S. Han, "**Chemical synthesis of p-type nanocrystalline copper selenide thin films for heterojunction solar cells**", *Applied Surface Science*, **253** (2006) 2123-2126.
- [38] M.T. Neshkova, V.D. Nikolova, A.M. Bond, V. Petrov, "**Electrodeposition of ternary CuAgSe thin films Use of the electrochemical quartz crystal microbalance approach for real-time phase quantification**", *Electrochimica Acta*, **50** (2005) 5606-5615.
- [39] I. B. Assaker, H. Elbedoui, R. Chtourou, "**Electrodeposited and characterization of Cu–Cd–Se semiconductor thin films**", *Electrochimica Acta*, **81** (2012) 149-154.
- [40] B. Pejova and I. Grozdanov, "**Chemical Deposition and Characterization of Cu₃Se₂ and Thin Films**", *Journal of Solid State Chemistry*, **158** (2001) 49-54.
- [41] T. Ohtani, M. Shohno, "**Room temperature formation of Cu₃Se₂ by solid-state reaction between a-Cu₂Se and a-CuSe**", *Journal of Solid State Chemistry*, **177** (2004) 3886-3890.
- [42] T.P. Hsieh, C.C. Chuang, C. S. Wu, J. C. Chang, J. W. Guo, W.C. Chen, "**Effects of residual copper selenide on CuInGaSe₂ solar cells**", *Solid-State Electronics*, **56** (2011) 175-178.

- [43] J. Li, T. Ma, M. Wei, W. Liu, G. Jiang, C. Zhu, "**The $\text{Cu}_2\text{ZnSnSe}_4$ thin films solar cells synthesized by electrodeposition route**", *Applied Surface Science*, **258** (2012) 6261- 6265.
- [44] R. A Wibowo, K. H. Kim, "**Band gap engineering of RF-sputtered CuInZnSe_2 thin films for indium-reduced thin-film solar cell application**", *Solar Energy Materials & Solar Cells*, **93** (2009) 941-944.
- [45] P. Kumar, J. Singh, M. K. Pandey, "**Wet chemical synthesis, structural and spectroscopic studies of CuSe-Ag Hierarchical sphere and drum-like micro porous structure**", *Spectro chimica Acta Part A: Molecular and Bio molecular Spectroscopy*, **110** (2013) 67-71.
- [46] R. AL-Kerm, "**Modification of CuSe thin film electrodes prepared by electrodeposition: Enhancement of photoelectrochemical characteristics by controlling cooling rate and covering with polymer/metalloporphyrin**", Master's Thesis, An-Najah National University, Nablus, Palestine, (2013).
- [47] T. Liu, Z. Jin, Jia Li, J. Wang, D. Wang, J. Lai and H. Du, "**Monodispersed octahedral-shaped pyrite CuSe_2 particles by polyol solution chemical synthesis**", *CrystEngComm*, Issue 44, 2013.
- [48] M. Sharin, A. Razak, Z.Zainal, "**Electrophoretic deposition and characterization of copper selenide thin films**", *The Malaysian Journal of Analytical Sciences*, **11** (2007) 324-330.

- [49] B. Hop, H. Trinh, K. Dat, P. Bao, "**Growth of CdS thin films by chemical bath deposition technique**", *VNU Journal of Science, Mathematics – Physics*, **24** (2008) 119-123.
- [50] S. Ambadea, R. Mane, S. Kale, S. Sonawane, A. Shaikh, S.Han, "**Chemical synthesis of p-type nanocrystalline copper selenide thin films for heterojunction solar cells**", *Applied Surface Science*, **253** (2006) 2123-2126.
- [51] S. Bingham, A. Black, Y. Calm, K. Garand, J. Throckmorton, **Electrochemical Deposition**, Center of Hierarchical Manufacturing, http://www.umassk12.net/nanodev/NanoEd/Electrochemical_Deposition/ (Accessed on 2014, April, 05).
- [52] J. Li, L. Jiang, B. Wang, F. Liu, J. Yang, D. Tang, Y. Lai, J. Li, "**Electrodeposition and characterization of copper bismuth selenidesemiconductor thin films**", *Electrochimica Acta*, **87** (2013) 153-157.
- [53] S. Soundeswaran, O. Senthil Kumar, R. Dhanasekaran, "**Effect of ammonium sulphate on chemical bath deposition of CdS thin films**", *Materials Letters*, **58** (2004) 2381- 2385.
- [54] K. S. Ramaiah, R.D. Pilkington, A.E. Hill, R.D. Tomlinson, A.K. Bhatnagar, "**Structural and optical investigations on CdS thin films grown by chemical bath technique**", *Materials chemistry and physics*, **68** (2001) 22-30.
- [55] B.G. Durdu, U. Alver, A. Kucukonder, Ö. Söğüt and M. Kavgaci, "**Investigation on Zinc Selenide and Copper Selenide Thin Films**

Produced by Chemical Bath Deposition", *ACTA PHYSICA POLONICA A*, 124 (2013) 1.

- [56] http://upload.wikimedia.org/wikipedia/commons/f/f0/Reflux_English.svg (Accessed on 2014, April, 05).
- [57] W. Mansour, "**Hydrosilation reaction catalyzed by novel Metalloporphyrin catalysts intercalated inside Nano- and micro particles**", Master's Thesis, An-Najah National University, Nablus, Palestine, (2013).
- [58] M. Mari'e, "**Thin Film CdS/FTO/Glass Electrodes Prepared by Combined Electrodeposition/ Chemical Bath Deposition: Enhancement of PEC Characteristics by Coating with Metalloporphyrinate/ Polysiloxane Matrices**", Master's Thesis, An-Najah National University, Nablus, Palestine, (2012).
- [59] H. S. Hilal, S. Shakhshir, M. Masoud, "**Metalloporphyrin/polysiloxane modified n-GaAs surfaces: effect on photoelectrochemical efficiency and surface stability**", *Journal of Electroanalytical Chemistry*, **527** (2002) 47-55.
- [60] H. S. Hilal, M. Masoud, S. Shakhshir, N. Jisrawi, "**n-GaAs band-edge reposition by modification with metalloporphorin-polysiloxane matrices**", *Active and Passive Electronic Components*, **26(1)** (2003) 11-21.
- [61] H. S. Hilal, W.M. Ateereh, T. Al-Tel, R. Shubeita, I. Saadeddin, G. Campet, "**Enhancement of n-GaAs characteristics by combined**

- heating, cooling rate and metalloporphyrin modification techniques"**, *Solid State Sciences*, **6** (2004) 139-146.
- [62] A. Zyoud, I. Saadeddin, S. Khurduj, M. Mari'e, Z. M. Hawash, M. I. Faroun, G. Campet, D. Park, H. S. Hilal, "**Combined electrochemical/chemical bath depositions to prepare CdS film electrodes with enhanced PEC characteristics**", *Journal of Electroanalytical Chemistry*, **707** (2013) 117–121.
- [63] H. Sabri, S. Saleh, A. Zyoud, N. N. Abdel-Rahman, I. Saadeddin, G. Campet, D. Park, M. Faroun, H. S. Hilal, "**Enhancement of CdSe film electrode PEC characteristics by metalloporphyrin/polysiloxane matrices**", *Electrochimica Acta*, **136** (2014) 138–145.
- [64] W. Chang, Y. Cheng, W. Yu, Y. Yao, C. Lee and H. Ko, "**Enhancing performance of ZnO dye-sensitized solar cells by incorporation of multiwalled carbon nanotubes**", *Nanoscale Research Letters*, **7** (2012) 166.
- [65] R. Yu, T. Ren, K. Sun, Z. Feng, G. Li, and C. Li, "**Shape-Controlled Copper Selenide Nanocubes Synthesized by an Electrochemical Crystallization Method**", *The Journal of Physical Chemistry Letters*, **113** (2009) 10833–10837.
- [66] http://wikieducator.org/User:Sakshi_grover/my-sandbox (Accessed on 2014, August, 07).
- [67] S. K. Salih, H. S. Hilal, I. A. Sa'deddin, E. Sellir and G. Campet, "**Modification of n-Si Characteristics By Annealing And Cooling At Different Rates**", *Active and Passive Electronic Components*, **26** (2003) 213–230.

جامعة النجاح الوطنية
كلية الدراسات العليا

تحضير أفلام CuSe كأقطاب في عمليات الطاقة الشمسية بطريقة الجمع ما بين الترسيب الكهربي والترسيب الكيميائي

إعداد

خالد علي قاسم مرتضى

إشراف

أ.د. حكمت هلال

قدمت هذه الأطروحة استكمالاً لمتطلبات الحصول على درجة الماجستير في الكيمياء بكلية الدراسات العليا في جامعة النجاح الوطنية في نابلس فلسطين.

2014

ب

تحضير أفلام CuSe كأقطاب في عمليات الطاقة الشمسية بطريقة الجمع ما بين الترسيب

الكهربي والترسيب الكيميائي

إعداد

خالد علي قاسم مرتضى

إشراف

أ.د. حكمت هلال

الملخص

تم تحضير أفلام سيلينيوم النحاس (CuSe) الرقيقة باستخدام طرق مختلفة منها الترسيب الكهربي (ECD) والترسيب الكيميائي (CBD) ثم طريقة الجمع بين الطريقتين سابقتي الذكر، على شرائح من الزجاج الموصل (FTO/coated).

وقد تم دراسة خصائص كافة الأفلام المحضرة في تحويل الضوء الى كهرباء بالطريقة الفوتوكهروكيميائية. وقد تم معاملة الأفلام المحضرة بعدة طرق مختلفة وظروف تجريبية مختلفة. وقد تم التحكم بعدة متغيرات منها: زمن الترسيب (2، 4، 6 ساعة)، درجة التسخين (الشيء)، وطريقة التبريد. تم كذلك دراسة تأثير الشيء (التسخين) عند درجة حرارة 250 مئوية ولمدة ساعة زمنية واحدة على خصائص الأفلام المحضرة. وقد تم تبريد الأفلام المشوية إلى درجة حرارة الغرفة باستخدام طريقتين مختلفتين (التبريد البطيء والسريع). وتم أيضاً استخدام زوج التأكسد والاختزال $K_3Fe(CN)_6/K_4Fe(CN)_6/LiClO_4$ في قياس تحويل الضوء الى كهرباء. حيث بنيت هذه الدراسة على قياس عدة عوامل مثل: جهد الدارة المفتوح (V_{oc})، كثافة تيار الدارة القصيرة (J_{sc})، منحنيات كثافة تيار الظلمة (dark $J-V$ plots) مقابل الجهد، منحنيات كثافة تيار الاضاءة (Photo $J-V$ plots) مقابل الجهد، وكفاءة الخلية في تحويل الضوء الى كهرباء (% efficiency)، وتضاريس السطح، علاوة على ثباتها مع الوقت.

وقد وجد ان زمن الترسيب لمدة (2 ساعة) يعطي افضل كفاءة في تحويل الضوء الى كهرباء مقارنة بنظائره الاخرى. كما وجد ان الافلام المشوية على درجة حرارة 250 مئوية، متبوعة بالتبريد

ت

السريع أو التبريد البطيء اعطت اقل كفاءة في تحويل الضوء الى كهرباء مقارنة بنظائرها غير المشوية.

علاوة على ذلك فقد تم طلاء سطوح افلام CuSe المحضرة بمركبات البورفينات/ بوليمر بولي سايلوكسين (MP-Sil) حيث وجد ولأول مرة ان عملية الطلاء تقلل من كفاءة وثبات الالكتروود في عمليات التحويل الضوئي الى تيار كهربائي.